



REPUBLIC OF TURKEY
ACIBADEM MEHMET ALİ AYDINLAR UNIVERSITY
INSTITUTE OF HEALTH SCIENCES

**PHOTODYNAMIC THERAPY ACTIVITIES OF
PHTHALOCYANINES ON CANCER**

ŞEYMA IŞIK

MASTER THESIS

DEPARTMENT OF MEDICAL BIOTECHNOLOGY

SUPERVISOR

Associate Prof. Dr. Özge Can

Second Supervisor

Dr. Müge Serhatlı

İSTANBUL-2020

DECLARATION

This thesis is my work, from the planning to writing of the thesis that I have no unethical behavior at all stages; all the information and interpretations not obtained by this thesis. That I have cited sources and included these sources in the list of references. And declare that I am not infringing any patents or copyrights at the time of writing.

08/01/2020

Şeyma Işık



FOREWORD AND ACKNOWLEDGMENTS

I want to express my appreciation to my supervisors, Dr. Müge Serhatlı, and Assoc. Prof. Dr. Özge Can. They convincingly guided and encouraged me to be professional and to do the right thing even when the road got tough. Their office doors were always open whenever I ran into a trouble spot or had a question about my research or writing.

I want to thank each member of the Immunogenetics Laboratory in Genetic Engineering and Biotechnology Institute of Marmara Research Center of TUBITAK for their help and motivation. I want to thank Prof. Dr. Esin Hamuryudan for providing me phthalocyanine molecules that were used in this work.

I am grateful to my little sister, Ceren Işık, for having always motivated me with her presence, life energy, smile, and joy. I want to express my sincere appreciation to my family for their support and great love. I also want to thank my friend, Mert Işık for his love and support.

This study was supported by TUBITAK 1003-SBAG, Project number 216S387. No opinion and determination of the publication is the official opinion of TUBITAK.

CONTENTS

Page

THESIS APPROVAL	i
DECLARATION	iii
FOREWORD AND ACKNOWLEDGMENTS	iv
TABLE LIST	ix
FIGURE LIST	xviii
LIST OF SYMBOLS	xviii
LIST OF ABBREVIATIONS	xx
SUMMARY	1
ÖZET	3
1. INTRODUCTION	5
2. BACKGROUND	7
2.1. Cancer	7
2.2. Hallmark of Cancer	7
2.3. Photodynamic Therapy	8
2.4. History of Photodynamic Therapy	9
2.5. Component of Photodynamic Therapy	10
2.5.1. Photosensitizer	10
2.5.1.1. Selective tumor distribution of photosensitizer	11
2.5.1.2. Phthalocyanines	12

2.5.2.	Light.....	12
2.5.3.	Oxygen.....	13
2.6.	Mechanism of PDT.....	14
2.7.	Cell Death Mechanisms Triggered by PDT: Apoptosis or Necrosis.....	16
2.8.	Subcellular Localization of Photosensitizer.....	16
3.	MATERIALS AND METHODS.....	18
3.1.	Materials.....	18
3.1.1.	Light-emitting diode system.....	20
3.2.	Methods.....	21
3.2.1.	Phthalocyanine molecules.....	21
3.2.2.	Cell culture.....	23
3.2.2.1.	Culture condition of cell lines.....	23
3.2.2.2.	Cell cryopreservation.....	24
3.2.2.3.	Continuous culture of cell lines.....	24
3.2.2.4.	Determination of population doubling time.....	25
3.2.2.5.	Mycoplasma detection.....	26
3.2.3.	Cellular uptake of Pc.....	26
3.2.4.	Biocompatibility.....	27
3.2.5.	Dark cytotoxicity.....	29
3.2.6.	Photo-irradiated cytotoxicity.....	30
3.2.7.	Oxidative stress evaluation.....	31

4.	RESULTS	32
4.1.	Determination of Population Doubling Time	32
4.2.	Mycoplasma Detection	32
4.3.	Cellular Uptake of Phthalocyanine Molecules	33
4.4.	Biocompatibility of Phthalocyanine Molecules.....	39
4.5.	Pc-induced Dark Cytotoxicity on Cancer Cell Lines.....	43
4.6.	Photo-induced Cytotoxicity of the Phthalocyanine Molecules on Cancer Cell Lines.....	48
4.7.	PDT-mediated Oxidative Stress Evaluation	58
4.8.	Comparison of PDT-induced Cytotoxicity of Nine Phthalocyanine Molecules on Cancer Cell Lines.....	68
4.9.	Comparison of PDT-induced Immediate and Late ROS Production of Nine Phthalocyanine Molecules on Cancer Cell Lines.....	70
4.10.	Tables of Results.....	74
4.10.1.	Tables of dark cytotoxicity	74
4.10.2.	Comparative table of experiments with EH1 phthalocyanine	78
4.10.3.	Comparative table of experiments with EH2 phthalocyanine	83
4.10.4.	Comparative table of experiments with EH3 phthalocyanine	89
4.10.5.	Comparative table of experiments with EH4 phthalocyanine	94
4.10.6.	Comparative table of experiments with HQH ₂ Pc phthalocyanine.....	100
4.10.7.	Comparative table of experiments with HQZnPc phthalocyanine	103
4.10.8.	Comparative table of experiments with HQInPc phthalocyanine.....	109

4.10.9.	Comparative table of experiments with SQH ₂ Pc phthalocyanine	114
4.10.10.	Comparative table of experiments with SQZnPc phthalocyanine	119
4.11.	Statistical Analysis	124
5.	DISCUSSION	140
6.	BIBLIOGRAPHY	148
7.	RESUME	152



TABLE LIST

Page

Table 1 Currently used photosensitizer molecules with FDA approval, and their commercial names.....	11
Table 2 List of cell lines.....	18
Table 3 List of equipment	18
Table 4 List of Buffer, Solution, and Kits.....	19
Table 5 List of EH Series Phthalocyanines.....	21
Table 6 List of HQ Series Phthalocyanines	22
Table 7 List of SQ Series Phthalocyanines	22
Table 8 Population doubling time of A253, FaDu, HT29 and T47D cell lines.	32
Table 9 Mycoplasma detection on the cell lines	33
Table 10 How many times Pc molecules was taken by cells relative to untreated control.	39
Table 11 Relative percentage cell viability of cancer cell lines following 24 hours of EH1 phthalocyanine administrations at dark.	75
Table 12 Relative percentage cell viability of cancer cell lines following 24 hours of EH2 phthalocyanine administrations at dark.	75
Table 13 Relative percentage cell viability of cancer cell lines following 24 hours of EH3 phthalocyanine administrations at dark.	75
Table 14 Relative percentage cell viability of cancer cell lines following 24 hours of EH4 phthalocyanine administrations at dark.	76
Table 15 Relative percentage cell viability of cancer cell lines following 24 hours of HQH ₂ Pc phthalocyanine administrations at dark.....	76
Table 16 Relative percentage cell viability of cancer cell lines following 24 hours of HQZnPc phthalocyanine administrations at dark.	76
Table 17 Relative percentage cell viability of cancer cell lines following 24 hours of HQInPc phthalocyanine administrations at dark.	77
Table 18 Relative percentage cell viability of cancer cell lines following 24 hours of SQH ₂ Pc phthalocyanine administrations at dark.	77

Table 19 Relative percentage cell viability of cancer cell lines following 24 hours of SQZnPc phthalocyanine administrations at dark.	77
Table 20 Relative percentage cell viability and ROS formation of cancer cell lines after photodynamic therapy with EH1 phthalocyanine at 624 nm (light fluence of 2 joules/cm ²).....	78
Table 21 Relative percentage cell viability and ROS formation of cancer cell lines after photodynamic therapy with EH1 phthalocyanine at 650-670 nm (light fluence of 2 joules/cm ²).....	79
Table 22 Relative percentage cell viability and ROS formation of cancer cell lines after photodynamic therapy with EH1 phthalocyanine at 690-710 nm (light fluence of 2 joules/cm ²).....	80
Table 23 Relative percentage cell viability and ROS formation of cancer cell lines after photodynamic therapy with EH1 phthalocyanine at 720-740 nm (light fluence of 2 joules/cm ²).....	81
Table 24 Relative percentage cell viability and ROS formation of cancer cell lines after photodynamic therapy with EH1 phthalocyanine at 725-755 nm (light fluence of 2 joules/cm ²).....	82
Table 25 Relative percentage cell viability and ROS formation of cancer cell lines after photodynamic therapy with EH2 phthalocyanine at 624 nm (light fluence of 2 joules/cm ²).....	84
Table 26 Relative percentage cell viability and ROS formation of cancer cell lines after photodynamic therapy with EH2 phthalocyanine at 650-670 nm (light fluence of 2 joules/cm ²).....	85
Table 27 Relative percentage cell viability and ROS formation of cancer cell lines after photodynamic therapy with EH2 phthalocyanine at 690-710 nm (light fluence of 2 joules/cm ²).....	86
Table 28 Relative percentage cell viability and ROS formation of cancer cell lines after photodynamic therapy with EH2 phthalocyanine at 720-740nm (light fluence of 2 joules/cm ²).....	87
Table 29 Relative percentage cell viability and ROS formation of cancer cell lines after photodynamic therapy with EH2 phthalocyanine at 725-755 nm (light fluence of 2 joules/cm ²).....	88

Table 30 Relative percentage cell viability and ROS formation of cancer cell lines after photodynamic therapy with EH3 phthalocyanine at 624 nm (light fluence of 2 joules/cm ²).....	89
Table 31 Relative percentage cell viability and ROS formation of cancer cell lines after photodynamic therapy with EH3 phthalocyanine at 650-670 nm (light fluence of 2 joules/cm ²).....	90
Table 32 Relative percentage cell viability and ROS formation of cancer cell lines after photodynamic therapy with EH3 phthalocyanine at 690-710 nm (light fluence of 2 joules/cm ²).....	91
Table 33 Relative percentage cell viability and ROS formation of cancer cell lines after photodynamic therapy with EH3 phthalocyanine at 720-740nm (light fluence of 2 joules/cm ²).....	92
Table 34 Relative percentage cell viability and ROS formation of cancer cell lines after photodynamic therapy with EH3 phthalocyanine at 725-755 nm (light fluence of 2 joules/cm ²).....	93
Table 35 Relative percentage cell viability and ROS formation of cancer cell lines after photodynamic therapy with EH4 phthalocyanine at 624 nm (light fluence of 2 joules/cm ²).....	95
Table 36 Relative percentage cell viability and ROS formation of cancer cell lines after photodynamic therapy with EH4 phthalocyanine at 650-670 nm (light fluence of 2 joules/cm ²).....	96
Table 37 Relative percentage cell viability and ROS formation of cancer cell lines after photodynamic therapy with EH4 phthalocyanine at 690-710 nm (light fluence of 2 joules/cm ²).....	97
Table 38 Relative percentage cell viability and ROS formation of cancer cell lines after photodynamic therapy with EH4 phthalocyanine at 720-740 nm (light fluence of 2 joules/cm ²).....	98
Table 39 Relative percentage cell viability and ROS formation of cancer cell lines after photodynamic therapy with EH4 phthalocyanine at 725-755 nm (light fluence of 2 joules/cm ²).....	99

Table 40 Relative percentage cell viability and ROS formation of cancer cell lines after photodynamic therapy with HQH ₂ Pc phthalocyanine at 624 nm (light fluence of 2 joules/cm ²).....	100
Table 41 Relative percentage cell viability and ROS formation of cancer cell lines after photodynamic therapy with HQH ₂ Pc phthalocyanine at 650-670 nm (light fluence of 2 joules/cm ²).....	101
Table 42 Relative percentage cell viability and ROS formation of cancer cell lines after photodynamic therapy with HQH ₂ Pc phthalocyanine at 690-710 nm (light fluence of 2 joules/cm ²).....	101
Table 43 Relative percentage cell viability and ROS formation of cancer cell lines after photodynamic therapy with HQH ₂ Pc phthalocyanine at 720-740 nm (light fluence of 2 joules/cm ²).....	102
Table 44 Relative percentage cell viability and ROS formation of cancer cell lines after photodynamic therapy with HQH ₂ Pc phthalocyanine at 725-755 nm (light fluence of 2 joules/cm ²).....	103
Table 45 Relative percentage cell viability and ROS formation of cancer cell lines after photodynamic therapy with HQZnPc phthalocyanine at 624 nm (light fluence of 2 joules/cm ²).....	104
Table 46 Relative percentage cell viability and ROS formation of cancer cell lines after photodynamic therapy with HQZnPc phthalocyanine at 650-670 nm (light fluence of 2 joules/cm ²).....	105
Table 47 Relative percentage cell viability and ROS formation of cancer cell lines after photodynamic therapy with HQZnPc phthalocyanine at 690-710 nm (light fluence of 2 joules/cm ²).....	106
Table 48 Relative percentage cell viability and ROS formation of cancer cell lines after photodynamic therapy with HQZnPc phthalocyanine at 720-740 nm (light fluence of 2 joules/cm ²).....	107
Table 49 Relative percentage cell viability and ROS formation of cancer cell lines after photodynamic therapy with HQZnPc phthalocyanine at 725-755 nm (light fluence of 2 joules/cm ²).....	108

Table 50 Relative percentage cell viability and ROS formation of cancer cell lines after photodynamic therapy with HQInPc phthalocyanine at 624 nm (light fluence of 2 joules/cm ²).....	109
Table 51 Relative percentage cell viability and ROS formation of cancer cell lines after photodynamic therapy with HQInPc phthalocyanine at 650-670 nm (light fluence of 2 joules/cm ²).....	110
Table 52 Relative percentage cell viability and ROS formation of cancer cell lines after photodynamic therapy with HQInPc phthalocyanine at 690-710 nm (light fluence of 2 joules/cm ²).....	111
Table 53 Relative percentage cell viability and ROS formation of cancer cell lines after photodynamic therapy with HQInPc phthalocyanine at 720-740 nm (light fluence of 2 joules/cm ²).....	112
Table 54 Relative percentage cell viability and ROS formation of cancer cell lines after photodynamic therapy with HQInPc phthalocyanine at 725-755 nm (light fluence of 2 joules/cm ²).....	113
Table 55 Relative percentage cell viability and ROS formation of cancer cell lines after photodynamic therapy with SQH ₂ Pc phthalocyanine at 624 nm (light fluence of 2 joules/cm ²).....	114
Table 56 Relative percentage cell viability and ROS formation of cancer cell lines after photodynamic therapy with SQH ₂ Pc phthalocyanine at 650-670 nm (light fluence of 2 joules/cm ²).....	115
Table 57 Relative percentage cell viability and ROS formation of cancer cell lines after photodynamic therapy with SQH ₂ Pc phthalocyanine at 690-710 nm (light fluence of 2 joules/cm ²).....	116
Table 58 Relative percentage cell viability and ROS formation of cancer cell lines after photodynamic therapy with SQH ₂ Pc phthalocyanine at 720-740 nm (light fluence of 2 joules/cm ²).....	117
Table 59 Relative percentage cell viability and ROS formation of cancer cell lines after photodynamic therapy with SQH ₂ Pc phthalocyanine at 725-755 nm (light fluence of 2 joules/cm ²).....	118

Table 60 Relative percentage cell viability and ROS formation of cancer cell lines after photodynamic therapy with SQZnPc phthalocyanine at 624 nm (light fluence of 2 joules/cm ²).....	119
Table 61 Relative percentage cell viability and ROS formation of cancer cell lines after photodynamic therapy with SQZnPc phthalocyanine at 650-670 nm (light fluence of 2 joules/cm ²).....	120
Table 62 Relative percentage cell viability and ROS formation of cancer cell lines after photodynamic therapy with SQZnPc phthalocyanine at 690-710 nm (light fluence of 2 joules/cm ²).....	121
Table 63 Relative percentage cell viability and ROS formation of cancer cell lines after photodynamic therapy with SQZnPc phthalocyanine at 720-740 nm (light fluence of 2 joules/cm ²).....	122
Table 64 Relative percentage cell viability and ROS formation of cancer cell lines after photodynamic therapy with SQZnPc phthalocyanine at 725-755 nm (light fluence of 2 joules/cm ²).....	123
Table 65 Significance of EH1-mediated PDT (at 624 nm with light fluence 2 joules/cm ²), two-way ANOVA results.....	124
Table 66 Significance of EH1-mediated PDT (at 650-670 nm with light fluence 2 joules/cm ²), two-way ANOVA results.....	124
Table 67 Significance of EH1-mediated PDT (at 690-710 nm with light fluence 2 joules/cm ²), two-way ANOVA results.....	125
Table 68 Significance of EH1-mediated PDT (at 720-740 nm with light fluence 2 joules/cm ²), two-way ANOVA results.....	125
Table 69 Significance of EH1-mediated PDT (at 725-755 nm with light fluence 2 joules/cm ²), two-way ANOVA results.....	125
Table 70 Significance of EH2-mediated PDT (at 624 nm with light fluence 2 joules/cm ²), two-way ANOVA results.....	126
Table 71 Significance of EH2-mediated PDT (at 650-670 nm with light fluence 2 joules/cm ²), two-way ANOVA results.....	126
Table 72 Significance of EH2-mediated PDT (at 690-710 nm with light fluence 2 joules/cm ²), two-way ANOVA results.....	126

Table 73 Significance of EH2-mediated PDT (at 720-740 nm with light fluence 2 joules/cm ²), two-way ANOVA results.....	127
Table 74 Significance of EH2-mediated PDT (at 725-755 nm with light fluence 2 joules/cm ²), two-way ANOVA results.....	127
Table 75 Significance of EH3-mediated PDT (at 624 nm with light fluence 2 joules/cm ²), two-way ANOVA results.....	127
Table 76 Significance of EH3-mediated PDT (at 650-670 nm with light fluence 2 joules/cm ²), two-way ANOVA results.....	128
Table 77 Significance of EH3-mediated PDT (at 690-710 nm with light fluence 2 joules/cm ²), two-way ANOVA results.....	128
Table 78 Significance of EH3-mediated PDT (at 720-740 nm with light fluence 2 joules/cm ²), two-way ANOVA results.....	128
Table 79 Significance of EH3-mediated PDT (at 725-755 nm with light fluence 2 joules/cm ²), two-way ANOVA results.....	129
Table 80 Significance of EH4-mediated PDT (at 624 nm with light fluence 2 joules/cm ²), two-way ANOVA results.....	129
Table 81 Significance of EH4-mediated PDT (at 650-670 nm with light fluence 2 joules/cm ²), two-way ANOVA results.....	129
Table 82 Significance of EH4-mediated PDT (at 690-710 nm with light fluence 2 joules/cm ²), two-way ANOVA results.....	130
Table 83 Significance of EH4-mediated PDT (at 720-740 nm with light fluence 2 joules/cm ²), two-way ANOVA results.....	130
Table 84 Significance of EH4-mediated PDT (at 725-755 nm with light fluence 2 joules/cm ²), two-way ANOVA results.....	130
Table 85 Significance of H ₂ QHPc-mediated PDT (at 624 nm with light fluence 2 joules/cm ²), two-way ANOVA results.....	131
Table 86 Significance of H ₂ QHPc-mediated PDT (at 650-670 nm with light fluence 2 joules/cm ²), two-way ANOVA results.....	131
Table 87 Significance of H ₂ QHPc-mediated PDT (at 690-710 nm with light fluence 2 joules/cm ²), two-way ANOVA results.....	131
Table 88 Significance of H ₂ QHPc-mediated PDT (at 720-740 nm with light fluence 2 joules/cm ²), two-way ANOVA results.....	132

Table 89 Significance of HQH ₂ Pc-mediated PDT (at 725-755 nm with light fluence 2 joules/cm ²), two-way ANOVA results.....	132
Table 90 Significance of HQZnPc-mediated PDT (at 624 nm with light fluence 2 joules/cm ²), two-way ANOVA results.....	132
Table 91 Significance of HQZnPc-mediated PDT (at 650-670 nm with light fluence 2 joules/cm ²), two-way ANOVA results.....	133
Table 92 Significance of HQZnPc-mediated PDT (at 690-710 nm with light fluence 2 joules/cm ²), two-way ANOVA results.....	133
Table 93 Significance of HQZnPc-mediated PDT (at 720-740 nm with light fluence 2 joules/cm ²), two-way ANOVA results.....	133
Table 94 Significance of HQZnPc-mediated PDT (at 725-755 nm with light fluence 2 joules/cm ²), two-way ANOVA results.....	134
Table 95 Significance of HQInPc-mediated PDT (at 624 nm with light fluence 2 joules/cm ²), two-way ANOVA results.....	134
Table 96 Significance of HQZnPc-mediated PDT (at 650-670 nm with light fluence 2 joules/cm ²), two-way ANOVA results.....	134
Table 97 Significance of HQZnPc-mediated PDT (at 690-710 nm with light fluence 2 joules/cm ²), two-way ANOVA results.....	135
Table 98 Significance of HQZnPc-mediated PDT (at 720-740 nm with light fluence 2 joules/cm ²), two-way ANOVA results.....	135
Table 99 Significance of HQZnPc-mediated PDT (at 725-755 nm with light fluence 2 joules/cm ²), two-way ANOVA results.....	135
Table 100 Significance of SQH ₂ Pc-mediated PDT (at 624 nm with light fluence 2 joules/cm ²), two-way ANOVA results.....	136
Table 101 Significance of SQH ₂ Pc-mediated PDT (at 650-670 nm with light fluence 2 joules/cm ²), two-way ANOVA results.....	136
Table 102 Significance of SQH ₂ Pc-mediated PDT (at 670-710 nm with light fluence 2 joules/cm ²), two-way ANOVA results.....	136
Table 103 Significance of SQH ₂ Pc-mediated PDT (at 720-740 nm with light fluence 2 joules/cm ²), two-way ANOVA results.....	137
Table 104 Significance of SQH ₂ Pc-mediated PDT (at 725-755 nm with light fluence 2 joules/cm ²), two-way ANOVA results.....	137

Table 105 Significance of SQZnPc-mediated PDT (at 624 nm with light fluence 2 joules/cm ²), two-way ANOVA results.....	137
Table 106 Significance of SQZnPc-mediated PDT (at 650-670 nm with light fluence 2 joules/cm ²), two-way ANOVA results.....	138
Table 107 Significance of SQZnPc-mediated PDT (at 690-710 nm with light fluence 2 joules/cm ²), two-way ANOVA results.....	138
Table 108 Significance of SQZnPc-mediated PDT (at 720-740 nm with light fluence 2 joules/cm ²), two-way ANOVA results.....	138
Table 109 Significance of SQZnPc-mediated PDT (at 725-755 nm with light fluence 2 joules/cm ²), two-way ANOVA results.....	139



FIGURE LIST

Page

Figure 1 Milestones of Photodynamic Therapy.....	9
Figure 2 Optical window in tissue.. ..	13
Figure 3 Photophysical changes of photosensitizer agent shown by Jablonski diagram.	15
Figure 4 Schematic represent of photochemical reactions through PDT in order to cause reactive oxygen species formation and cellular damage.....	16
Figure 5 Cellular signaling cascade triggered through ROS generation following PDT, leads to programmed cell death depend on subcellular localization of PS.....	17
Figure 6 LED configuration of CETONI 96 led array.....	20
Figure 7 Flow cytometry forward and side scatters, and fluorescence histograms to demonstrate cellular uptake of phthalocyanine molecules through A253 cell line. ..	34
Figure 8 Flow cytometry forward and side scatters, and fluorescence histograms to demonstrate cellular uptake of phthalocyanine molecules through FaDu cell line. ..	35
Figure 9 Flow cytometry forward and side scatters, and fluorescence histograms to demonstrate cellular uptake of phthalocyanine molecules through HT29 cell line...	36
Figure 10 Flow cytometry forward and side scatters, and fluorescence histograms to demonstrate cellular uptake of phthalocyanine molecules through T47D cell line...	37
Figure 11 Fluorescence histograms overlays of cell lines to compare cellular uptake of phthalocyanine molecules relative to untreated control and each other.. ..	38
Figure 12 Graph shows cellular uptake of Pc molecules based on how many times the signal was received by flow cytometry compared to the untreated control.	38
Figure 13 Dose dependent A. dark and B. photo-induced cytotoxicity of EH1 phthalocyanine on L929 cell line.....	40
Figure 14 Dose dependent A. dark and B. photo-induced cytotoxicity of EH2 phthalocyanine on L929 cell line.	40
Figure 15 Dose dependent A. dark and B. photo-induced cytotoxicity of EH3 phthalocyanine on L929 cell line.	40
Figure 16 Dose dependent A. dark and B. photo-induced cytotoxicity of EH4 phthalocyanine on L929 cell line.	41

Figure 17 Dose dependent A. dark and B. photo-induced cytotoxicity of HQH ₂ Pc phthalocyanine on L929 cell line.	41
Figure 18 Dose dependent A. dark and B. photo-induced cytotoxicity of HQZnPc phthalocyanine on L929 cell line	41
Figure 19 Dose dependent A. dark and B. photo-induced cytotoxicity of HQInPc phthalocyanine on L929 cell line.	42
Figure 20 Dose dependent A. dark and B. photo-induced cytotoxicity of SQH ₂ Pc phthalocyanine on L929 cell line.	42
Figure 21 Dose dependent A. dark and B. photo-induced cytotoxicity of SQZnPc phthalocyanine on L929 cell line	42
Figure 22 Dose dependent dark cytotoxicity of EH1 phthalocyanine on A. A253 B FaDu C. HT29 D. T47D cell lines.	43
Figure 23 Dose dependent dark cytotoxicity of EH2 phthalocyanine on A. A253 B FaDu C. HT29 D. T47D cell lines.	44
Figure 24 Dose dependent dark cytotoxicity of EH3 phthalocyanine on A. A253 B FaDu C. HT29 D. T47D cell lines.	44
Figure 25 Dose dependent dark cytotoxicity of EH4 phthalocyanine on A. A253 B FaDu C. HT29 D. T47D cell lines..	45
Figure 26 Dose dependent dark cytotoxicity of HQH ₂ Pc phthalocyanine on A. A253 B FaDu C. HT29 D. T47D cell lines.....	45
Figure 27 Dose dependent dark cytotoxicity of HQZnPc phthalocyanine on A. A253 B FaDu C. HT29 D. T47D cell lines.....	46
Figure 28 Dose dependent dark cytotoxicity of HQInPc phthalocyanine on A. A253 B FaDu C. HT29 D. T47D cell lines.	46
Figure 29 Dose dependent dark cytotoxicity of SQH ₂ Pc phthalocyanine on A. A253 B FaDu C. HT29 D. T47D cell lines	47
Figure 30 Dose dependent dark cytotoxicity of SQZnPc phthalocyanine on A. A253 B FaDu C. HT29 D. T47D cell lines	47
Figure 31 Dose dependent photo-induced cytotoxicity of EH1 phthalocyanine on cancer cell lines by WST-1 assay.....	49
Figure 32 Dose dependent photo-induced cytotoxicity of EH1 phthalocyanine on cancer cell lines by resazurin assay.....	49

Figure 33 Dose dependent photo-induced cytotoxicity of EH2 phthalocyanine on cancer cell lines by WST-1 assay.....	50
Figure 34 Dose dependent photo-induced cytotoxicity of EH2 phthalocyanine on cancer cell lines by resazurin assay.....	50
Figure 35 Dose dependent photo-induced cytotoxicity of EH3 phthalocyanine on cancer cell lines by WST-1 assay.....	51
Figure 36 Dose dependent photo-induced cytotoxicity of EH3 phthalocyanine on cancer cell lines by resazurin assay.....	51
Figure 37 Dose dependent photo-induced cytotoxicity of EH4 phthalocyanine on cancer cell lines by WST-1 assay.....	52
Figure 38 Dose dependent photo-induced cytotoxicity of EH4 phthalocyanine on cancer cell lines by resazurin assay.....	52
Figure 39 Dose dependent photo-induced cytotoxicity of HQH ₂ Pc phthalocyanine on cancer cell lines by WST-1 assay.....	53
Figure 40 Dose dependent photo-induced cytotoxicity of HQH ₂ Pc phthalocyanine on cancer cell lines by resazurin assay.....	53
Figure 41 Dose dependent photo-induced cytotoxicity of HQZnPc phthalocyanine on cancer cell lines by WST-1 assay.....	54
Figure 42 Dose dependent photo-induced cytotoxicity of HQZnPc phthalocyanine on cancer cell lines by resazurin assay.....	54
Figure 43 Dose dependent photo-induced cytotoxicity of HQInPc phthalocyanine on cancer cell lines by WST-1 assay.....	55
Figure 44 Dose dependent photo-induced cytotoxicity of HQInPc phthalocyanine on cancer cell lines by resazurin assay.....	55
Figure 45 Dose dependent photo-induced cytotoxicity of SQH ₂ Pc phthalocyanine on cancer cell lines by WST-1 assay.....	56
Figure 46 Dose dependent photo-induced cytotoxicity of SQH ₂ Pc phthalocyanine on cancer cell lines by resazurin assay.....	56
Figure 47 Dose dependent photo-induced cytotoxicity of SQZnPc phthalocyanine on cancer cell lines by WST-1 assay.....	57
Figure 48 Dose dependent photo-induced cytotoxicity of SQZnPc phthalocyanine on cancer cell lines by resazurin assay.....	57

Figure 49 Dose dependent post-30 minutes photo-induced ROS formation of EH1 phthalocyanine on cancer cell lines.....	59
Figure 50 Dose dependent post-24 hours photo-induced ROS formation of EH1 phthalocyanine on cancer cell lines.....	59
Figure 51 Dose dependent post-30 minutes photo-induced ROS formation of EH2 phthalocyanine on cancer cell lines.....	60
Figure 52 Dose dependent post-24 hours photo-induced ROS formation of EH2 phthalocyanine on cancer cell lines.....	60
Figure 53 Dose dependent post-30 minutes photo-induced ROS formation of EH3 phthalocyanine on cancer cell lines	61
Figure 54 Dose dependent post-24 hours photo-induced ROS formation of EH3 phthalocyanine on cancer cell lines.....	61
Figure 55 Dose dependent post-30 minutes photo-induced ROS formation of EH4 phthalocyanine on cancer cell lines.....	62
Figure 56 Dose dependent post-24 hours photo-induced ROS formation of EH4 phthalocyanine on cancer cell lines.....	62
Figure 57 Dose dependent post-30 minutes photo-induced ROS formation of HQH ₂ Pc phthalocyanine on cancer cell lines.....	63
Figure 58 Dose dependent post-24 hours photo-induced ROS formation of HQH ₂ Pc phthalocyanine on cancer cell lines.....	63
Figure 59 Dose dependent post-30 minutes photo-induced ROS formation of HQZnPc phthalocyanine on cancer cell lines.....	64
Figure 60 Dose dependent post-24 hours photo-induced ROS formation of HQZnPc phthalocyanine on cancer cell lines.....	64
Figure 61 Dose dependent post-30 minutes photo-induced ROS formation of HQInPc phthalocyanine on cancer cell lines.....	65
Figure 62 Dose dependent post-24 hours photo-induced ROS formation of HQInPc phthalocyanine on cancer cell lines.....	65
Figure 63 Dose dependent post-30 minutes photo-induced ROS formation of SQH ₂ Pc phthalocyanine on cancer cell lines.....	66
Figure 64 Dose dependent post-24 hours photo-induced ROS formation of SQH ₂ Pc phthalocyanine on cancer cell lines.....	66

Figure 65 Dose dependent post-30 minutes photo-induced ROS formation of SQZnPc phthalocyanine on cancer cell lines.....	67
Figure 66 Dose dependent post-24 hours photo-induced ROS formation of SQZnPc phthalocyanine on cancer cell lines.....	67
Figure 67 PDT-mediated cytotoxicity of nine phthalocyanine molecules on A253 cell line.....	68
Figure 68 PDT-mediated cytotoxicity of nine phthalocyanine molecules on FaDu cell line.....	68
Figure 69 PDT-mediated cytotoxicity of nine phthalocyanine molecules on HT29 cell line.....	69
Figure 70 PDT-mediated cytotoxicity of nine phthalocyanine molecules on T47D cell line.....	69
Figure 71 PDT-mediated immediate ROS production of nine phthalocyanine molecules on A253 cell line.....	70
Figure 72 PDT-mediated late ROS production of nine phthalocyanine molecules on A253 cell line.....	71
Figure 73 PDT-mediated immediate ROS production of nine phthalocyanine molecules on FaDu cell line.....	71
Figure 74 PDT-mediated late ROS production of nine phthalocyanine molecules on FaDu cell line.....	71
Figure 75 PDT-mediated immediate ROS production of nine phthalocyanine molecules on HT29 cell line.....	72
Figure 76 PDT-mediated late ROS production of nine phthalocyanine molecules on HT29 cell line.....	72
Figure 77 PDT-mediated immediate ROS production of nine phthalocyanine molecules on T47D cell line.....	72
Figure 78 PDT-mediated late ROS production of nine phthalocyanine molecules on T47D cell line.....	73

LIST OF SYMBOLS

%	Percentage
-O ₂	Singlet Oxygen
μg	Microgram
μm	Micrometer
μl	Microliters
μs	Microsecond
C°	Celsius
Al	Aluminum
cm ²	Centimeter Square
CO ₂	Carbon Dioxide
Fe	Iron
g	Gram
H ₂ O	Water
H ₂ O ₂	Hydrogen Peroxide
In	Indium
kcal	Kilo Calorie
kDa	Kilo Daltons
<i>l</i>	Liter
M	Molar
mg	Milligram
Mg	Magnesium
ml	Milliliter
mM	Millimolar
mV	Millivolt
ng	Nanograms

nm	Nanometer
ns	Nanoseconds
O ₂	Molecular Oxygen
pH	Potential of Hydrogen
rpm	Revolutions per minute
SD	Standard Deviation
SOD	Superoxide Dismutase
Sn	Tin
Zn	Zinc



LIST OF ABBREVIATIONS

3D	Three-Dimensional
ALA	5-Aminolevulinic acid
AMD	Age-related macular degeneration
ATCC	American Type Culture Collection
Ce6-PVP	Chlorin e-6-polyvinpyrrolidone
DCFDA	2',7'-Dichlorodihydrofluorescein diacetate
DMSO	Dimethylsulfoxide
DNA	Deoxyribonucleic Acid
DNase	Deoxyribonuclease
DPBS	Dulbecco's phosphate-buffered saline
EDTA	Ethylenediaminetetraacetic Acid
FBS	Fetal Bovine Serum
FDA	The Food and Drug Administration
HBSS	Hank's Balanced Salt Solution
HpD	Hematoporphyrin derivative
HPPH	2-(1-hexyloxyethyl)-2devinyl pyropheophorbide-a
IR	Infrared radiation
LED	Light-emitting diode
MACE	Mono-(L)-aspartylchlorin-e6
min.	Minute
mTHPC	m-tetrahydroxyphenylchlorin
PBS	Phosphate-Buffered Saline
Pc	Phthalocyanine
PDT	Photodynamic Therapy
PS	Photosensitizer

RNase Ribonuclease
ROS Reactive Oxygen Species
TUBITAK Scientific and Technological Research
 Council of Turkey



SUMMARY

Cancer is one of the most death-causing health problems in the world. There are many treatment approaches to cure this disease. Photodynamic therapy is one of the most promising cancer treatments since their advantages including being less invasive than radiotherapy, surgery, and have the ability to bypass the mechanisms that make the cell resistant to chemotherapeutic drugs and ionizing radiation. Photodynamic therapy is based on light excitation of a photosensitizer molecule that transfers its energy/photon to nearby molecular oxygen. This mechanism leads to the formation of harmful singlet oxygen and reactive oxygen species, by the way, cellular damage. Phthalocyanine molecules, synthetic macrocyclic chemical compounds with absorption spectrum and fluorescent characteristic and capability to create energy to form singlet oxygen that leads to cellular death by triggering mechanisms within the cell, are suitable to be used in photodynamic therapy as a photosensitizer agent.

In this thesis, in-vitro photodynamic therapy effects of nine specifically synthesized tetra-substituted symmetric water-soluble phthalocyanine molecules were investigated in many terms. By using their self-fluorescent features, cellular uptake of the molecules was revealed through proper channels of flow cytometry without any need to label the phthalocyanine molecules. Biocompatibility of the molecules was studied on mouse L929 cell line considering prescription of International Organization for Standardization, ISO10993. After revealing biocompatibility of the molecules, firstly dark cytotoxicity experiments were carried out to determine the non-toxic concentration range to be used for PDT studies. Among different light fluence, proper light fluence was determined, by the way, at the proper Pc concentrations and light fluence, in-vitro photodynamic therapy was applied on different cancer cell lines, salivary gland carcinoma, pharynx carcinoma, colorectal adenocarcinoma, and breast carcinoma. Further, whether the PDT-mediated cellular damage is triggered through reactive oxygen species formation or not, for each treatment group, oxidative stress was evaluated.

It has been shown that all the molecules used in the study are biocompatible, have cellular uptake properties, do not have cytotoxicity in the dark. Moreover, each phthalocyanine molecule except non-metallo phthalocyanine with morpholinyl moieties, HQH2Pc, causes significant cell death due to photodynamic therapy and this cell death is related to ROS production. The highest PDT effect was determined in the salivary gland carcinoma cells and in the cationic zinc phthalocyanine, EH1. In conclusion, these molecules are powerful candidates that can be used as photosensitizer agents in photodynamic therapy for further studies.

Keywords: Cancer, Photodynamic therapy, Phthalocyanines, Reactive oxygen species, Singlet oxygen

ÖZET

Ftalosiyenin Moleküllerinin Kansere Üzerindeki Fotodinamik Tedavi Etkileri

Kanser, dünyada ölüme en çok sebebiyet veren hastalıklardan bir tanesidir. Kanser tedavisi için farklı yaklaşımlar söz konusudur. Fotodinamik tedavi, radyoterapi ve cerrahi yöntemlerinden daha az invaziv olması, ayrıca hücreyi kemoterapötik ilaçlara ve iyonlaştırıcı radyasyona dirençli hale getiren mekanizmaları elimine edebilmesi, kıyasla ucuz bir tedavi yöntemi olması gibi pek çok avantaja sahip olmasından dolayı ümit vaat eden kanser tedavilerinden biridir. Fotodinamik tedavi temelde, enerjisini / fotonunu yakındaki moleküler oksijene aktaran ışığa duyarlılaştırıcı bir molekülün belirli dalga boyunda ışık ile uyarılmasına dayanır. Bu mekanizma, zararlı singlet oksijenin ve reaktif oksijen parçacıklarının oluşumuna neden olarak hücresel hasara yol açar. Ftalosiyenin molekülleri sentetik makrosiklik kimyasal bileşiklerdir. Absorpsiyon spektrum karakteristikleri ve hücresel hasara yol açan singlet oksijeni oluşturmak için gerekli olan enerjiyi üretebilme kapasiteleri sayesinde, fotodinamik tedavide bir ışığa duyarlılaştırıcı madde olarak kullanılabilirler.

Bu tez çalışmasında, dokuz tane özel olarak sentezlenmiş simetrik yapıda olan suda çözünür ftalosiyenin molekülünün in vitro fotodinamik tedavi etkileri birçok açıdan incelenmiştir. Floresan özellikleri olan bu moleküller, bu özellikleri kullanılarak, hücrelere bağlanma kapasiteleri, floresan başka bir madde ile boyanmaya gerek duyulmaksızın akış sitometrisinin uygun kanalları ile gösterilmiştir. Moleküllerin biyouyumluluğu, fare fibroblast L929 hücreleri üzerinde çalışılmıştır. Moleküllerin biyouyumluluğunun gösterilmesinden sonra, ilk önce PDT çalışmaları için kullanılacak toksik olmayan konsantrasyon aralığının belirlenmesi için karanlıkta sitotoksikite deneyleri yapılmıştır. Belirlenen uygun Pc konsantrasyonu ve ışık dozunda, farklı kanser hücre hatlarında fotodinamik tedavi uygulaması gerçekleştirilmiştir. Ayrıca, fotodinamik tedavi kaynaklı hücresel hasarın, reaktif

oksijen parçacıklarının oluşumu ile tetiklenip tetiklenmediğini göstermek amacıyla, her tedavi grubu için oksidatif stres değerlendirilmesi yapılmıştır.

Çalışmada kullanılan tüm moleküllerin biyouyumlu oldukları, hücrel alım özelliklerine sahip oldukları, karanlıkta sitotoksitelerinin bulunmadığı gösterilmiştir. Ayrıca, merkez metali bulundurmeyen morfolinil gruplu ftalosiyanın molekülü olan HQH_2Pc molekülü hariç her molekül, fotodinamik tedaviye bağlı hücre ölümüne neden olmuştur ve bu hücre ölümünün reaktif oksijen parçacığı üretimine bağlı olduğu gösterilmiştir. En yüksek PDT etkisi, tükürük bezi karsinom hücrelerinde ve katyonik çinko ftalosiyanın molekülü olan EH1 molekülünde belirlenmiştir. Sonuç olarak, bu moleküller ileri çalışmalar için fotodinamik tedavide ışığa duyarlılaştırıcı ajanlar olarak kullanılabilir güçlü adaylardır.

Anahtar Kelimeler: Fotodinamik tedavi, Ftalosiyanın, Kanser, Reaktif oksijen parçacığı, Singlet oksijen.

1. INTRODUCTION

In order to meet the demands of developing technology, hybrid compounds formed by combining two or more compounds are important among high technology materials. The absorption spectrum characteristics of the synthetic macrocyclic compounds, phthalocyanines, make them used photosensitizers and the molecules have become interesting materials for photodynamic therapy (PDT) applications in recent years (1, 2). Photodynamic therapy is one of the most promising treatment modalities due to its low side effects. The basis of photodynamic cancer treatment is light, specific photo sensor, photosensitizer, and oxygen that can absorb light in the near IR region (3). The first step in treatment begins with the administration of the photosensitizer (PS) agent into the body. The agent is absorbed by all the cells of the body, but it is held in cancer cells more than normal cells. 24-72 hours after the injection, the agent is completely excreted from normal cells but remains retained by cancerous cells (4). When the light exposure at a specific wavelength occurs, the PS molecules are stimulated and change their energy state from the baseline to the excited state. As it returns from the excited level to the basic state, the released energy is transferred to molecular oxygen within the cell, causing singlet oxygen and reactive oxygen species (ROS) formation (4, 5). The resulting singlet oxygen and ROS causes damage and death to cancerous cells. Since this reaction is very short-lived (10-350 ns) and local (approximately 10-55 nm in the cell), tissues other than cancerous tissues are not damaged. In addition to these instant effects of PDT application, there are two other important advantages that show its effect for a long time. The first is that the vascularization in the tumor is disrupted after therapy, and the structure is left without food, and the second is that T cells attack cancer cells as a result of activation of the immune system (6).

The response to PDT at the cellular level depends on the internal and external parameters. External parameters are including factors such as PS concentration, light dose, incubation conditions. Internal parameters are including factors such as metabolic properties of the cell, the oxygen level in tissue, cell genotype, and cell cycle

phase (7). The mechanism of PDT is also directly related to the intracellular localization of the PS molecule. This is because the life of singlet oxygen, the most effective photoproduct in PDT, is shorter than 0.05 μ s. Owing to its high reactive property, $^1\text{O}_2$ can diffuse only 0.02 μ m from the region of release (8, 9). Therefore, the localization of PS within the cell determines which organelle is primarily damaged. Because most PSs are localized outside the nucleus and have a short lifespan of singlet oxygen, the mutagenic effect of PDT is quite low. PDT mediated direct cell death occurs in the form of apoptosis, necrosis or combination. In many cases, PDT has been shown to be highly effective in inducing apoptosis (10, 11).

In this thesis study, in-vitro PDT effects of nine specifically synthesized cationic water-soluble phthalocyanine (Pc) derivatives (12, 18) on Salivary gland carcinoma, A253 cell line, Pharynx carcinoma, FaDu, Colorectal adenocarcinoma, HT29, Breast carcinoma, T47D cell lines has been aimed. Respectively, the binding status of the molecules to the cells, their biocompatibility, cytotoxic effects in the dark, the fluency of the light to be used, and photodynamic therapy-induced cell death, and the ability to trigger the formation of reactive oxygen species due to photodynamic therapy were investigated and reported.

2. BACKGROUND

2.1. Cancer

Cancer is a branch of a group of diseases with the capacity of abnormal cell growth and invading and spreading surrounding parts of the body (20).

2.2. Hallmark of Cancer

In 2000, Douglas Hanahan and Robert A Weinberg reported 6 hallmarks of cancer that are acquired during the progression of tumorigenesis. One of the hallmarks is that resistance to cell death where healthy cells are induced cell death by different mechanisms including apoptosis, autophagy, and necrosis. Also, cancer cells have the capacity to limitless growth due to evading growth suppression where healthy cell growth is restricted and suppressed. They activate cellular proliferation signaling pathways by producing an excessive amount of growth factors and also producing abnormal growth factor receptors that do not require ligand to trigger cascade in order to proliferate unstoppably. Additionally, cancer cells have the ability to replicate limitless due to their genetic material alteration where healthy cells can replicate for only an amount of time. To address the oxygen and nutrition needs due to their rapid growth capacities, cancer cells trigger angiogenesis that is the formation of new blood vessels through angiogenic growth factors. Further, Cancer cells have the ability to invade other local tissues and metastasize to the distant sites on the body by blood and lymph circulation (21). In addition to these 6 hallmarks of cancer, in 2011 Douglas Hanahan and Robert A Weinberg expand their understanding of cancer by hallmarks of cancer: generation. They have put in 4 additional hallmarks of cancer in their previous reports. One of these hallmarks is genome instability and mutation. Instability of genetic material can lead to mutations that can be normally altered by check mechanism, in this case, these gathered mutation results in the formation of cancer

cells by triggering unrestricted cell growth. Also, they reported that the destruction of this immune system is one of the hallmarks to progress cancer where cancer progression normally restricted by natural immunity of the body. Moreover, in contrast to healthy cells, cancer cells regulate their glucose metabolism to fulfill their excessive energy needs by limiting it mostly to glycolysis even in the presence of oxygen, called aerobic glycolysis. Lastly, they stated that cancer cell proliferation and progress is also supported by tumor promoted inflammatory cells (22).

23. Photodynamic Therapy

There is various cancer treatment currently used with FDA approval such as chemotherapy, radiotherapy, immunotherapy, targeted drug therapy, etc. (national cancer institute). Among cancer treatments, photodynamic therapy is one of the most promising therapy due to its low side effect, selectivity, long term efficiency, and eliminating possible drug-resistant (23).

PDT application is based on 3 elements that are a light source, a photosensitizer agent, and molecular oxygen. The first step of this treatment begins with the administration of tumor localizing photosensitizer agent that is activated by a light source of an appropriate wavelength (3, 10).

The photosensitizer changes its energy state to short-lived singlet excited state as a result of the absorption of a photon of light. When changing its state from singlet to longer-lived triplet state, exchange its energy with nearby molecular oxygen yielding singlet oxygen as well as reactive oxygen species that trigger cell damage and death (10).

24. History of Photodynamic Therapy

The history of PDT underlies before the century, however first recognition of cell death triggered by a chemical compound and light was reported 100 years ago, in 1900 by a medical student Oscar Raab following his study on malaria-causing protozoa. As a change, he found that acridine red and light combination had a lethal effect on Infusoria. Following his studies, he found that the lethal effect was a result of energy transfer from light to chemical compound as like photosynthesis in plants (7, 24).

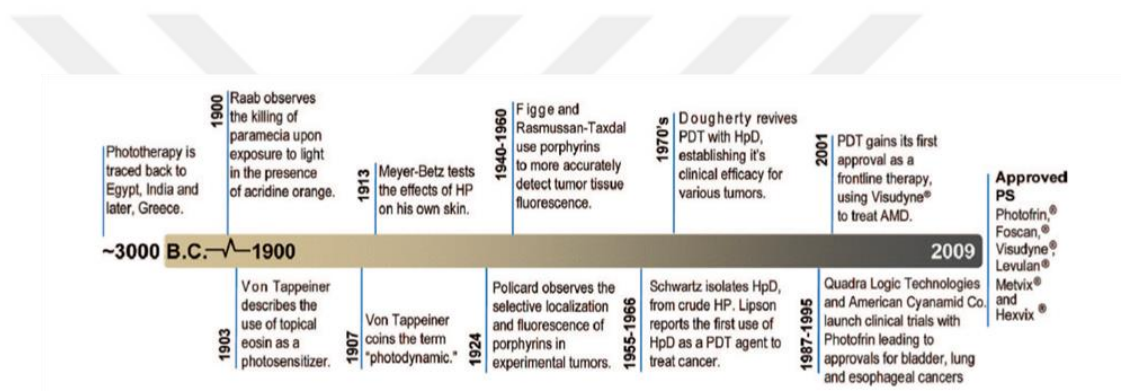


Figure 1 Milestones of Photodynamic Therapy.

Reference: Reprinted with permission from (Celli JP, Spring BQ, Rizvi I, Evans CL, Samkoe KS, Verma S, et al. Imaging and photodynamic therapy: Mechanisms, monitoring, and optimization. Chem Rev. 2010; 110(5): 2795–2838.)

In 1903, the first usage to treat skin tumors, eosin and the white light combination were used by von Tappeiner. Then, von Tappeiner with Jodlbauer revealed oxygen requirement in photoreaction in 1907, and they described this phenomenon as “photodynamic action” (25). In 1913, Friedrich Meyer-Betz injected himself with hematoporphyrin to see the effects in humans. In 1924 Frenchman Policard reported the localization of porphyrin in a malignant tumor. In 1948, Figge and Weiland studied on porphyrin localization in each tumor type to the application of porphyrin in diagnosis and treatment and reported that in normal tissues, excepted to lymph nodes, fetal and placental tissue and healing wounds,

fluorescent was not monitored (26). In 1955, Schwartz showed hematoporphyrin was composed of various porphyrin with different features. After some purification and dissolving procedures, he produced hematoporphyrin derivative (HpD) that had a much more cytotoxic effect than crude hematoporphyrin (27). The first treatment with photo induced HpD on a tumor was in 1975 as a result of the studies of Dougherty and coworkers. In the 2001 verteporfin, menzoporphyrin derivative monoacid ring A, commercially named as Visudyne, was approved by FDA to primarily treat age-related macular degeneration (7).

25. Component of Photodynamic Therapy

The working principle of photodynamic therapy includes three components: light source, photosensitizer, and oxygen (23).

25.1. Photosensitizer

Photosensitizers are chemical molecules that induce a photochemical reaction in other molecules through photosensitization. Photosensitizers are one of the main components of photodynamic therapy.

Currently, various photosensitizer agents with Food Drug Administration approval are used in the clinic (Table 1) to treat different types of diseases including cancer. Some of them are Photofrin, Foscan, Visudyne®, Levulan®, and Metvix®. On the other hand, there are many photosensitizer candidates are currently under

clinical trials including but not limited to HPPH, motexafin lutetium, NPe6, SnET2 (28).

Table 1 Currently used photosensitizer molecules with FDA approval, and their commercial names.

Photosensitizer	Structure	Wavelength (nm)	Approved	Trials	Cancer type
Porfimer sodium (Photofrin) (HpD)	Porphrin	630	Worldwide		Lung, esophagus, bile,duct, bladder, brain, ovarian
ALA	Porphrin precursor	635	Worldwide		Skin, bladder, brain, esophagus
ALA esters	Porphrin precursor	635	Europe		Skin, bladder
Temoporfin (Foscan) (mTHPC)	Chlorin	652	Europe	United States	Head and neck, lung, brain, skin, bile,duct
Verteporfin	Chlorin	690	Worldwide (AMD)	United Kingdom	Ophthalmic, pancreatic,skin
HPPH	Chlorin	665		United States	Head and neck, esophagus, lung
SnEt2 (Purlytin)	Chlorin	660		United States	Skin, breast
Talaporfin (LS11, MACE, NPe6)	Chlorin	660		United States	Liver, colon, brain
Ce6-PVP (Fotolon)	Chlorin	660		Belarus, Russia	Nasopharyngeal, sarcoma, brain
Silicon phthalocyanine (Pc4)	Phthalocyanine	675		United States	Cutaneous T-cell lymphoma
Padoporfin (TOOKAD)	Bacteriochlorin	762		United States	Prostate
Motexafin lutetium (Lutex)	Texaphyrin	732		United States	Breast

Reference: Reprinted with permission (lisence number, 4724860266940) from (Agostinis P, Berg K, Cengel KA, Foster TH, Girotti AW, Gollnick SO, et al. Photodynamic therapy of cancer: An update. CA Cancer J Clin. 2011; 61(4): 250–281.)

2.5.1.1. Selective tumor distribution of photosensitizer

Although tumor-specific localization of photosensitizers is not fully understood, some features of tumor tissues can be used to understand these selective distributions. Excessive low-density protein receptors, the presence of macrophage (29, 30) and low pH are some of the differences between tumor tissues and normal tissues. Tumor tissues due to their lower pH and higher lactic acid content of interstitial fluid (31) can preferentially uptake photosensitizers compared to normal tissues (32, 33). Furthermore, the large interstitial space of tumor tissues, a leaking vessel, damaged lymphatic drainage, a large amount of newly synthesized collagen (34, 35), and a high amount of lipids are also effective for the preferential distribution of photosensitizers (36).

2.5.1.2. Phthalocyanines

Phthalocyanines that are synthetic macrocyclic compounds have been used as photosensitizers and become interesting materials for photodynamic therapy (PDT) applications in recent years due to their absorption spectral characteristics with high molecular extinction coefficient in the red Q band. PCs that have to produce 26-30 kcal/mole energy at their triplet state can give yield appropriate energy for efficient photodynamic therapy where singlet oxygen formation requires 23 kcal/mole energy (37, 38).

Moreover, PCs have some properties that make them useful in research and clinical including tumor selectivity, non-toxicity, effective as a photosensitizer, fluorescence capacities, and long-lived triplet state production efficiency upon irradiation, photochemical and chemical stability (38, 40). PCs can be altered by adding groups to the surrounding of their ring structure. Also, different metal ions can be inserted on the central ring of non-metallo PCs. Blue and green colors and photo energy transfer features of PCs allow them used in different industries. Photo reduction rates of PCs depend on the metal group on the central ring of metallo-PCs respectively as $Zn > Al > Mg > Sn > Fe$ (37, 41).

2.5.2. Light

In photodynamic therapy, currently, a large range of light source has been used. One of them is laser light source with having some disadvantages including powerful irradiation, being highly expensive compared to alternatives, and requiring an optical system that widens the beam of laser in order to be effective in a large area. As a non-laser source, conventional lamps lead to overheating of the cell during photo illumination by its high irradiance capacities. In addition to these light sources with limitations, light-emitting diodes (LEDs) have been also used in photodynamic

therapy application as an appropriate source due to being safe, irradiation features on large areas, wide emission wavelength range, and thermally being non-destructive (42, 43).

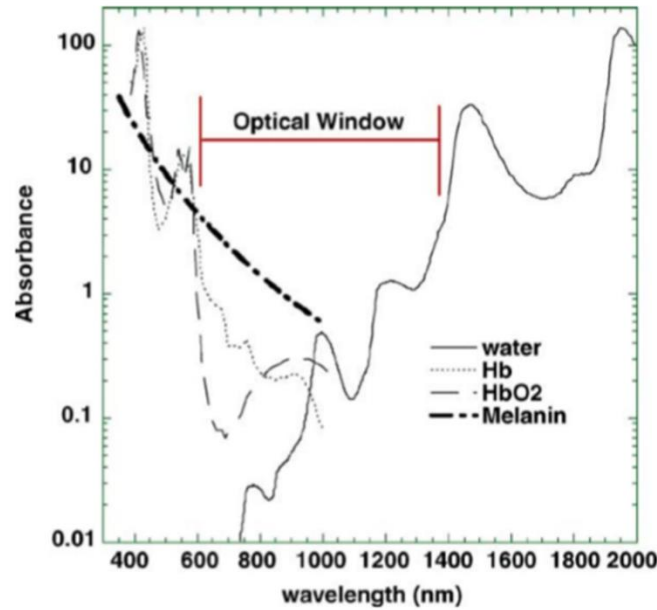


Figure 2 Optical window in tissue. In tissue, water, de-oxy/oxyhemoglobin (Hb/HbO₂), cytochromes and melanin are the most important chromophores, and their absorbance spectrums describe the optical window for photodynamic therapy.

Reference: Reprinted with permission (license number, 4724840999158) from (Castano AP, Demidova TN, Hamblin MR. Mechanisms in photodynamic therapy: Part one - Photosensitizers, photochemistry and cellular localization. *Photodiagnosis Photodyn Ther.* 2004; 1(4): 279–93.)

2.5.3. Oxygen

The role of molecular oxygen in photodynamic therapy is absolute, the oxygen concentration is one of the key factors that affect photodynamic therapy efficiency. However, it is one of the limiting factors. Hypoxia through the rapid proliferation of cancer cells, further vascular damage, and ROS production by PDT limit efficiency of PDT on solid tumors (44).

Peroxisome and metabolic activities of cancer cells make them produce a higher amount of ROS compared to the non-cancerous cell. Among ROS produced by cancer cells, hydrogen peroxide is predominantly more abundant. Decomposition capacity of hydrogen peroxide to molecular oxygen by Fenton reaction enhances PDT efficiency by increasing oxygen concentration in the presence of metal ions (44, 45). Additionally, hydroxyl radicals can trigger cancer cell apoptosis by oxidizing and damaging organelles. Singlet oxygen has a short lifetime(<40ns) with low diffusion rate(20nm) limits the area effected by PDT, therefore non-cancerous cells where the photosensitizers are cleaned up after a time scale are protected from PDT induced damage (46).

26. Mechanism of PDT

After activation through a light of specific wavelengths, PS pass from ground energy state to triplet energy state that leads to two types of photochemical response in nearby molecules, mostly molecular oxygen in PDT. Photo physical activation of ground-state oxygen takes place in two different reactions (43, 47). During type-I reaction, electrons or photons transfer to molecular oxygen to reactive oxygen formation, however in type-II reaction, rather than the electron, energy transfer takes place. Electron transfer by type I reaction results in reactive oxygen species, superoxide anions formation. Due to its short lifetime of superoxide anion in biological systems, at the end of the reaction hydrogen peroxide is formed (5, 47).

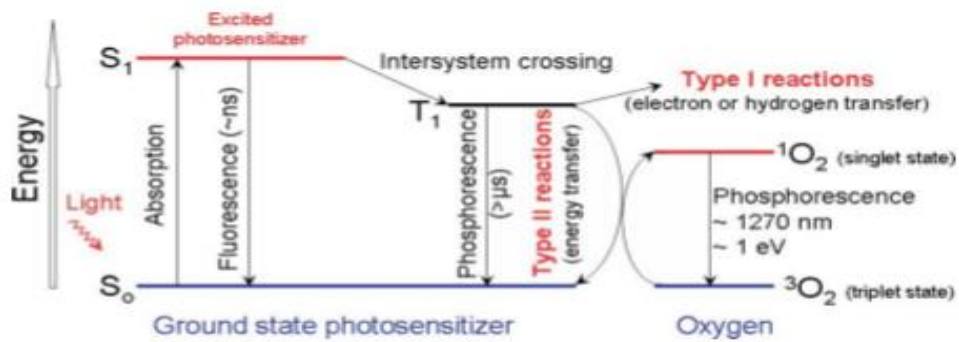


Figure 3 Photophysical changes of photosensitizer agent shown by Jablonski diagram.

Reference: Reprinted with permission (license number, 4724860651423) from (Agostinis P, Berg K, Cengel KA, Foster TH, Girotti AW, Gollnick SO, et al. Photodynamic therapy of cancer: An update. CA Cancer J Clin. 2011; 61(4): 250–281.)

The damage by hydrogen peroxide is not limited to cellular component due to its capacity to diffusion through the membrane. Further, the higher concentration of hydrogen peroxide causes it to react with superoxide anions and the formation of hydroxyl radicals that can also be formed by Fenton reaction in presence of metal ions (5, 43). On the other hand, Energy transfer by type 2 reaction end up with very reactive singlet oxygen formation from molecular ground state oxygen. Both reactions can take place together following PDT, however, type two reaction takes place predominantly (43, 49). The damage by hydrogen peroxide is not limited to cellular component due to its capacity to diffusion through the membrane. Further, the higher concentration of hydrogen peroxide causes it to react with superoxide anions and the formation of hydroxyl radicals that can also be formed by Fenton reaction in the presence of metal ions (5).

Symbols of Figure 6 are H_2O_2 , hydrogen peroxide; $\text{O}_2(1\Delta\text{g})$ $\text{O}_2(1\Delta\text{g})$, singlet oxygen (excited state); $\text{O}_2(3\Sigma\text{-g})$ $\text{O}_2(3\Sigma\text{g-})$, triplet oxygen (ground state); $\text{O}^{\cdot-}$ $2\text{O}_2^{\cdot-}$, superoxide anion; OH^{\cdot} OH^{\cdot} , hydroxyl radical; SOD, superoxide dismutase; X^- $+$ X^- $+$ X^- $+$, anion/cation species; $\text{X}\cdot$ $\text{X}\cdot$, radical species (43).

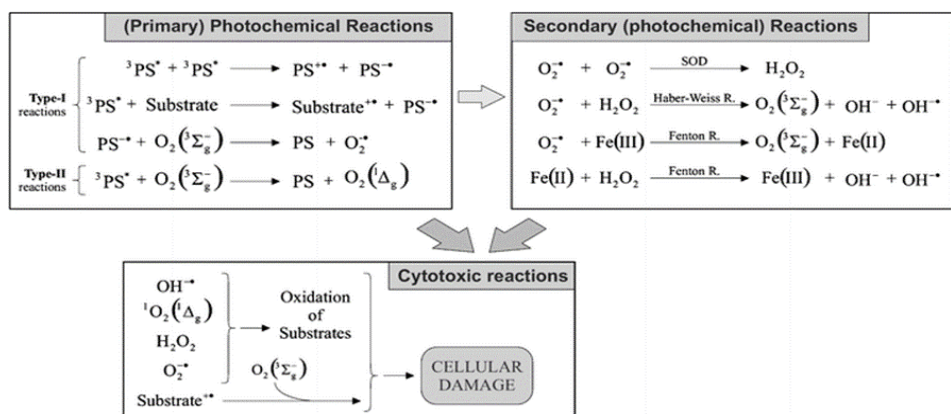


Figure 4 Schematic represent of photochemical reactions through PDT in order to cause reactive oxygen species formation and cellular damage.

Reference: Reprinted with permission from (Plaetzer K, Krammer B, Berlanda J, Berr F, Kiesslich T. Photophysics and photochemistry of photodynamic therapy: Fundamental aspects. *Lasers Med Sci.* 2009; 24(2): 259–68.)

27. Cell Death Mechanisms Triggered by PDT: Apoptosis or Necrosis

Cell death following photo irradiation in photodynamic therapy takes place either necrosis or apoptosis due to some factors that are light dose, subcellular localization of photosensitizer, and cell type (11). Normally, lower light doses trigger apoptotic cell death while higher doses cause more necrotic cell death as a result of that apoptosis-related enzymes and components such as caspases can be inactivated by high doses PDT (50). After PDT, 70 percent or less cell death is a result of apoptosis where 99 percent of cell death generally occurs due to necrosis (51).

28. Subcellular Localization of Photosensitizer

Subcellular localization photosensitizer is one of the significant factors that determine the localization of primary cellular damage, type of cell death whether apoptotic or necrotic and rescue response including the changes in gene and protein expression levels (6).

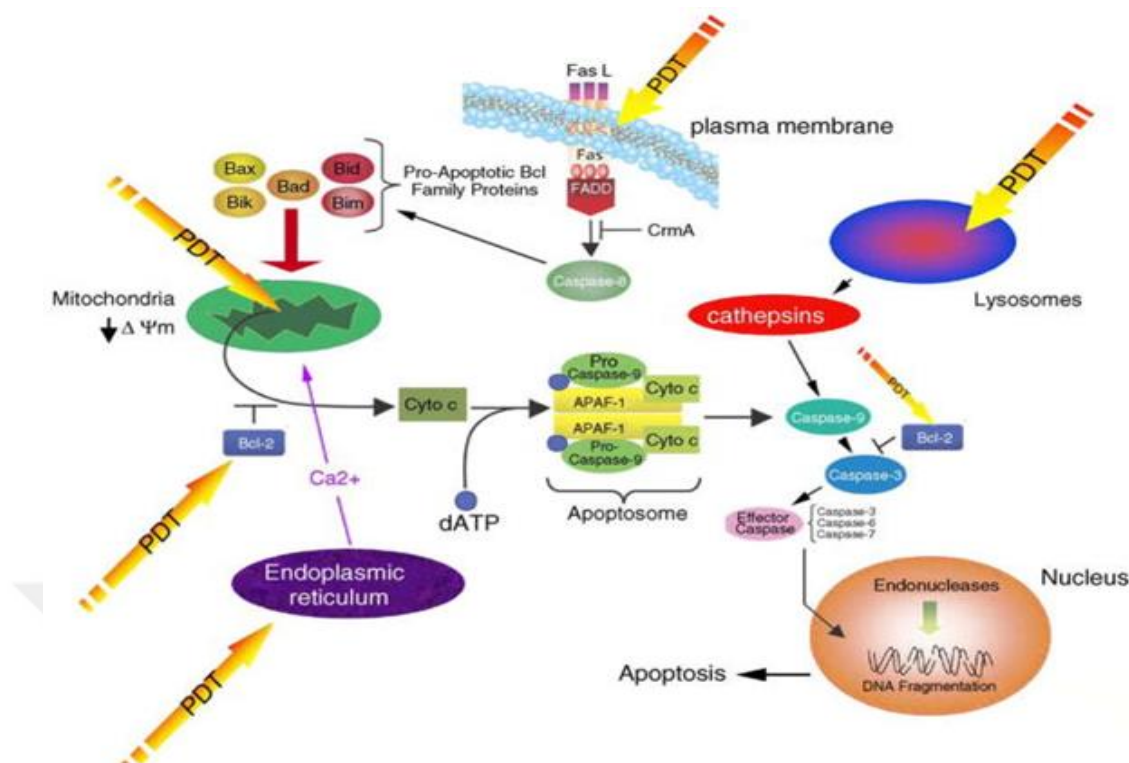


Figure 5 Cellular signaling cascade triggered through ROS generation following PDT, leads to programmed cell death depend on subcellular localization of PS.

Reference: Reprinted with permission (lisence number, 4724850332368) from (Castano AP, Demidova TN, Hamblin MR. Mechanisms in photodynamic therapy: Part two - Cellular signaling, cell metabolism and modes of cell death. Photodiagnosis and Photodynamic Therapy. 2005; 2(1): 1–23.)

PS have a cationic charge as well as hydrophobic residues can localize mitochondria in the cell through mitochondrial membrane potential and membrane lipid bilayer (20, 54). Mitochondrial localization of photosensitizer during photo illumination can trigger such signaling pathways that are responsible for programmed cell death (55). Firstly, PDT with this subcellular localization causes releasing of pro-apoptotic proteins, such as cytochrome c and apoptosis-inducing factor from mitochondria into the cytosol, also rapid membrane potential loss (56, 57). Cytochrome c release from mitochondria induces caspase 3 activity which is the key compartment in triggering the apoptotic pathway. Plasma membrane localization of PS can trigger necrotic cell death by causing integrity loss of plasma membrane, and depletion of intracellular ATP (58).

3. MATERIALS AND METHODS

3.1. Materials

List of cell lines used in this study is given in Table 2.

Table 2 List of cell lines

Cell line	Cat No, Brand, Country
A253, Human salivary gland epidermoid carcinoma	HTB-41, ATCC, USA
FaDu, Human pharynx squamous cell carcinoma	HTB-43, ATCC, USA
HT29, Human colon colorectal adenocarcinoma	HTB-38, ATCC, USA
T47D, Human breast infiltrating ductal carcinoma	HTB-133, ATCC, USA
L929, Mouse connective tissue fibroblast	CCL-1, ATCC, USA

List of equipment used in this study is given in Table 3.

Table 3 List of equipment

Name of Equipment	Cat No, Brand, Country
Class II Biological Safety Cabinets	AC2-4L1, ESCO, Southeast Asia
Vacuum glass	BORO 3.3, Isolab, Germany
Inverted light microscope	CKX41, Olympus, USA
Inbubator (for mouse cell lines)	BINDER, USA
Incubator (for human cell lines)	Sanyo, Japan
Imaging reader	Cytation 5, BioTek, USA
Flow Cytometer	Novocyte, Acea, USA
Water bath	Benchmark Scientific, USA
Heating and Cooling Thermostat	Ecoline RE206, Lauda, USA
Smart Personal Centrifuge	SPROUT, Heathrow Scientific, USA
Personal Centrifuge	M08, ThermoFisher, USA
Automated cell counter	LunaII, ThermoFisher, USA
Pipette	Easypet, Eppendorf, Germany

Pipette (10, 100, 200, 1000 uL)	Research Plus, Eppendorf, Germany
Centrifuge	5702R, Eppendorf, Germany
Freezer (+4)	Bosch, Germany
Freezer (-20)	Bosch, Germany
Freezer (-80)	U570, New Brunswick Scientific, USA
LED array	CELED 96, CETONI, Germany
LED controller	CETONI, Germany
Cryogenic vial	430488, Corning, USA
Liquid nitrogen tank	
Lucetta Luminometer	Lonza, Switzerland
XCELLigence	Acea, USA
E-plate (16 well)	Acea, USA

List of buffer, solution and kits used in this study is given in Table 4.

Table 4 List of Buffer, Solution, and Kits

Name of Buffer, Solution and Kits	Cat No, Brand, Country
McCoy5A Modified medium	30-2007, Gibco, USA
Minimum Essential Medium Eagle with jocklic modification	M0518, Sigma, USA
RPMI 1640 medium	61870044, Gibco, USA
Bovine insulin	Humulin N, Lilly
Heat-inactivated fetal bovine serum	16140071, Gibco, USA
Penicillin-streptomycin	15140122, Gibco, USA
Sodium bicarbonate	25080094, Gibco, USA
DPBS	14190250, Gibco, USA
Trypsin-EDTA 0,25%	25200056, Gibco, USA
alamarBlue cell viability reagent	DAL1025, Gibco, USA
2',7'-Dichlorofluorescein diacetate	D6883, Sigma Aldrich, USA
HBSS	14175129, Gibco, USA
WST-1	11 644 807 001, Roche, USA
DMSO cell culture grade	4-X, ATCC, USA
UltraPure™ DNase/RNase-Free Distilled Water	10977035, ThermoFisher, USA

3.1.1. Light-emitting diode system

The basis of photodynamic therapy is the stimulation of photosensitizer molecules by light at certain wavelengths (5). To achieve this, a light source is needed which can provide the desired wavelength in a controlled manner and is compatible with the plates used in cell culture. As a stimulating light source, CETONI 96 ceLED 96 LEDs were used. ceLED 96 is a standard LED array. Optimized for irradiation of all wells of 96 well plates at desired wavelengths (624-755 nm) and in the desired configuration. There is an external liquid cooling system to facilitate excessive power density in a small space. The ceLED Led Array is controlled by the QmixElements software, which enables simultaneous control of multiple irradiation zones. The software consists of a system kernel that provides basic functions and services, such as an application window, event log, or toolbar. Flexible grouping of multiple LED channels with irradiation groups allows simultaneous control of all channels of a group, rapid activation, deactivation of all LEDs, and simultaneous control of multiple LED arrays.

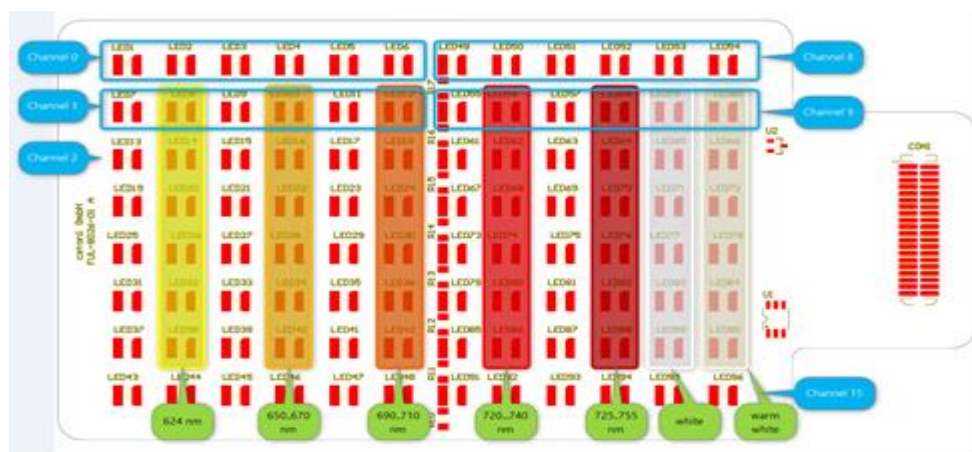


Figure 6 LED configuration of CETONI 96 led array.

3.2. Methods

3.2.1. Phthalocyanine molecules

Nine water-soluble cationic tetra-substituted symmetric phthalocyanines (47-52) were obtained from the Chemistry Department of Istanbul Technical University. They were suspended in RPMI 1640 medium (Gibco, Cat No 61870044) as the final concentration is 10 mg/ml. Structures, molecular weights (Mw), and UV-Vis spectrums of the Pc molecules used in the thesis was listed in Table 5, Table 6, and Table 7.

Table 5 List of EH Series Phthalocyanines

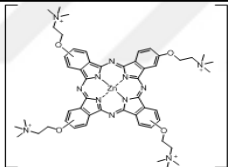
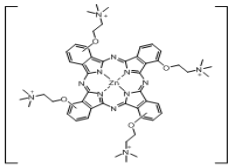
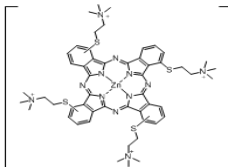
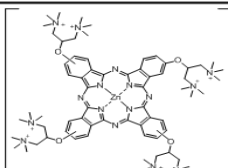
Pc Code	Molecular Structure	Mw	UV-Vis (nm)
EH1		1494,16 g/mol	In water: 340, 636, 670 nm
EH2		1494,16 g/mol	In water: 327, 653, 694 nm
EH3		1558,41 g/mol	In water: 329, 651, 693 nm
EH4		2290,30 g/mol	In water: 340, 633, 677 nm

Table 6 List of HQ Series Phthalocyanines

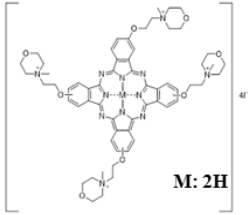
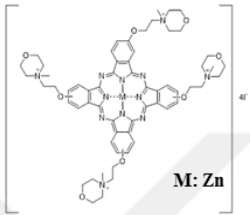
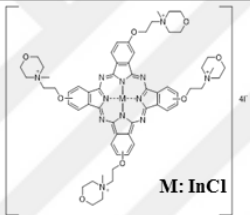
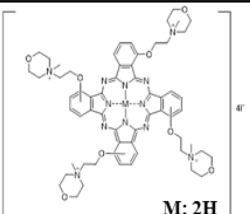
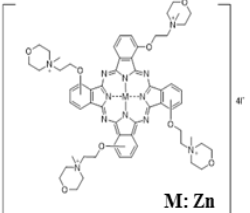
Pc Code	Molecular Structure	Mw	UV-Vis (nm)
HQH2Pc	 M: 2H	1598,95 g/mol	In water: 341, 623 nm
HQZnPc	 M: Zn	1662,31 g/mol	In water: 345, 634, 655 nm
HQInPc	 M: InCl	1747,20 g/mol	In water: 346, 650 nm

Table 7 List of SQ Series Phthalocyanines

Pc Code	Molecular Structure	Mw	UV-Vis (nm)
SQH2Pc	 M: 2H	1598,95 g/mol	In water: 314, 700 nm
SQZnPc	 M: Zn	1662,31 g/mol	In water: 320, 701 nm

3.2.2. Cell culture

3.2.2.1. Culture condition of cell lines

Cells that were used in this study were purchased from ATCC. A253 (ATCC, HTB-41), human submaxillary salivary gland epidermoid carcinoma cells were cultured in McCoy's 5a medium modified (Gibco, Cat No 30-2007) supplemented with final concentration 10% heat-inactivated fetal bovine serum (Gibco, Cat No 16140071) and 1% penicillin (10,000 Units/ml) - streptomycin (10,000 Units/ml) (Gibco, Cat No 15140122). FaDu (ATCC, HTB-43), human pharynx squamous cell carcinoma were cultured in Minimum Essential Medium Eagle with jocklic modification (Sigma Aldrich, Cat No M0518) supplemented with final concentration 2.0 g/L sodium bicarbonate (Gibco, Cat No 25080094), 10% heat-inactivated fetal bovine serum (Gibco, Cat No 16140071) and 1% penicillin (10,000 Units/ml) - streptomycin (10,000 Units/ml) (Gibco, Cat No 15140122). HT29 (ATCC, HTB-38), human colon colorectal adenocarcinoma cells cultured in McCoy's 5a Medium Modified (Gibco, Cat No 30-2007) supplemented with final concentration 10% heat-inactivated fetal bovine serum (Gibco, Cat No 16140071) and 1% penicillin (10,000 Units/ml) - streptomycin (10,000 Units/ml) (Gibco, Cat No 15140122). T47D (ATCC, HTB-133), human mammary gland ductal carcinoma cell were cultured in RPMI 1640 medium (Gibco, Cat No 61870044) supplemented with final concentration 0.2 Units/ml bovine insulin (Lilly, Cat No Humulin N), 10% heat-inactivated fetal bovine serum (Gibco, Cat No 16140071) and 1% penicillin (10,000 Units/ml) - streptomycin (10,000 Units/ml) (Gibco, Cat No 15140122). L929 (ATCC, CCL-1) mouse subcutaneous connective tissue fibroblast cells were cultured in Minimum Essential Medium Eagle with alpha modification supplemented with final concentration 10% heat-inactivated fetal bovine serum (Gibco, Cat No 16140071) and 1% penicillin-streptomycin (Gibco, Cat No 15140122).

3.2.2.2. Cell cryopreservation

The cell stocks were kept inside liquid nitrogen tank. Cells were detached from the flask through incubation with 0.25% trypsin-EDTA for around 5 minutes at 37°C. Then, trypsin was neutralized with 3 times more amount of serum-containing complete medium and centrifuged at 1300 rpm for 5 minutes to get rid of waste components. After discarding the supernatant, the cell pellet was suspended with cryopreservation media, and cell aliquots was prepared in Corning cryogenic vial with O-ring. The vials were placed into Mr. Frost that provides decreasing temperature 1°C per minutes and stored at -80 °C for min overnight max a week, and the vials were transferred into liquid nitrogen tank. Cryopreservation media for each cell line was 95% complete media with 5% DMSO (cell culture grade, ATCC).

3.2.2.3. Continuous culture of cell lines

Cell passage was carried out two to three times per week, considering their population doubling time. Firstly, the serum-containing medium was removed by washing with DPBS (Gibco, Cat No 14190250). Cells were detached from the flask through incubation with 0.25% trypsin-EDTA (Gibco, Cat No 25200056) for around 5 minutes at 37°C. Then, trypsin was neutralized with three times more amount of serum-containing complete medium and centrifuged at 1300 rpm for 5 minutes to get rid of waste components. After discarding the supernatant, the cell pellet was suspended with complete medium and seeded appropriate aliquots in new cell culture flasks.

During cell culture studies, cell counting was carried by trypan blue dye which is not cell permeable and could not pass from the membrane of healthy cells while can stain dead cells. Therefore, living cells appears white, and dead cells takes the color of

the dye, blue. Counting was performed using automated cell counting system, Luna II that also demonstrates percent viability.

3.2.2.4. Determination of population doubling time

The population doubling time of the cell lines was determined by XCELLigence equipment. The cells were detached from cell culture flask by 0.25% trypsin and centrifuged at 1300 rpm for 5 min when cell confluence around 70-80%. With cell viability higher than 90%, cells were suspended in their complete media as final concentration 5×10^4 cells/ml. On the other hand, complete media of each cell lines without cells was placed into the wells of E-plates to measure blanks. After blanking, the cells were seeded into the wells and the plates were placed on the XCELLigence equipment. The program was started, and the data was collected for 125 hours with intervals of 15 minutes.

The xCELLigence® RTCA device uses non-invasive electrical impedance monitoring to measure cell proliferation and morphology change in an unlabeled, real-time manner. The instrument is placed in a standard CO₂ cell culture incubator and fed and controlled by a cable connected to the control unit located outside the incubator. Real-time cell analysis (RTCA) software includes real-time data display and analysis functions and allows real-time interface creation. Real-time cell analysis with xCELLigence® RTCA greatly improves efficiency, bypassing estimates associated with endpoint analyzes.

The operating principle of the device is based on cellular impedance. The practical unit of this cellular impedance assay is a series of gold microelectrodes fused to the well base of a microtiter plate. When immersed in an electrically conductive solution, an electric capacity is applied alongside those electrodes, the electrons exit the negative terminal, pass via the solution, and then collect on the positive terminal, thereby

completing the circuit. The gold microelectrode biosensors inside the wells of ACEA's digital microtiter plates (E-Plate®) cover 70-80% of the surface area. The electrodes in each well of the E-Plate are related to the cords forming a sequence of interdigitates. This arrangement permits for simultaneous monitoring of populations of cells, thereby providing exquisite sensitivity for the number of cells introduced to the plate, size/morphology of cells, and cell-substrate binding quality

3.2.2.5. Mycoplasma detection

In cell culture studies, mycoplasma contamination disrupts the physiology and metabolism of the cells and negatively affects the efficiency and results of the researches. All the cell lines were periodically tested for mycoplasma by MycoAlert PLUSTRM kit from Lonza using the Lucetta Luminometer that is a single tube luminometer developed for the detection of bioluminescence and chemiluminescence.

Firstly, 2 ml of the cell culture samples to be tested were centrifuged at 200 xg for 5 min. After centrifugation, 100 µl of the supernatant was transferred to the luminometer (Lucetta) tube. 100 µl of MycoAlert PLUSTRM reagent was added to each sample, and incubated for 5 minutes. At the end of the period, the tubes were placed in the luminometer reader and the program was started (Reading A). Then 100 µl of MycoAlert TM PLUS substrate was added and incubated for 10 minutes. The program was started by placing the cuvette in the luminometer reader (Reading B). Ratio of the readings ($\text{Rate} = \text{Reading B} / \text{Reading A}$) was taken to detect mycoplasma.

3.2.3. Cellular uptake of Pc

Phthalocyanines are self-fluorescent molecules, and this feature allows them to be detected through the specific filters of flow cytometry without any need for extra labeling when binds to a cell. Therefore, cellular uptake of different Pc molecules was

evaluated by flow cytometry analysis. Cells were detached from cell culture plate by trypsinization, then suspended in DPBS as final cell concentration of 10×10^6 cell/ml. Each cell suspension including 100 $\mu\text{g/ml}$ Pc molecules was incubated at room temperature to binding of Pc molecules to the cells. Fluorescence of Pc molecules that binds to the cells was determined through determined cytometer settings as excitation at 637 nm and emission acquired 780/60 nm filter in Acea Novocyte Flow Cytometer.

A laser-based technology, flow cytometry is used to analyze and characterize cells in a fluidic system. Cells in a suspension are separated from each other through hydrodynamic focusing in a fluid stream and pass through lasers in the cytometer system. The lasers provide lights of specific wavelengths that excite fluorochrome on the cell, and this excitation causes light scattering that is detected by photomultiplier tubes. Through the tubes, detected light is amplified and converted to a voltage which can be analyzed digitally. Self-fluorescent features of phthalocyanine molecules make them possible to be detected by flow cytometry analysis without any labeling.

Cancer cell lines, A253, FaDu, HT29, and T47D, were incubated with phthalocyanines, then detection was done under cytometer settings as excitation at 637 nm and emission acquired 780/60 nm filter in Acea Novocyte Flow Cytometer. Firstly, forward and side scatters of all cell population was obtained. From all populations, singlet cells were selected to get rid of excessive fluorescence signaling of double cells and non-binding molecules. A fluorescence signaling histogram was created from the singlet cell population. As a control, untreated cells were used, and Pc containing samples was compared relative to untreated control.

3.2.4. Biocompatibility

To evaluate the biocompatibility of the nine phthalocyanine molecules, dark and photo-irradiated cytotoxicity of the molecules was analyzed on the mouse L929 cell

line. Firstly, dark cytotoxicity studies were carried out. In the biocompatible concentration range of the Pc molecules where control-related cytotoxicity is less than 30%, photo-irradiated cytotoxicity's were evaluated.

L929 cells were detached from cell culture flask by 0.25% trypsin and centrifuged at 1300 rpm for 5 min when cell confluence around 70-80%. With cell viability higher than 90%, cells were suspended in alpha mem media supplemented with 10% FBS and 1% penicillin-streptomycin as final concentration 5×10^4 cells/ml. Into 96 well plates, the cells were seeded (5×10^3 cells/well) and incubated in a 37°C, 5% CO₂ humidified incubator for 24 hours.

For the dark cytotoxicity group, after 24 hours incubation, phthalocyanine molecules in different concentrations (100 µg/mL, 10 µg/mL, 1 µg/mL, 0,1 µg/mL) that were prepared in complete cell culture media were applied onto the cells, and incubated in a 37°C, 5% CO₂ humidified incubator as covered with aluminum foil for 24 hours.

For the photo-irradiated cytotoxicity group, after 24 hours incubation, phthalocyanine molecules in determined concentration according to results of dark cytotoxicity were applied onto the cells and incubated in a 37°C, 5% CO₂ humidified incubator for an hour in order to cellular uptake of Pc molecules. After cellular uptake of Pc molecules, the cells were irradiated through different wavelengths for 5 minutes at 70 mV using Cetoni-LED. As a dark group, cells then were incubated in a 37°C, 5% CO₂ humidified incubator for 24 hours.

Post-24 hours of the treatment, cell viability evaluation was carried out by colorimetric WST-1 assay that is based on the cleavage of tetrazolium salts into formazan dye by mitochondrial dehydrogenases in viable cells. WST-1 solution is diluted 1:10 in complete media, and the media in each well was replaced with a 1:10

WST-1 solution. The cells were incubated to be avoided from light in a 37°C, 5% CO₂ humidified incubator for 3 hours. After incubation, endpoint absorbance of the wells was taken at 450 nm; references 650 nm through Cytation 5 multi-plate reader. Reference values were subtracted from an actual value. As a control, non-treated cells and cells treated with 10% DMSO were used. Percentage values were calculated respected to non-treated cells.

3.2.5. Dark cytotoxicity

In photodynamic therapy, photosensitizer molecules are non-toxic unless they are irradiated with light of specific wavelengths. In order to determine the non-toxic concentration range of phthalocyanine molecules on different cancer cell lines, cytotoxic assay with the nine phthalocyanine molecules and 4 cancer cell lines (A253, FaDu, HT29, and T47D) was set up in dark conditions.

The cells were detached from cell culture flask by 0.25% trypsin and centrifuged at 1300 rpm for 5 min when cell confluence around 70-80%. With cell viability higher than 90%, cells were suspended in their complete media as final concentration 5×10^4 cells/ml. Into 96 well plates, the cells were seeded (5×10^3 cells/well) and incubated in a 37°C, 5% CO₂ humidified incubator for 24 hours.

After 24 hours incubation, phthalocyanine molecules in different concentrations (100 µg/mL, 10 µg/mL, 1 µg/mL, 0,1 µg/mL) that were prepared in complete cell culture media were applied onto the cells, and incubated in a 37°C, 5% CO₂ humidified incubator as covered with aluminum foil for 24 hours.

Post-24 hours of the treatment, cell viability evaluation was carried out by colorimetric WST-1 assay that is based on the cleavage of tetrazolium salts into formazan dye by mitochondrial dehydrogenases in viable cells. WST-1 solution is

diluted 1:10 in complete media, and the media in each well was replaced with a 1:10 WST-1 solution. The cells were incubated to be avoided from light in a 37°C, 5% CO₂ humidified incubator for 3 hours. After incubation, endpoint absorbance of the wells was taken at 450 nm; references 650 nm through Cytation 5 multi-plate reader. Reference values were distracted from an actual value. As a control, non-treated cells and cells treated with 10% DMSO were used. Percentage values were calculated respected to non-treated cells. Respect to the dark cytotoxicity results, the concentration range of the nine phthalocyanine molecules for photodynamic therapy was determined.

3.2.6. Photo-irradiated cytotoxicity

Cells were prepared as mentioned in the dark cytotoxicity section and administered with Pc molecules with the concentration that determined as non-toxic respect to dark cytotoxicity studies. Following the administration of Pc molecules with different concentrations (10 µg/mL, 1 µg/mL), the cells were incubated in a 37°C, 5% CO₂ humidified incubator for an hour in order to cellular uptake of Pc molecules. After cellular uptake of Pc molecules, the cells were irradiated through different wavelengths for 5 minutes at 70 mV using Cetoni-LED. As a dark group, cells then were incubated in a 37°C, 5% CO₂ humidified incubator for 24 hours. As control non-treated cells were used. Beside each photo-irradiated cytotoxicity assay, a dark cytotoxicity experiment was set up.

Post-24 hours of treatment, cytotoxicity evaluation was carried out with WST-1 as in the dark cytotoxicity section. Further, to support the reliability of the WST-1 results, another cytotoxicity assay ends up with resazurin alamarBlue cell viability reagent (Gibco, Cat No DAL1025) that working principle is based on giving a colorimetric response to metabolic reduction of healthy cells and yielding proportional fluorescence relative to the number of cells respiring.

3.2.7. Oxidative stress evaluation

In photodynamic therapy, one of the photo damage processes is triggered through reactive oxygen species formation. In order to carry out ROS formation, the cells were detached from cell culture flask by 0,25% trypsin-EDTA and centrifuged at 1300 rpm for 5 min when cell confluence around 70-80%. With cell viability higher than 90%, cells were suspended in their complete media as the final concentration of 10×10^4 cells/ml. Into 96 well plates, the cells were seeded (10×10^3 cells/well) and incubated in a 37°C, 5% CO₂ humidified incubator for 24 hours. After 24 hours incubation, phthalocyanine molecules in different concentrations (10 µg/mL, 1 µg/mL) that were prepared in complete cell culture media were administrated into the cells. Following treatment with Pc molecules, the photo-irradiated group was irradiated with 2 joules/cm² with different wavelengths using CETONI-LED equipment after 1-hour incubation with Pc molecules. Following irradiation, dark and photo-irradiated groups incubated in a 37°C, 5% CO₂ humidified incubator as covered with aluminum foil for 30 minutes. At the end of the incubation, reactive oxygen species intensity was evaluated using 2', 7'-Dichlorofluorescein diacetate, DCFDA (sigma, D6883). DCFDA is a non-fluorescent cell-permeable probe that undergoes esterase reaction in the presence of reactive oxygen species and yields highly fluorescent 2', 7'-dichlorofluorescein. DCFDA that is used was prepared in ethanol as the final concentration is 20 mM. To carry out the experiment, old medium from treated and control groups were removed. Into the wells, 10 µM DCFDA in HBSS (Gibco, Cat No 14175129) were applied and incubated by avoiding light in a 37°C, 5% CO₂ humidified incubator for 30 minutes. After that, endpoint fluorescent intensity was read where the excitation wavelength is 504 nm and the emission wavelength are 529 nm. As a control to see the system was working, 50 µM H₂O₂ was used.

4. RESULTS

4.1. Determination of Population Doubling Time

Population doubling time of A253, FaDu, HT29, and T47D cell lines was determined using electrical impedance based XCELLigence device. Real time measurement for each cell line was collected for 125 hours with intervals of 15 min. After that, population doubling time was analyzed as shown in Table 8.

Table 8 Population doubling time of A253, FaDu, HT29 and T47D cell lines.

Cell line	Cell number seeded	Population doubling time (hours)
A253	5000 cells/well	13,905±1,189
FaDu	5000 cells/well	9,459±1,250
HT29	5000 cells/well	13,650±0,7432
T47D	5000 cells/well	15,627±3,885

4.2. Mycoplasma Detection

Each cell line was periodically tested for mycoplasma detection by MycoAlert PLUSTM kit from Lonza using the Lucetta Luminometer. Luminesce readings that were taken before (Reading A) and after (Reading B) MycoAlert TM PLUS substrate addition. Mycoplasma contamination was evaluated based on the ratio of the reading, and the results was shown in Table 9.

Table 9 Mycoplasma detection on the cell lines

Cell line	Ratio	Evaluation
A253	0,26	Negative
FaDu	0,43	Negative
HT29	0,16	Negative
T47D	0,38	Negative

ratio of < 1 refers negative for mycoplasma, > 1.2 refers mycoplasma contamination

43. Cellular Uptake of Phthalocyanine Molecules

Cancer cell lines, A253, FaDu, HT29, and T47D, were incubated with phthalocyanines, then detection was done under cytometer settings as excitation at 637 nm and emission acquired 780/60 nm filter in Acea Novocyte Flow Cytometer. A fluorescence signaling histogram was created from the singlet cell population. As a control, untreated cells were used, and Pc containing samples was compared relative to untreated control.

Cellular uptake of the ftalocyanine molecules through the A253 cell line was shown in Figure 7.

Cellular uptake of the ftalocyanine molecules through the FaDu cell line was shown in Figure 8.

Cellular uptake of the ftalocyanine molecules through the HT29 cell line was shown in Figure 9.

Cellular uptake of the ftalocyanine molecules through the T47D cell line was shown in Figure 10.

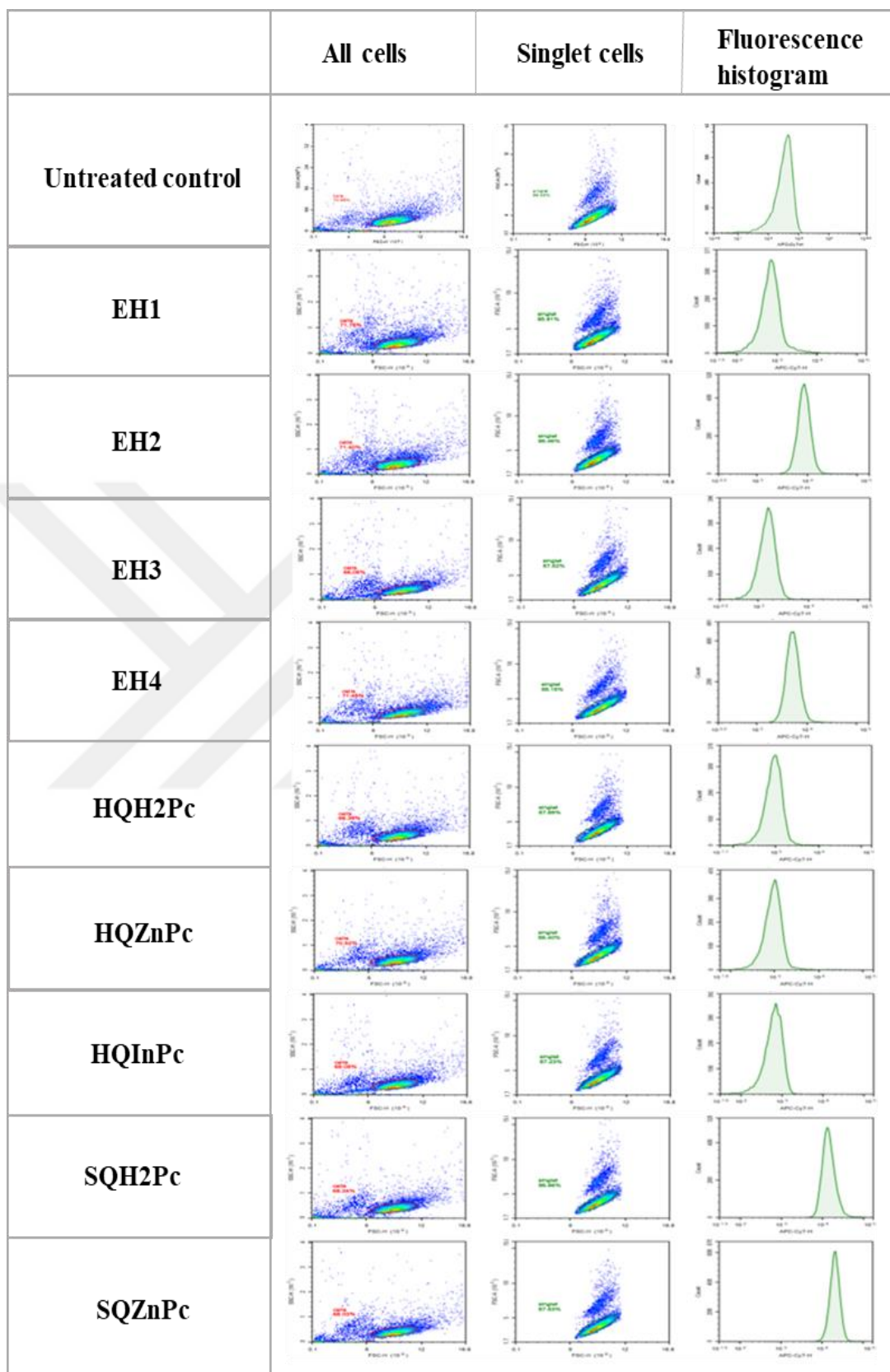


Figure 7 Flow cytometry forward and side scatters, and fluorescence histograms to demonstrate cellular uptake of phthalocyanine molecules through A253 cell line.

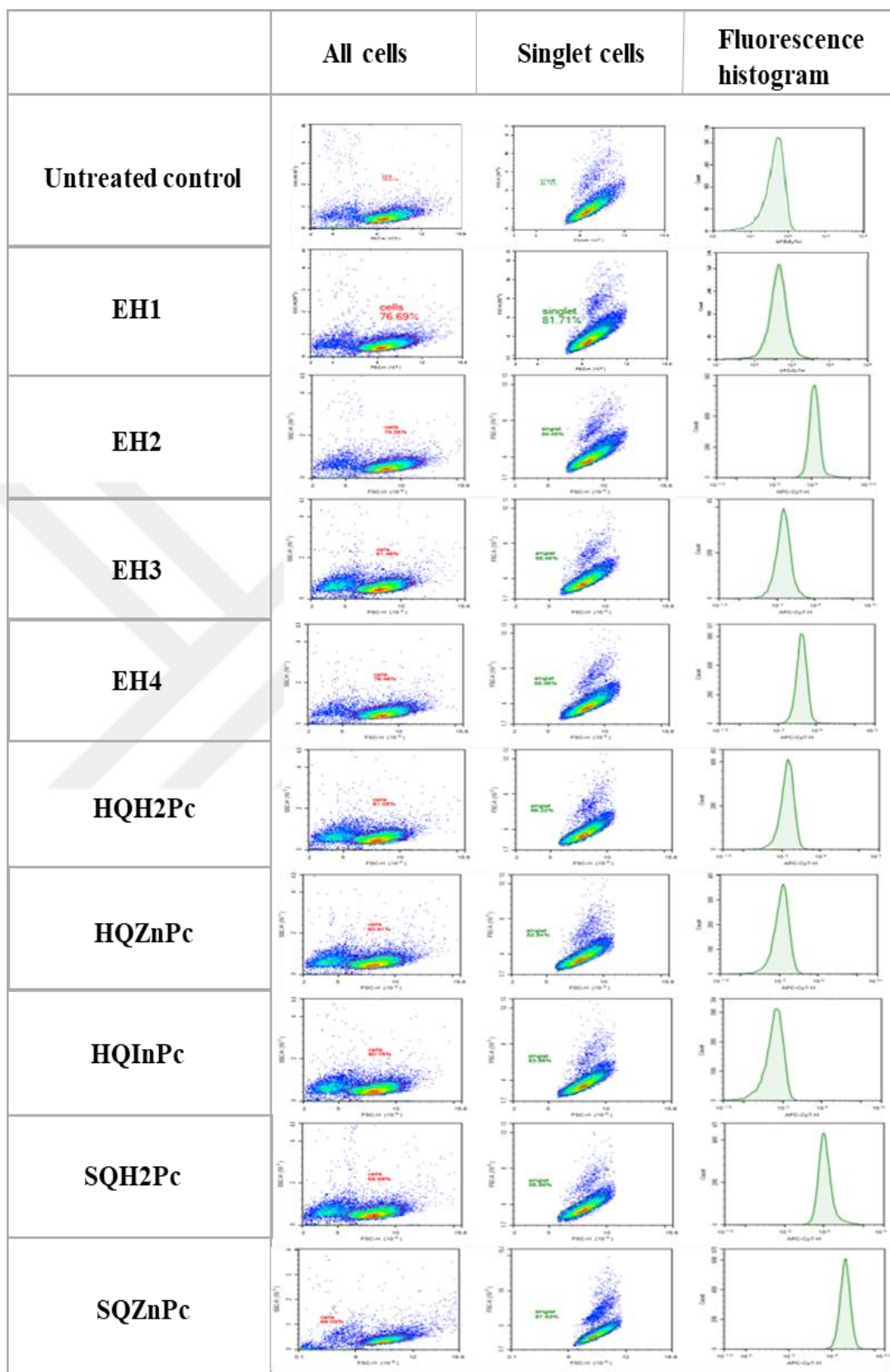


Figure 8 Flow cytometry forward and side scatters, and fluorescence histograms to demonstrate cellular uptake of phthalocyanine molecules through FaDu cell line.

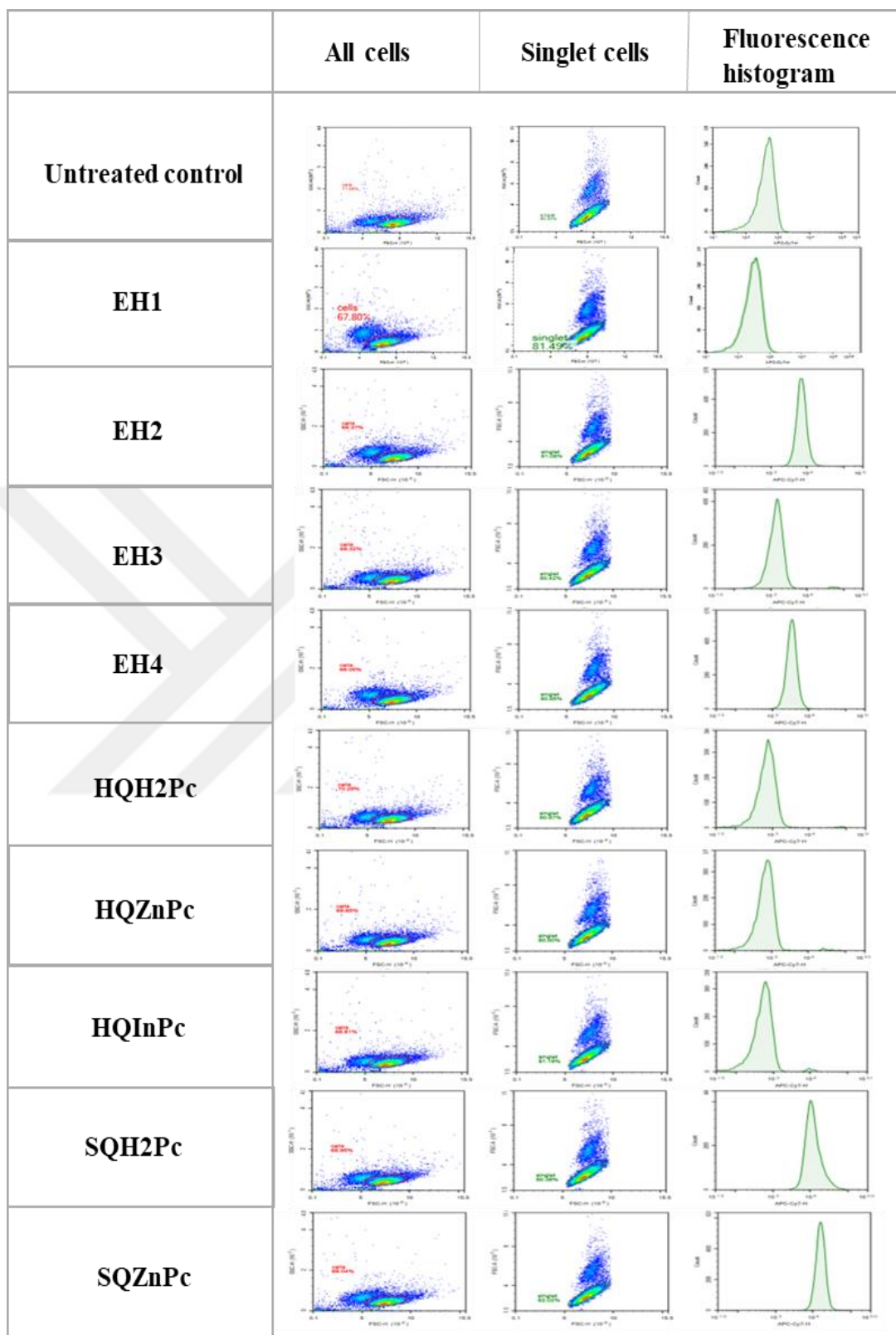


Figure 9 Flow cytometry forward and side scatters, and fluorescence histograms to demonstrate cellular uptake of phthalocyanine molecules through HT29 cell line.

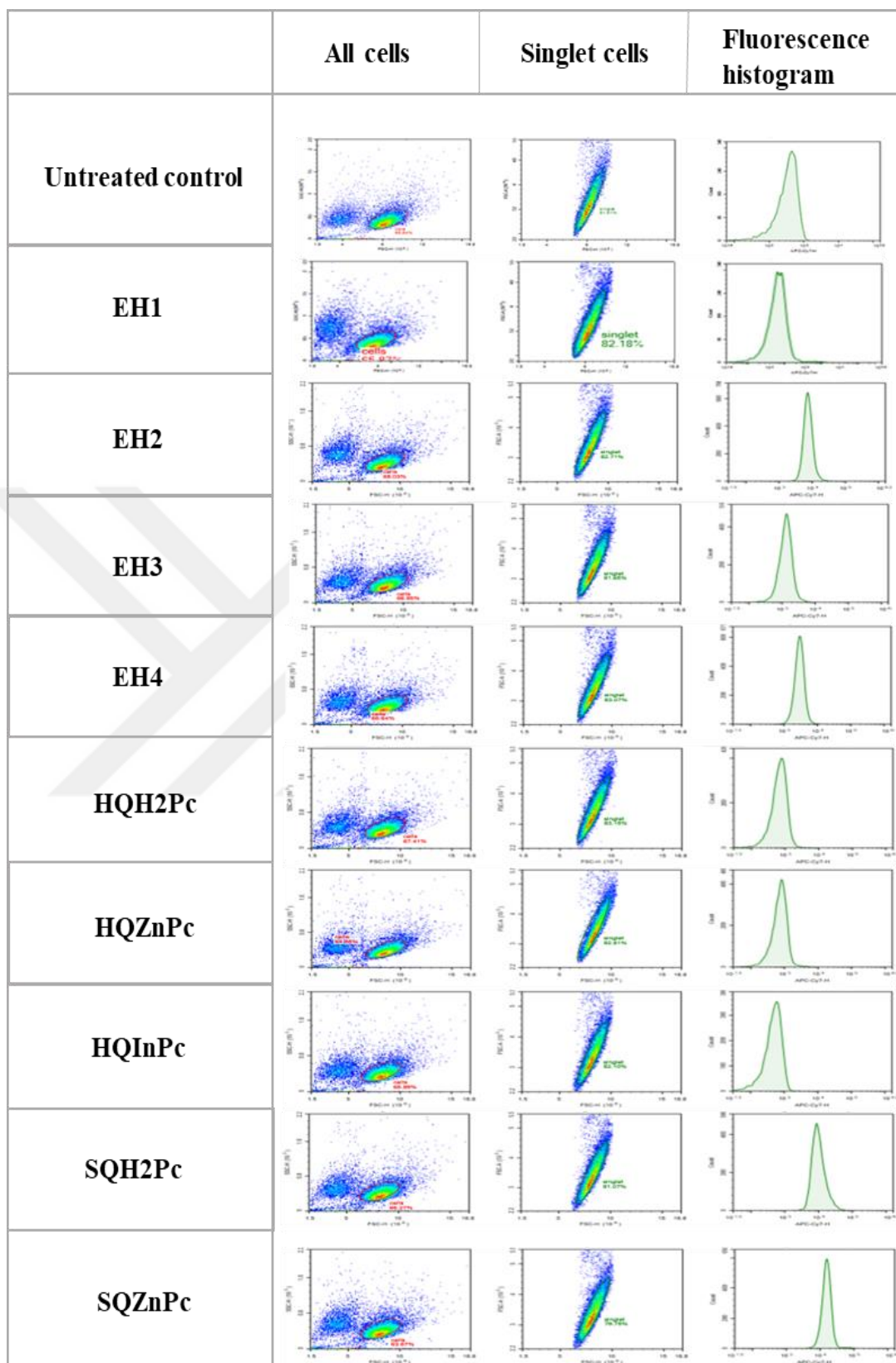


Figure 10 Flow cytometry forward and side scatters, and fluorescence histograms to demonstrate cellular uptake of phthalocyanine molecules through T47D cell line.

Overlaying fluorescence histograms created from the side and forward scatters of singlet cells allows making a comparison between Pc molecules by comparing fluorescence signaling as seen in Figure 11.

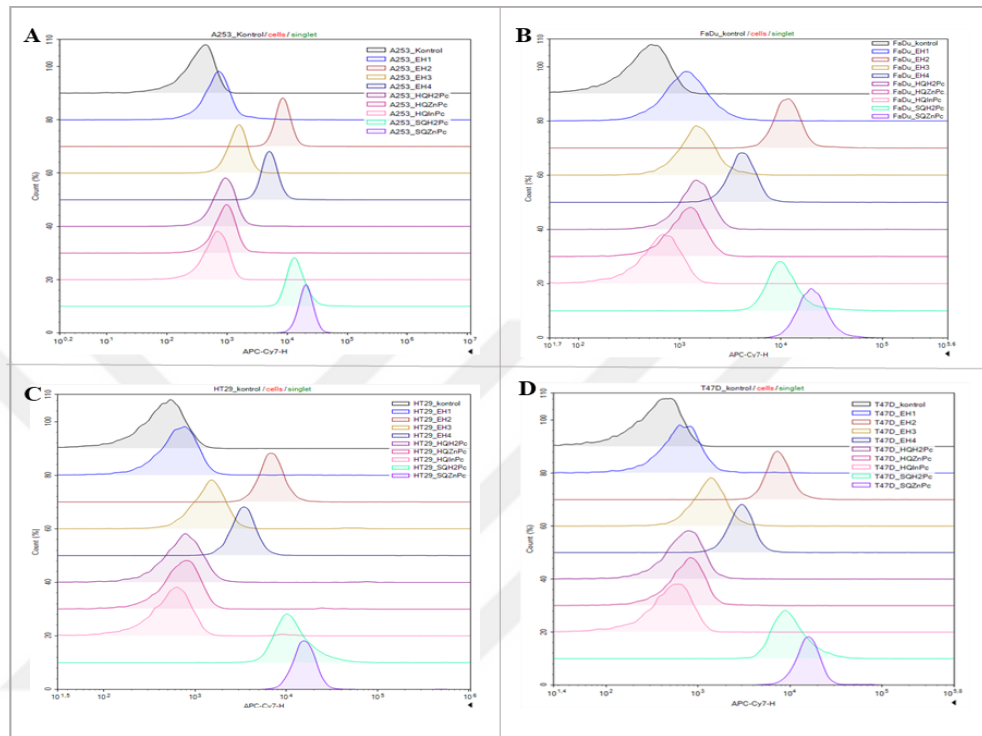


Figure 11 Fluorescence histograms overlays of cell lines to compare cellular uptake of phthalocyanine molecules relative to untreated control and each other. A. A253 B. FaDu C. HT29 D. T47D.

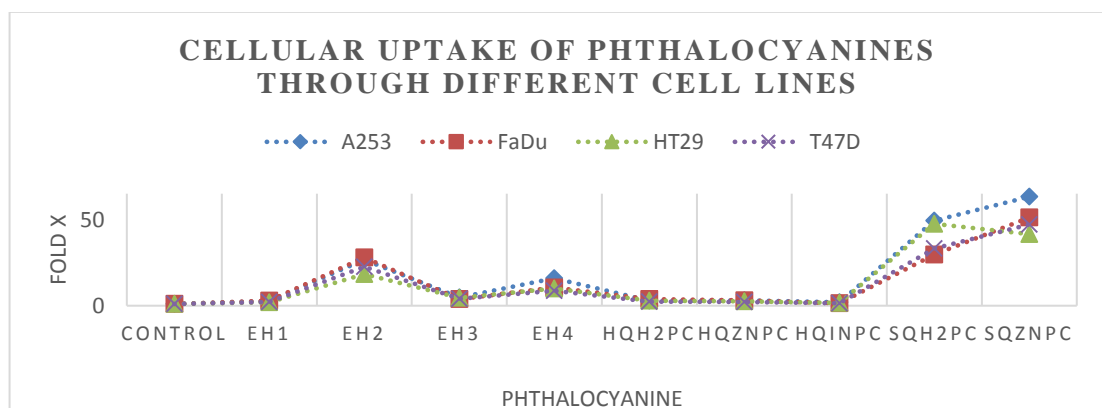


Figure 12 Graph shows cellular uptake of Pc molecules based on how many times the signal was received by flow cytometry compared to the untreated control.

Table 10 How many times Pc molecules was taken by cells relative to untreated control.

	Control	EH1	EH2	EH3	EH4	HQH ₂ Pc	HQZnPc	HQInPc	SQH ₂ Pc	SQZnPc
A253	1	3	27	5	16	3	3	2	49	63
FaDu	1	3	28	4	10	4	3	2	30	51
HT29	1	2	18	5	10	3	3	2	48	42
T47D	1	2	23	4	9	2	2	1	33	47

Following flow cytometry application, overall results demonstrated that SQ group Pcs, SQH₂Pc, and SQZnPc have a higher affinity to each cell line, following EH2 and EH4 Pcs compared to other Pc molecules. Further, it can be said that each nine Pc molecules were taken through each cell lines at least 2 times more than control groups according to obtained fluorescence signals relative to untreated controls.

4.4. Biocompatibility of Phthalocyanine Molecules

To determine the biocompatible concentration range of Pc molecules, different concentrations of the molecules exposed to the mouse L929 cell line firstly in dark conditions for 24 h. As to meet the requirement of ISO standards, the samples that are equal or exceed 70% viability conditions were confirmed as non-toxic. Photodynamic therapy application normally does not cause damage to non-cancerous cells, therefore, at the determined concentration as non-toxic at dark, photodynamic therapy was carried out at different wavelengths that range between 624 and 755 nm with light dose 2 joules/cm². The survival percentage of L929 cells was determined relative to the non-treated control. Values are shown as the mean±SD of three independent experimental repeats.

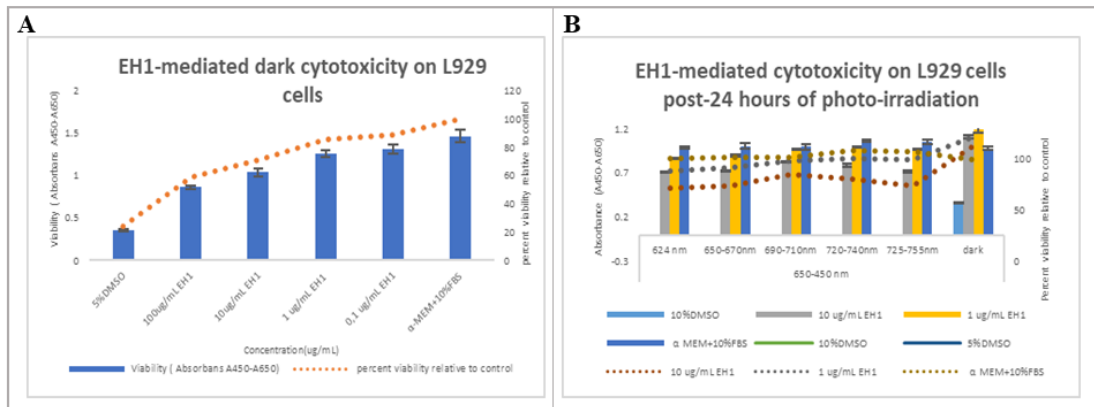


Figure 13 Dose dependent A. dark and B. photo-induced cytotoxicity of EH1 phthalocyanine. Viability was measured by WST-1 assay following 24h of PDT.

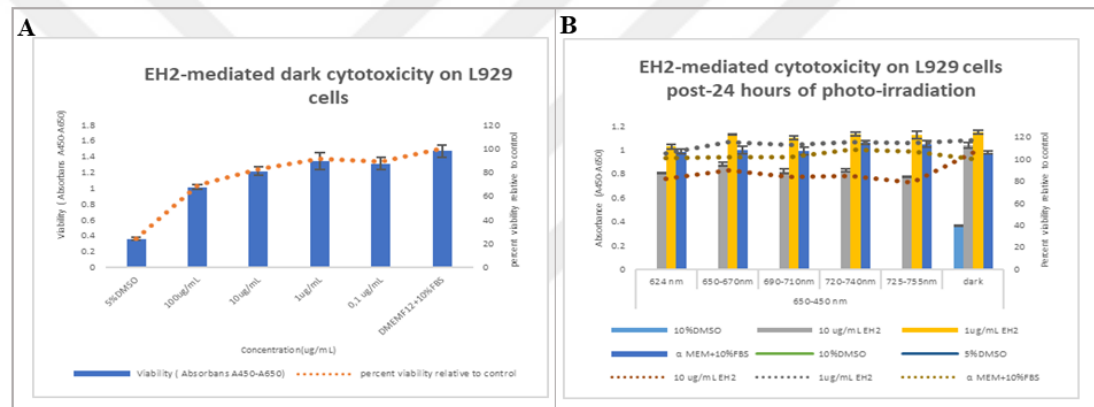


Figure 14 Dose dependent A. dark and B. photo-induced cytotoxicity of EH2 phthalocyanine. Viability was measured by WST-1 assay following 24h of PDT.

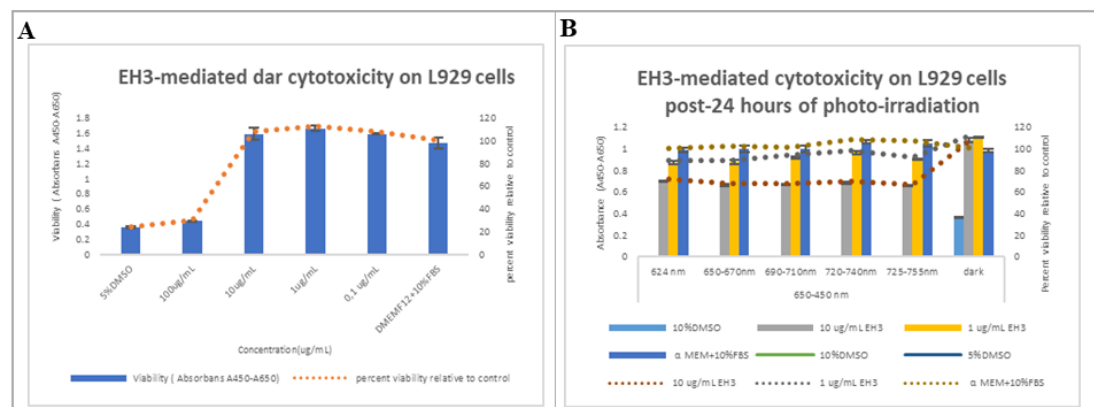


Figure 15 Dose dependent A. dark and B. photo-induced cytotoxicity of EH3 phthalocyanine. Viability was measured by WST-1 assay following 24h of PDT.

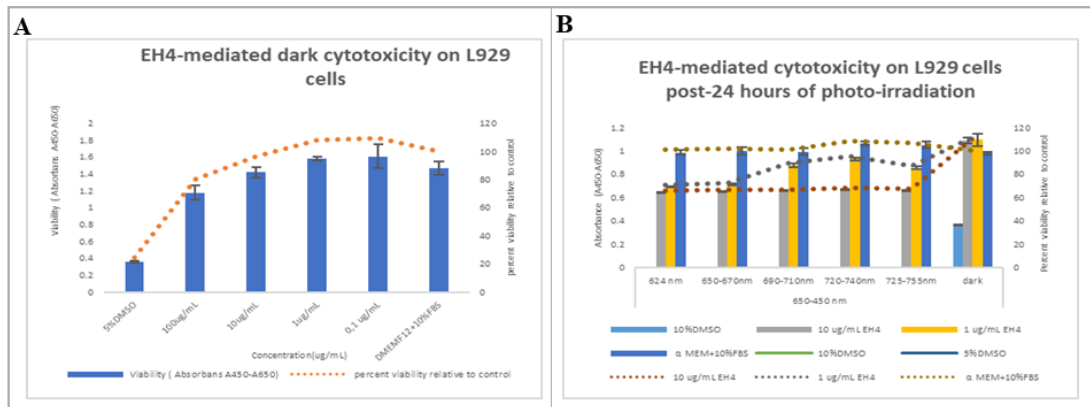


Figure 16 Dose dependent A. dark and B. photo-induced cytotoxicity of EH4 phthalocyanine. Viability was measured by WST-1 assay following 24h of PDT.

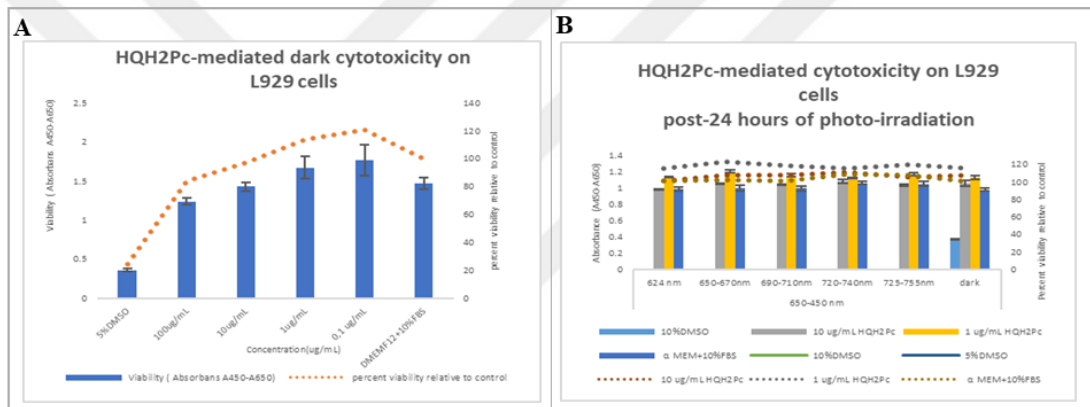


Figure 17 Dose dependent A. dark and B. photo-induced cytotoxicity of HQH₂Pc phthalocyanine. Viability was measured by WST-1 assay following 24h of PDT.

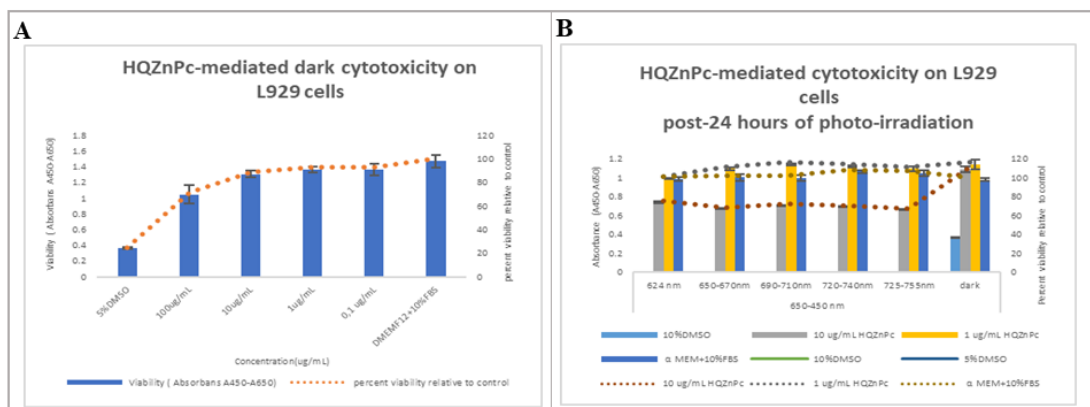


Figure 18 Dose dependent A. dark and B. photo-induced cytotoxicity of HQZnPc phthalocyanine. Viability was measured by WST-1 assay following 24h of PDT.

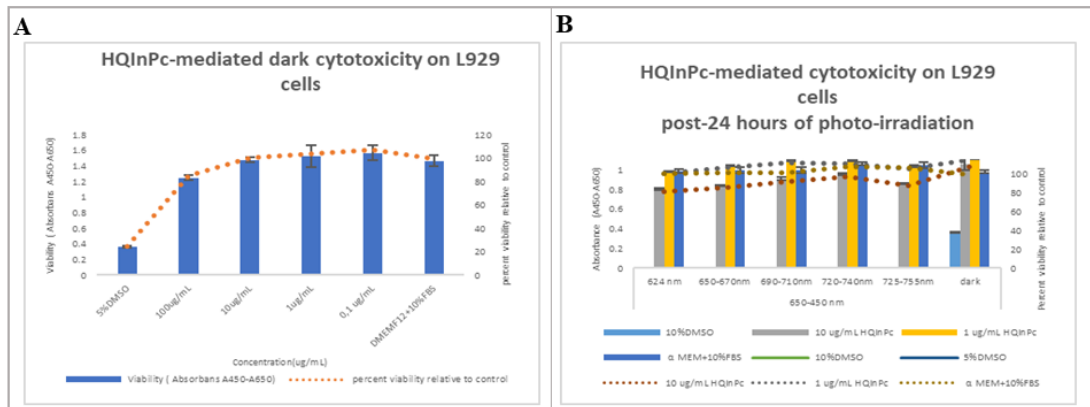


Figure 19 Dose dependent A. dark and B. photo-induced cytotoxicity of HQInPc phthalocyanine. Viability was measured by WST-1 assay following 24h of PDT.

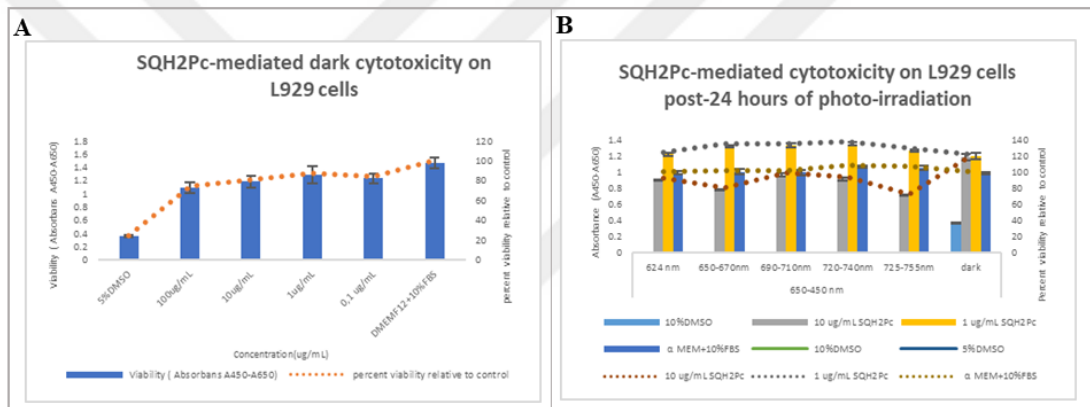


Figure 20 Dose dependent A. dark and B. photo-induced cytotoxicity of SQH2Pc phthalocyanine. Viability was measured by WST-1 assay following 24h of PDT.

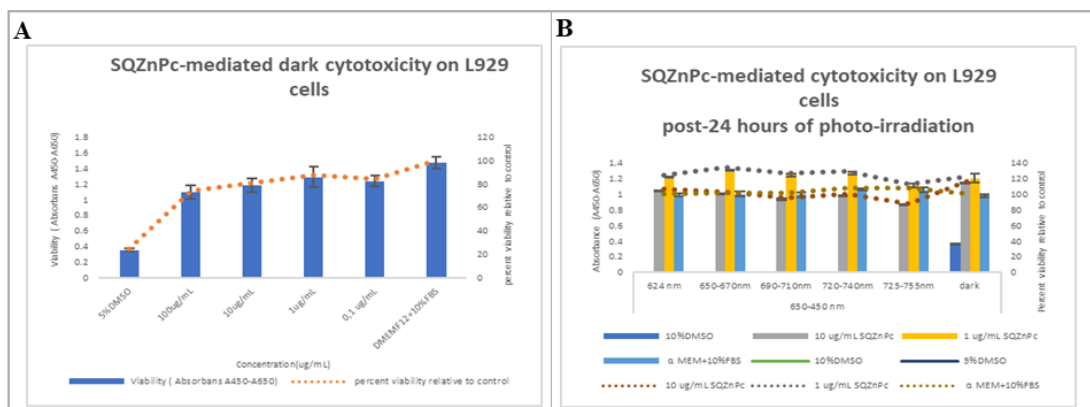


Figure 21 Dose dependent A. dark and B. photo-induced cytotoxicity of SQZnPc phthalocyanine. Viability was measured by WST-1 assay following 24h of PDT.

The phthalocyanine molecules without photo-exposure led to cytotoxicity where concentration is 100 $\mu\text{g/mL}$ or higher. Below this point, two concentrations, 10 $\mu\text{g/ml}$ and 1 $\mu\text{g/ml}$ were determined to be used for PDT. At the light dose of any wavelengths, both high and low doses of each Pc molecules did not cause a reduction in cell viability below 70% relative to the non-treated control. Based on this information, concentration $<10 \mu\text{g/mL}$ of each Pc molecules was selected as photosensitizers to be used for PDT studies for carcinoma cells.

45. Pc-induced Dark Cytotoxicity on Cancer Cell Lines

Photodynamic therapy only has cytotoxic effect when photosensitizer agent is irradiated with a proper wavelength of a light source so that it is not expected a cytotoxic response in dark condition. It should be well defined non-toxic concentration range of the Pc molecules to be used in photo-induced treatments. The survival percentage of the cells was determined relative to the non-treated control. Values are shown as the mean \pm SD of three independent experimental repeats.

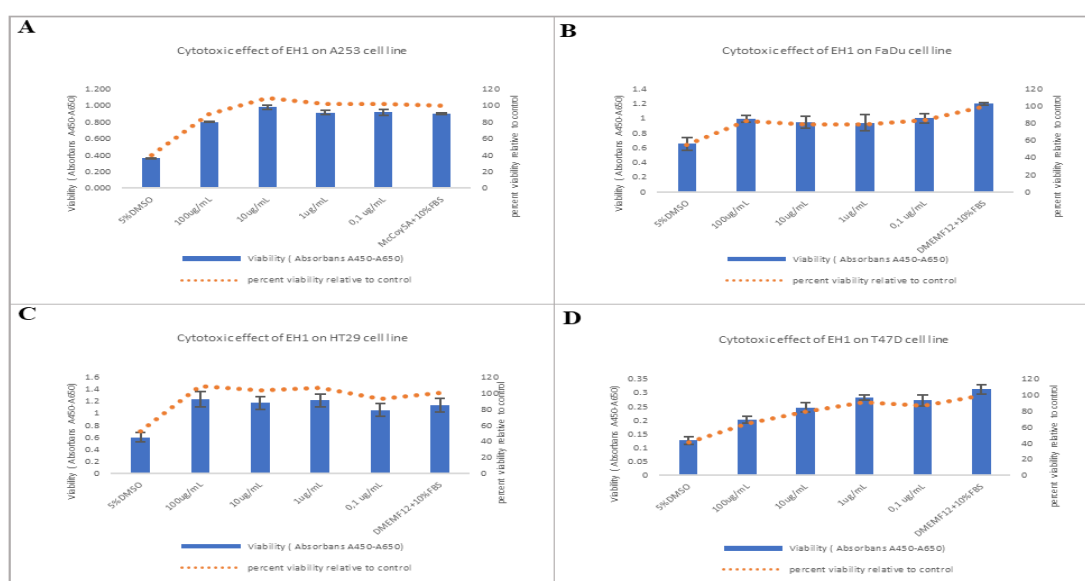


Figure 22 Dose dependent dark cytotoxicity of EH1 phthalocyanine on A. A253 B FaDu C. HT29 D. T47D cell lines. Viability was measured by WST-1 assay following 24h of drug administration.

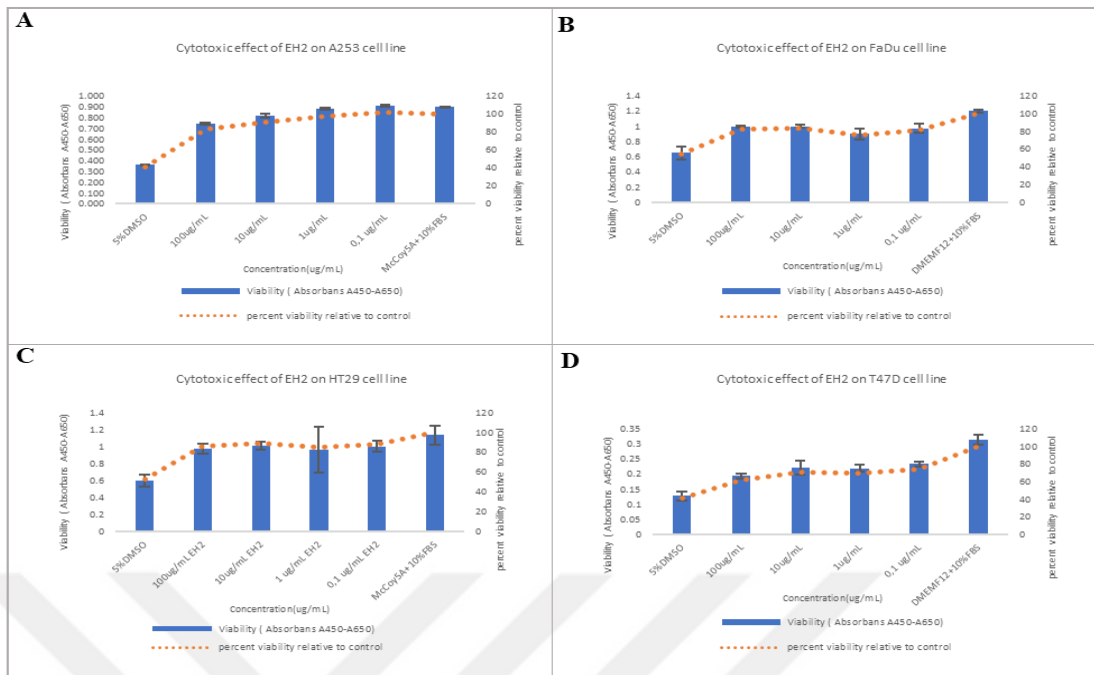


Figure 23 Dose dependent dark cytotoxicity of EH2 phthalocyanine on A. A253 B FaDu C. HT29 D. T47D cell lines. Viability was measured by WST-1 assay following 24h of drug administration.

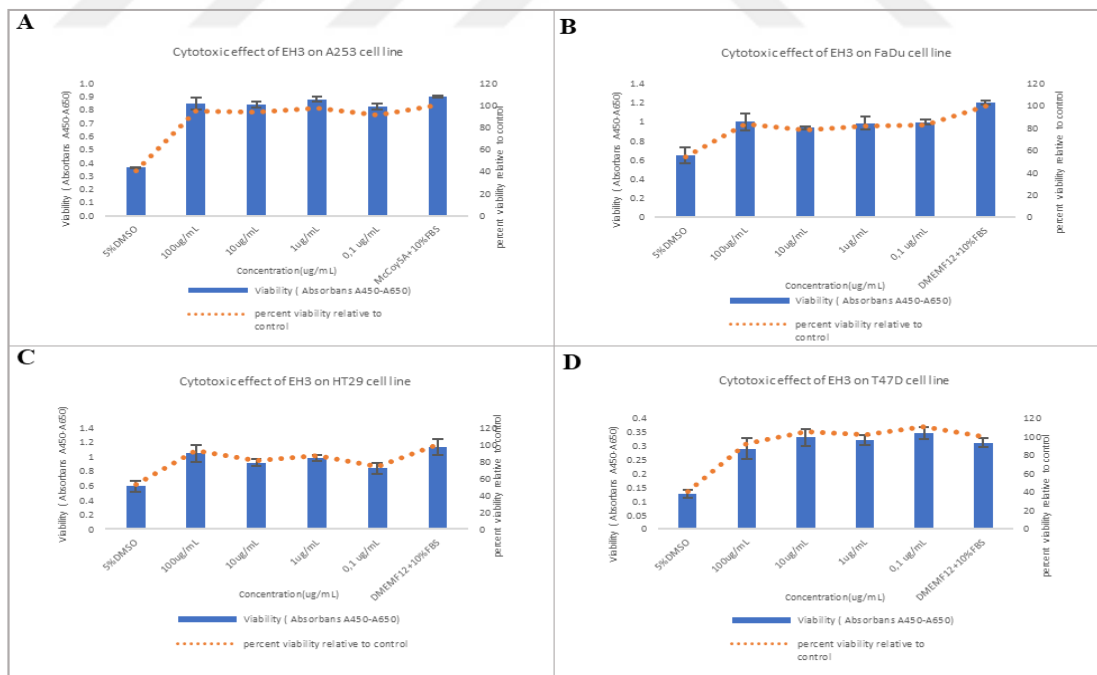


Figure 24 Dose dependent dark cytotoxicity of EH3 phthalocyanine on A. A253 B FaDu C. HT29 D. T47D cell lines. Viability was measured by WST-1 assay following 24h of drug administration.

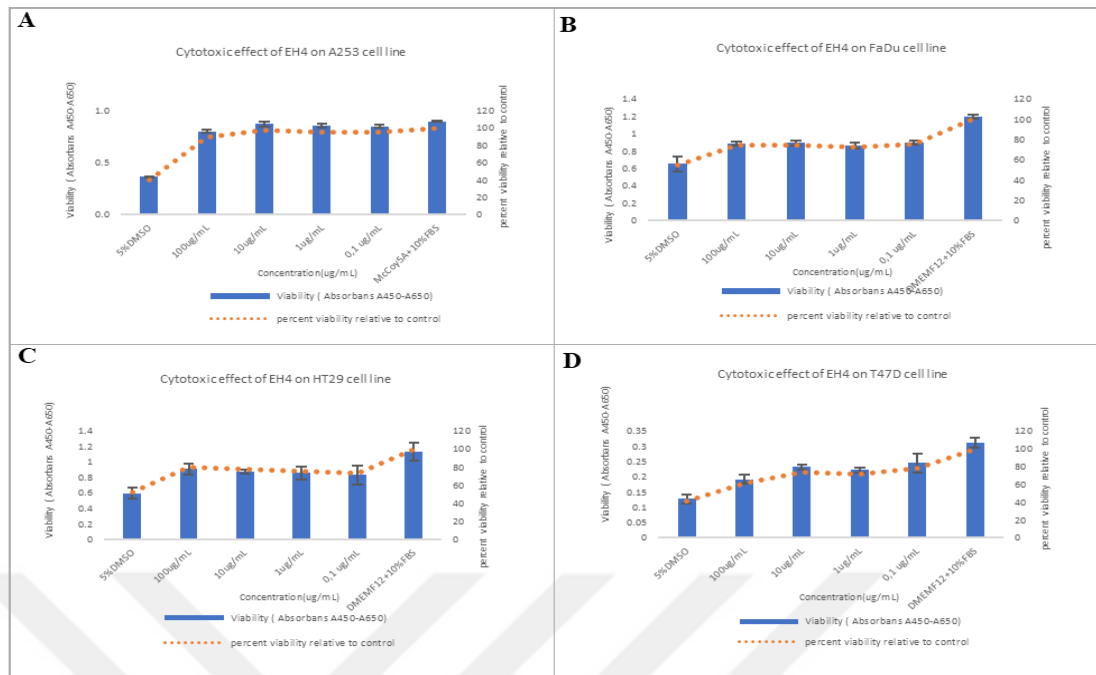


Figure 25 Dose dependent dark cytotoxicity of EH4 phthalocyanine on A. A253 B FaDu C. HT29 D. T47D cell lines. Viability was measured by WST-1 assay following 24h of drug administration.

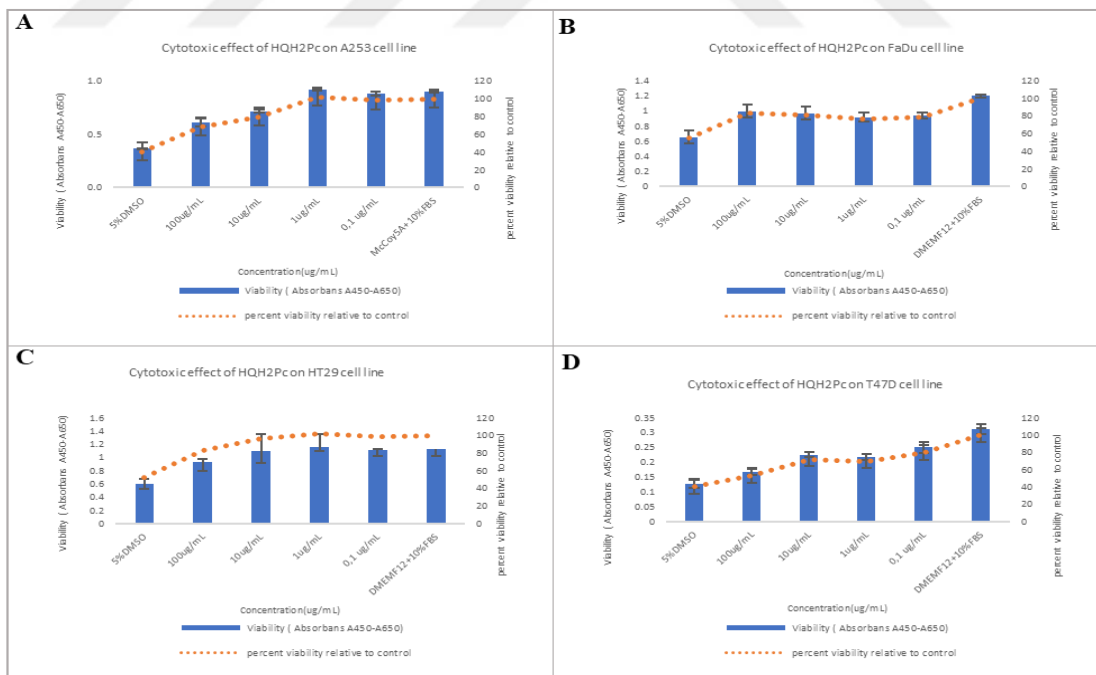


Figure 26 Dose dependent dark cytotoxicity of HQH₂Pc phthalocyanine on A. A253 B FaDu C. HT29 D. T47D cell lines. Viability was measured by WST-1 assay following 24h of drug administration.

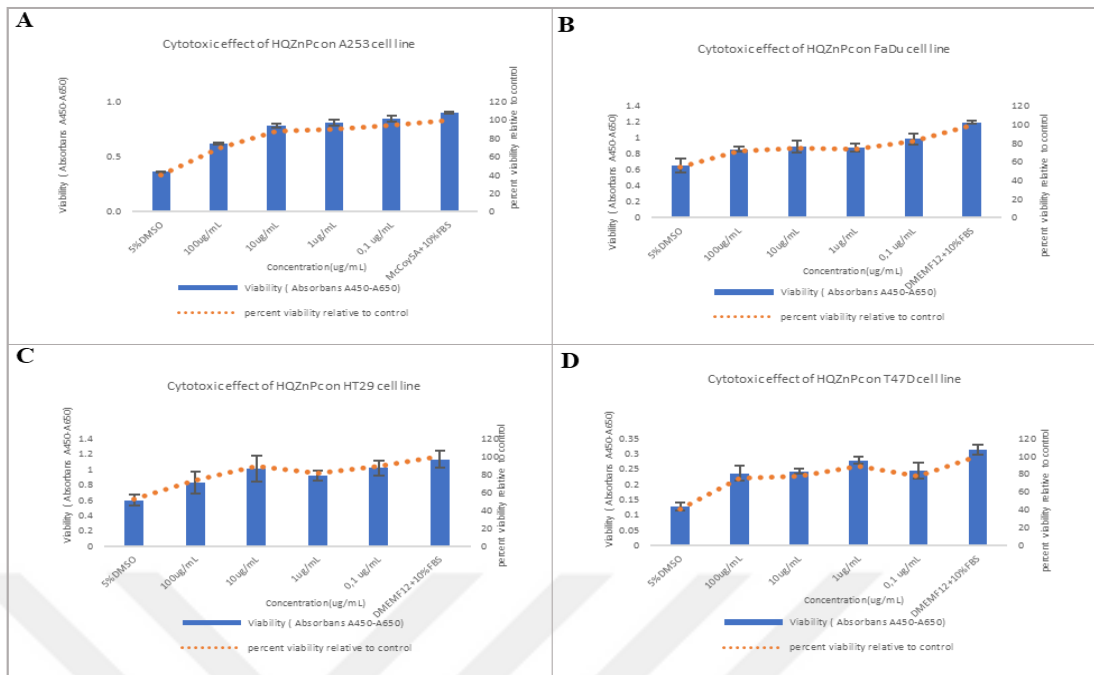


Figure 27 Dose dependent dark cytotoxicity of HQZnPc phthalocyanine on A. A253 B FaDu C. HT29 D. T47D cell lines. Viability was measured by WST-1 assay following 24h of drug administration.

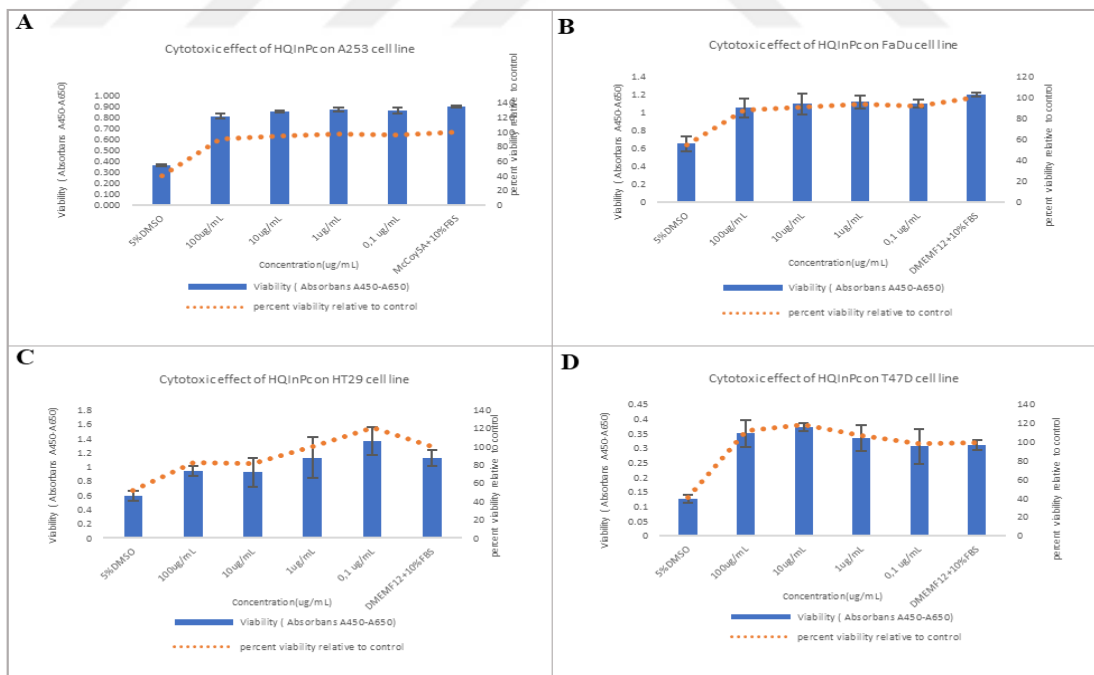


Figure 28 Dose dependent dark cytotoxicity of HQInPc phthalocyanine on A. A253 B FaDu C. HT29 D. T47D cell lines. Viability was measured by WST-1 assay following 24h of drug administration.

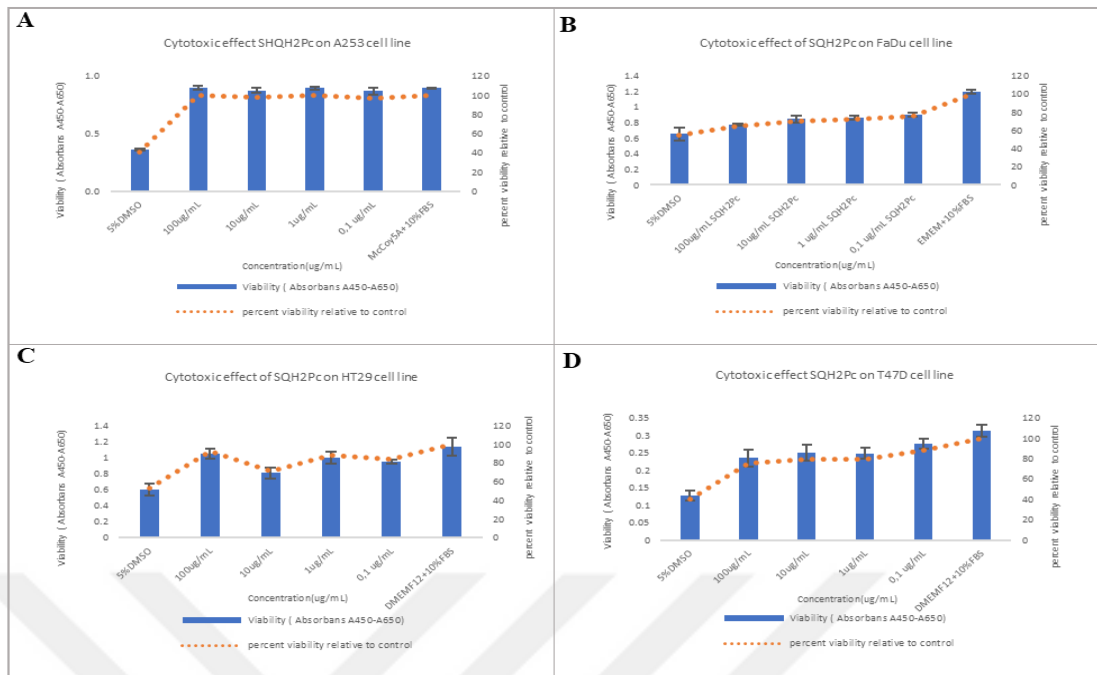


Figure 29 Dose dependent dark cytotoxicity of SQH₂Pc phthalocyanine on A. A253 B FaDu C. HT29 D. T47D cell lines. Viability was measured by WST-1 assay following 24h of drug administration.

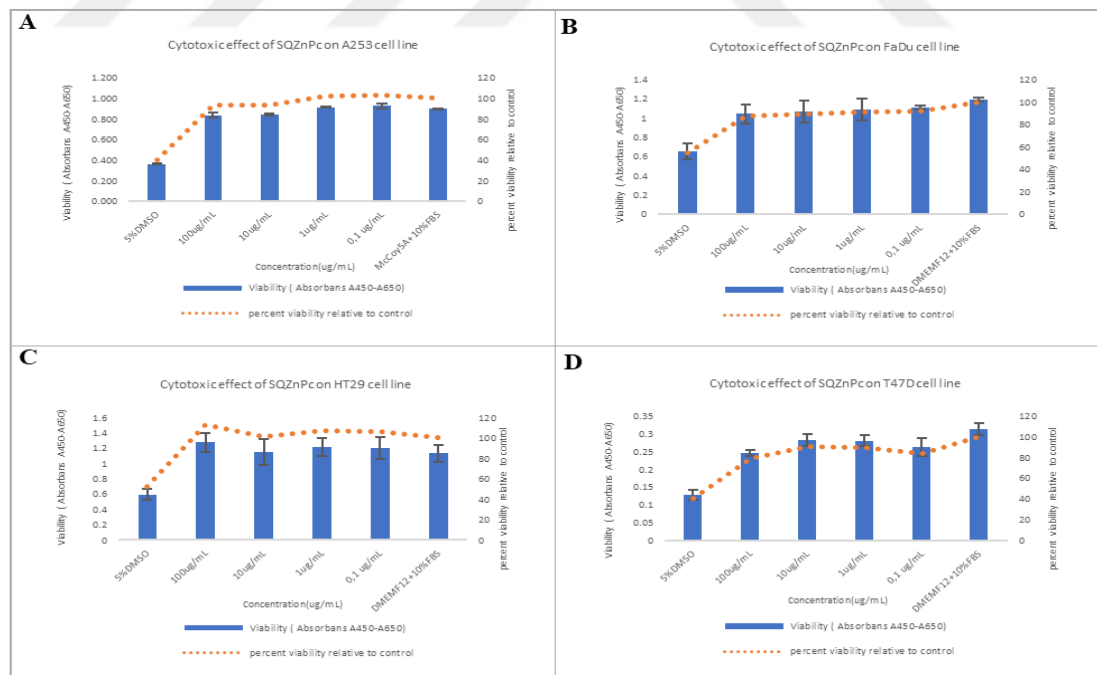


Figure 30 Dose dependent dark cytotoxicity of SQZnPc phthalocyanine on A. A253 B FaDu C. HT29 D. T47D cell lines. Viability was measured by WST-1 assay following 24h of drug administration.

At four different cancer cell lines, the Pc molecules were administrated, and the cytotoxic response was measured after 24h. Concentration, where the Pc molecules did not have any cytotoxic response which causes reduction cell viability below 70% in each cell line, was determined as 10 µg/ml and 1 µg/ml.

46. Photo-induced Cytotoxicity of the Phthalocyanine Molecules on Cancer Cell Lines

Two concentrations, 10 µg/ml and 1 µg/ml that was selected according to dark cytotoxicity studies of Pc molecules were administrated on the cell lines. The cytotoxic response that was created through energy/photon transfer from the Pc molecules to molecular oxygen was measured post 24h of photo-irradiation of 2 joules/cm² of the wavelength range of 624 nm-755 nm.

Viability was measured by both WST-1 and resazurin assays following 24h of PDT with an hour drug administration at 37 C° and 5% CO₂ humidified environment. Survival percentage of A253, FaDu, HT29, and T47D cells was determined relative to the non-treated control. At the different range of wavelength, constant light fluence was applied for each group. The temperature during light treatment was kept constant to 37 C° to avoid temperature-related damages. Values are shown as the mean±SD of three independent experimental replicates.

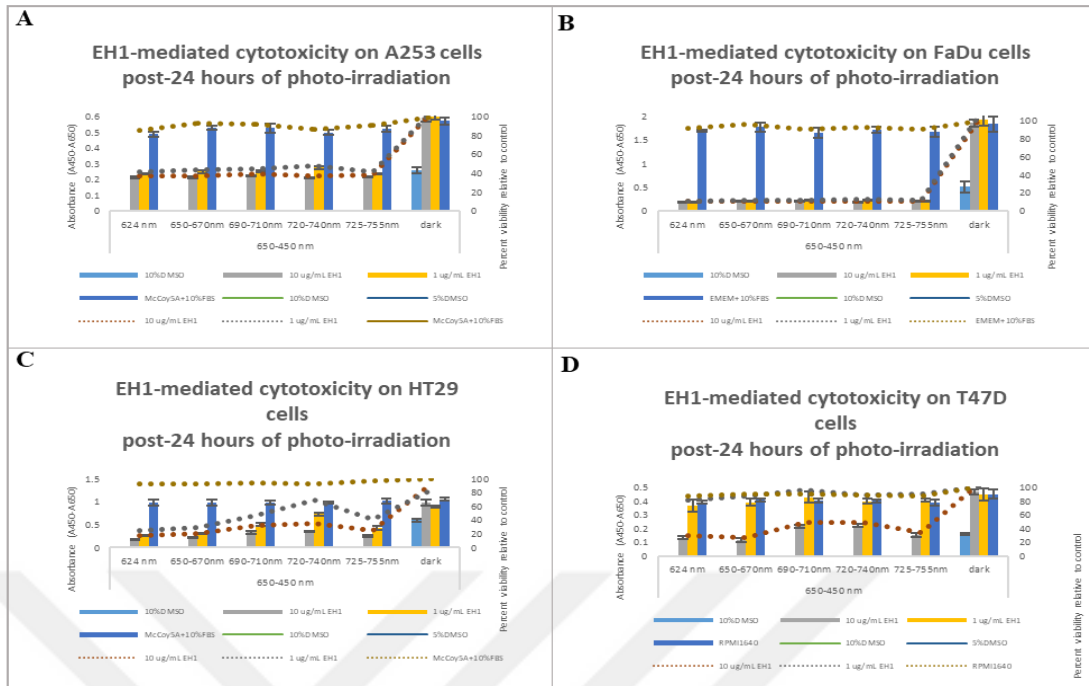


Figure 31 Dose dependent photo-induced cytotoxicity of EH1 phthalocyanine on A. Salivary gland carcinoma, A253, B. Pharynx carcinoma, FaDu, C. Colorectal adenocarcinoma, HT29, D. Breast carcinoma, T47D cell lines by WST-1 assay.

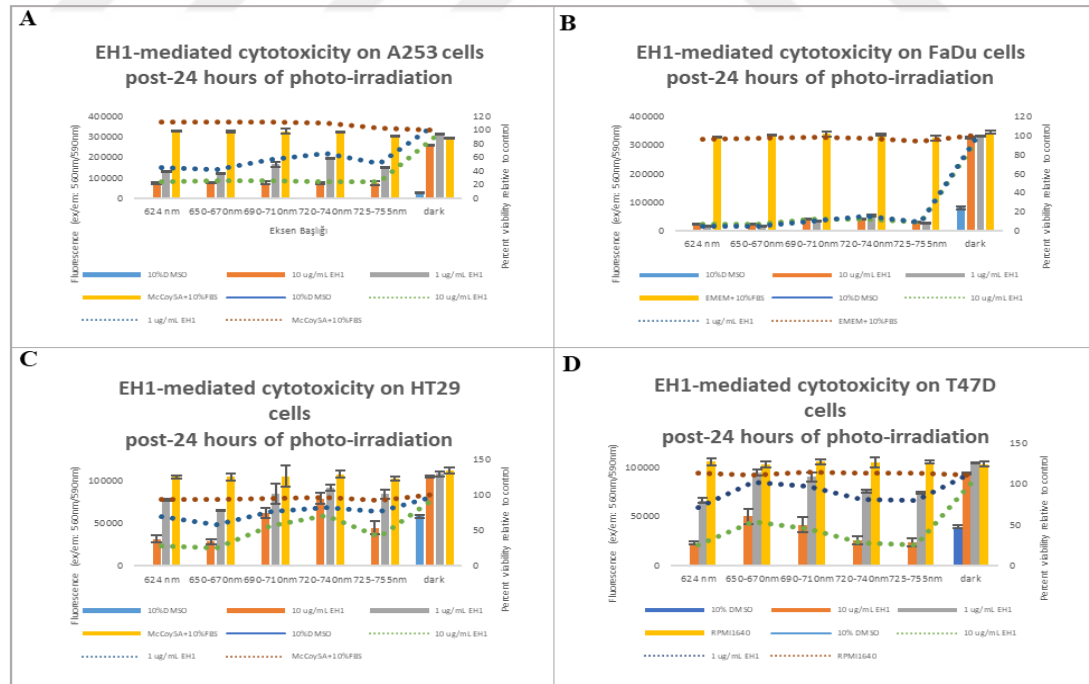


Figure 32 Dose dependent photo-induced cytotoxicity of EH1 phthalocyanine on A. Salivary gland carcinoma, A253, B. Pharynx carcinoma, FaDu, C. Colorectal adenocarcinoma, HT29, D. Breast carcinoma, T47D cell lines by resazurin assay.

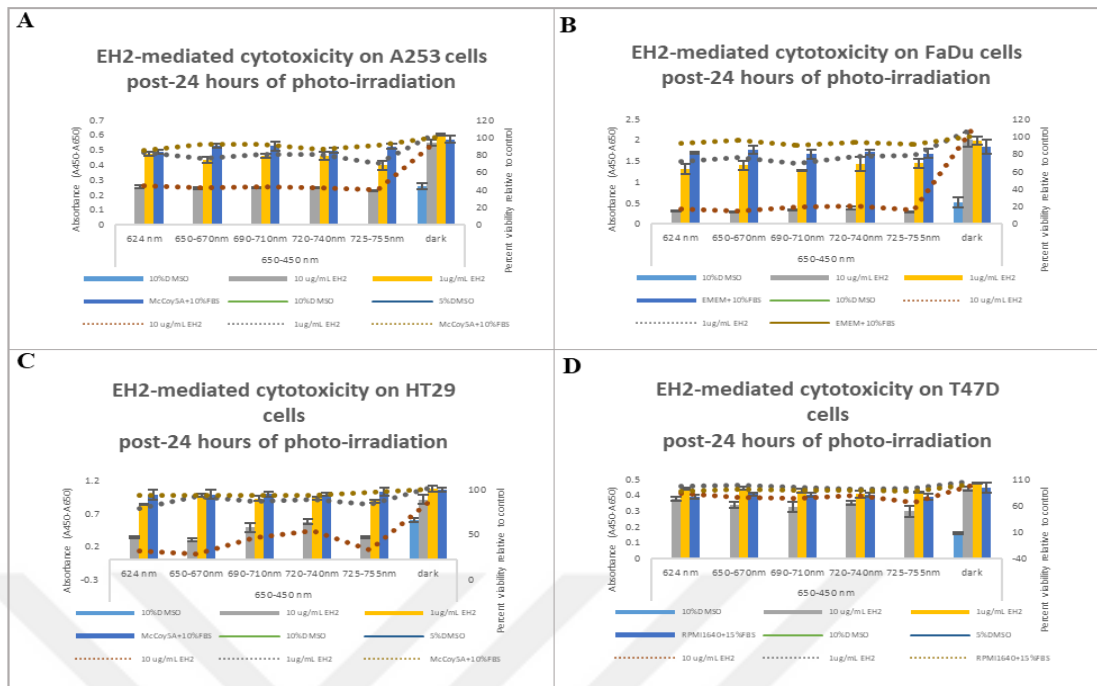


Figure 33 Dose dependent photo-induced cytotoxicity of EH2 phthalocyanine on A. Salivary gland carcinoma, A253, B. Pharynx carcinoma, FaDu, C. Colorectal adenocarcinoma, HT29, D. Breast carcinoma, T47D cell lines by WST-1 assay.

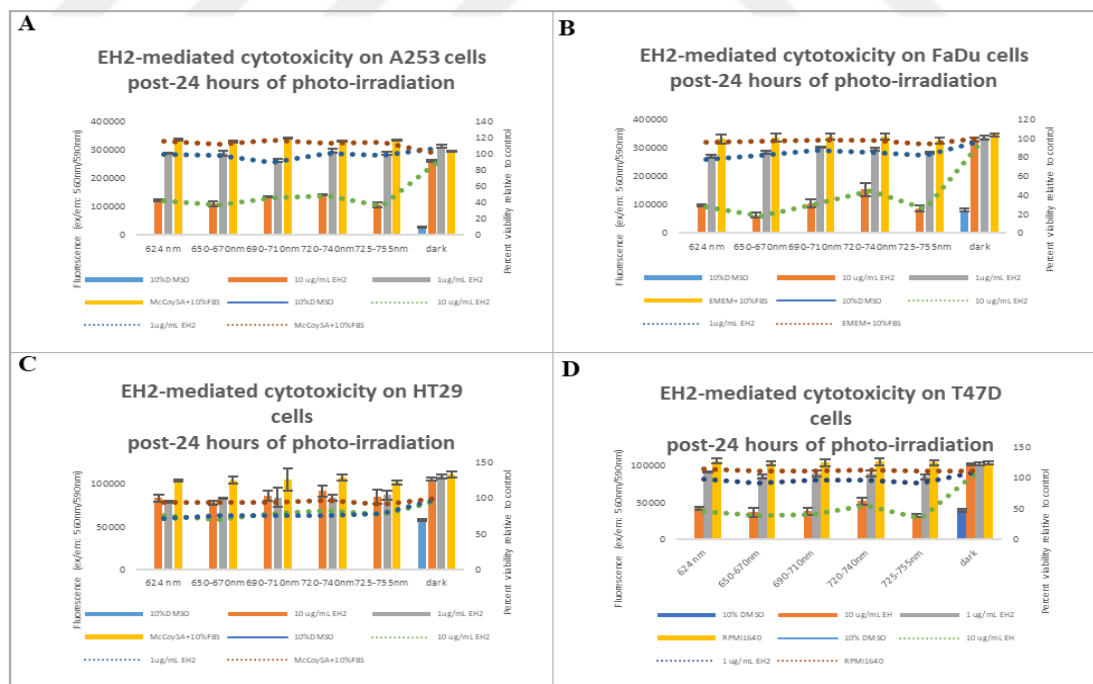


Figure 34 Dose dependent photo-induced cytotoxicity of EH2 phthalocyanine on A. Salivary gland carcinoma, A253, B. Pharynx carcinoma, FaDu, C. Colorectal adenocarcinoma, HT29, D. Breast carcinoma, T47D cell lines by resazurin assay.

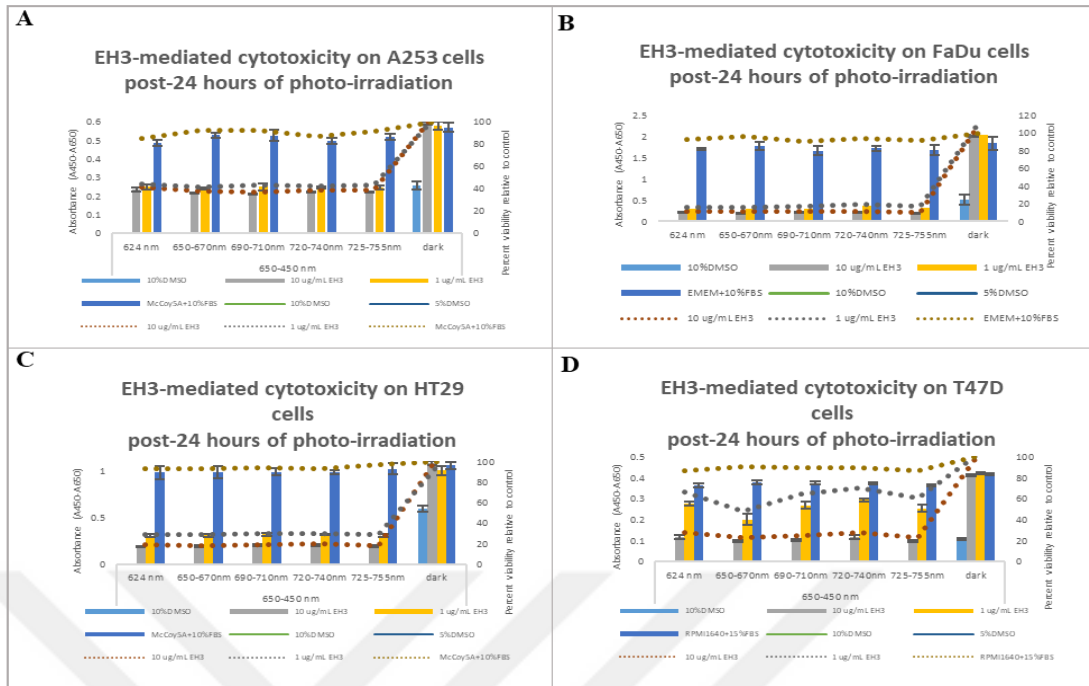


Figure 35 Dose dependent photo-induced cytotoxicity of EH3 phthalocyanine on A. Salivary gland carcinoma, A253, B. Pharynx carcinoma, FaDu, C. Colorectal adenocarcinoma, HT29, D. Breast carcinoma, T47D cell lines by WST-1 assay.

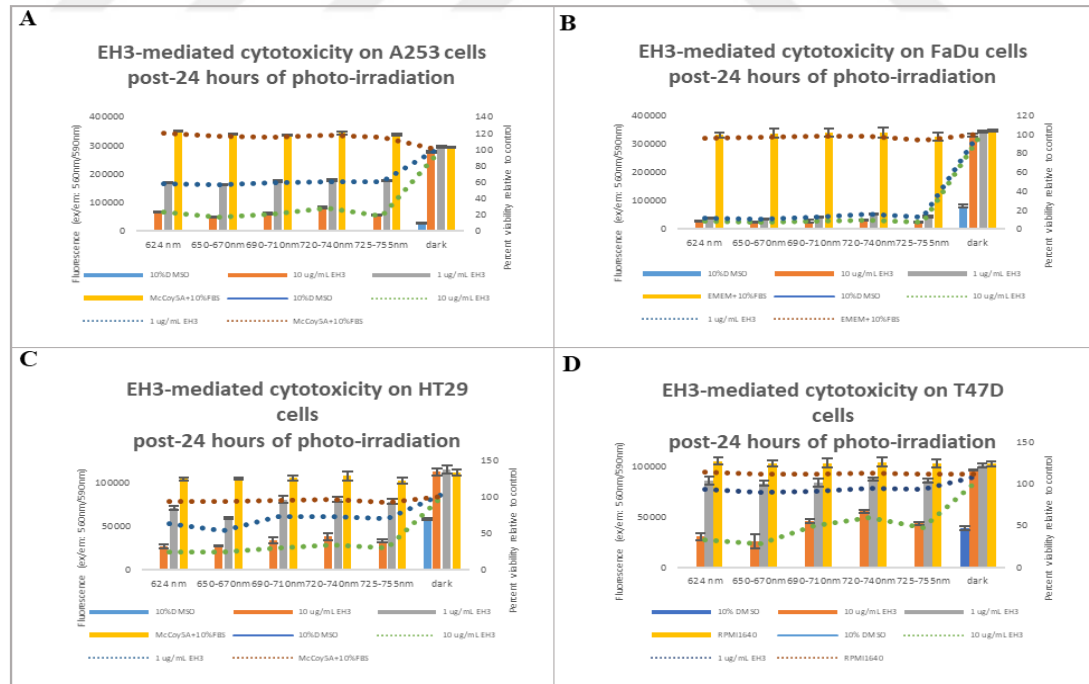


Figure 36 Dose dependent photo-induced cytotoxicity of EH3 phthalocyanine on A. Salivary gland carcinoma, A253, B. Pharynx carcinoma, FaDu, C. Colorectal adenocarcinoma, HT29, D. Breast carcinoma, T47D cell lines by resazurin assay.

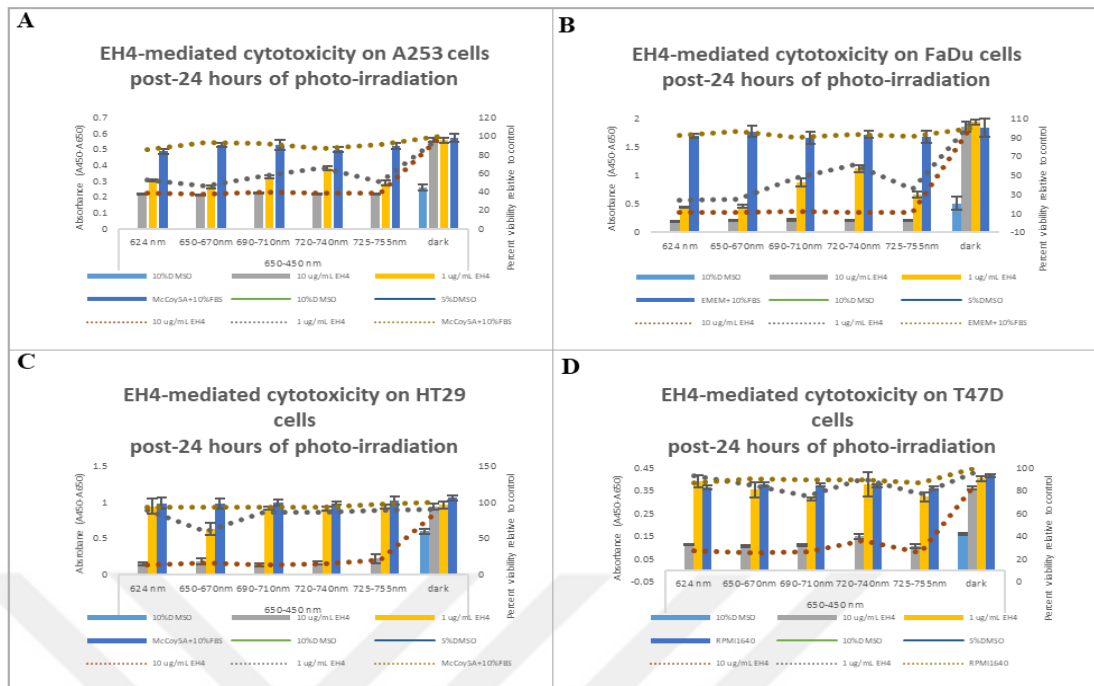


Figure 37 Dose dependent photo-induced cytotoxicity of EH4 phthalocyanine on A. Salivary gland carcinoma, A253, B. Pharynx carcinoma, FaDu, C. Colorectal adenocarcinoma, HT29, D. Breast carcinoma, T47D cell lines by WST-1 assay.

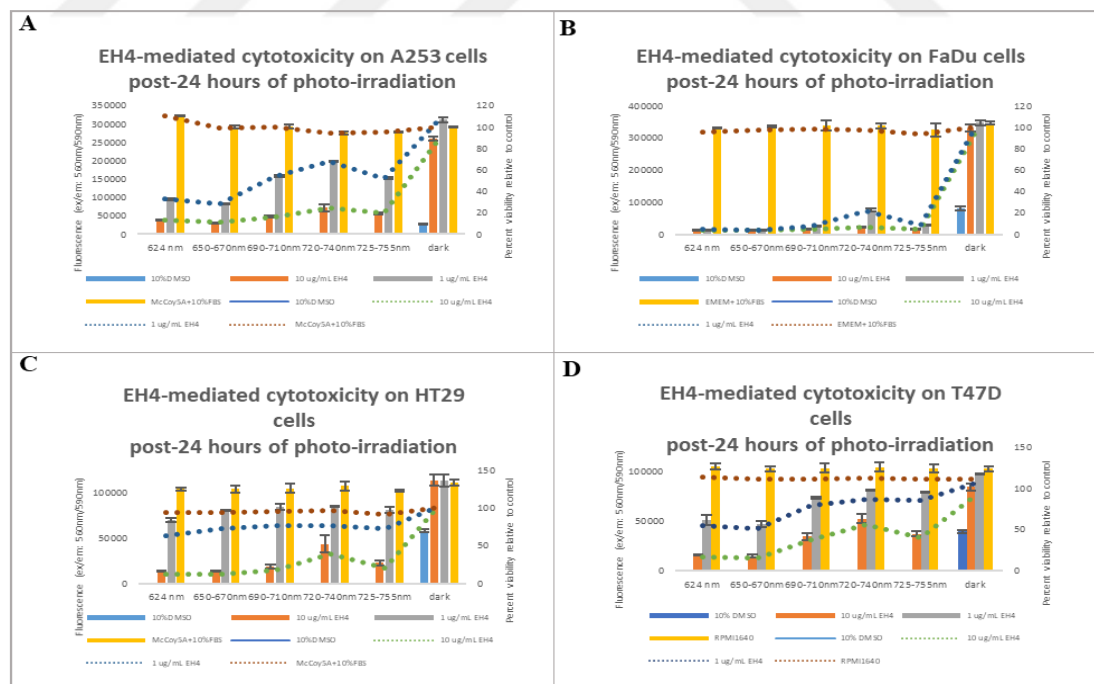


Figure 38 Dose dependent photo-induced cytotoxicity of EH4 phthalocyanine on A. Salivary gland carcinoma, A253, B. Pharynx carcinoma, FaDu, C. Colorectal adenocarcinoma, HT29, D. Breast carcinoma, T47D cell lines by resazurin assay

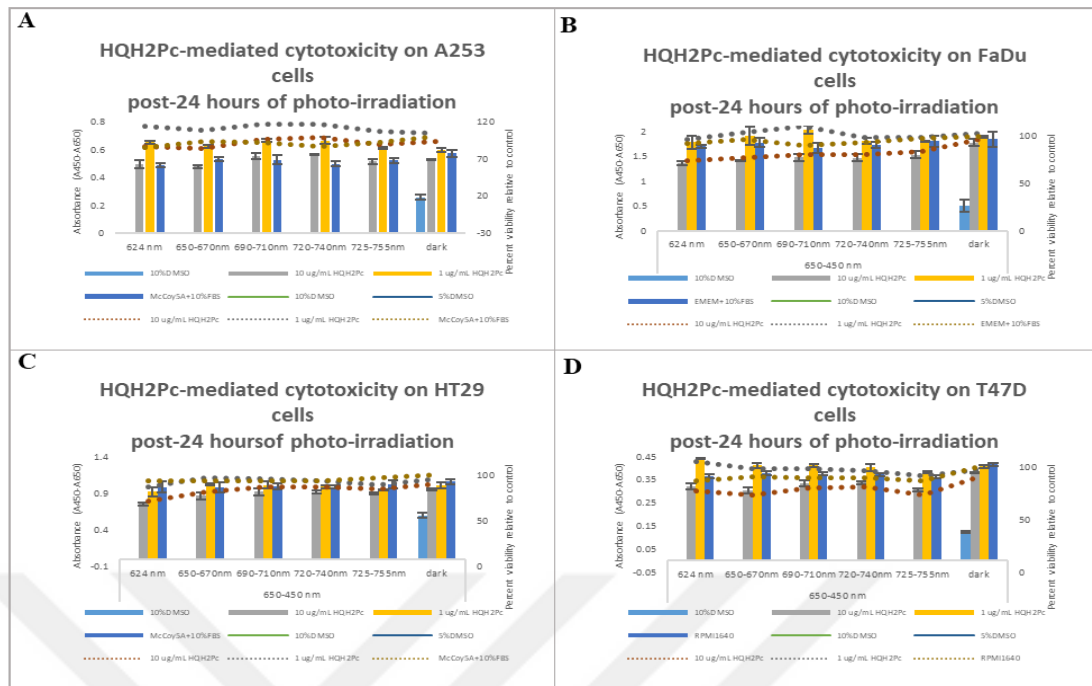


Figure 39 Dose dependent photo-induced cytotoxicity of HQH2Pc phthalocyanine on A. Salivary gland carcinoma, A253, B. Pharynx carcinoma, FaDu, C. Colorectal adenocarcinoma, HT29, D. Breast carcinoma, T47D cell lines by WST-1 assay.

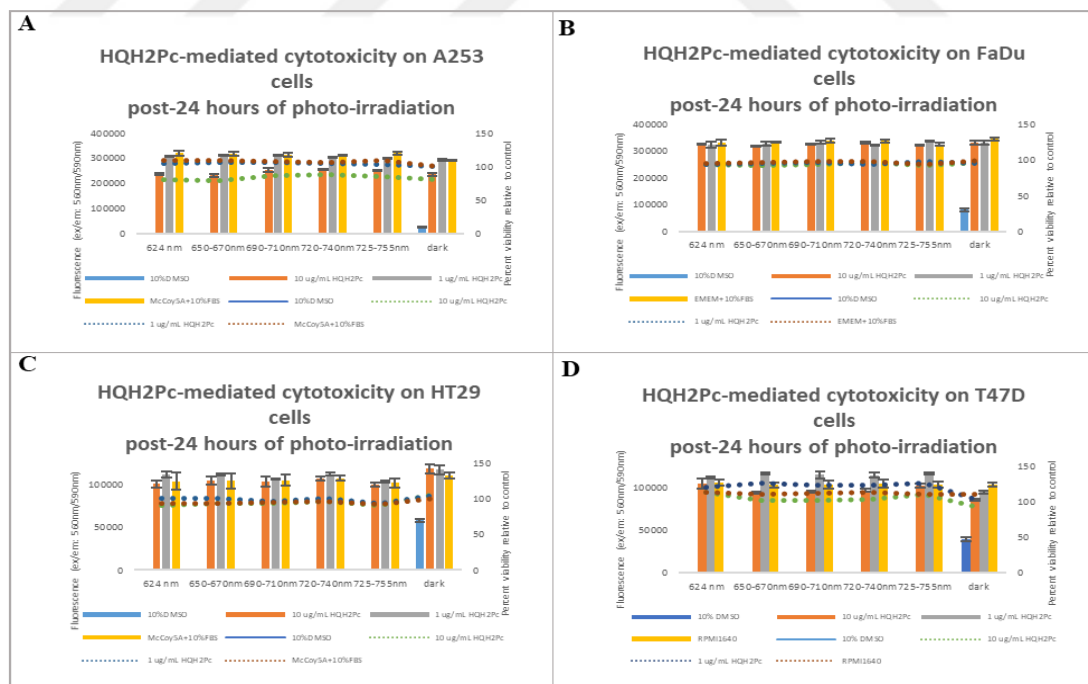


Figure 40 Dose dependent photo-induced cytotoxicity of HQH2Pc phthalocyanine on A. Salivary gland carcinoma, A253, B. Pharynx carcinoma, FaDu, C. Colorectal adenocarcinoma, HT29, D. Breast carcinoma, T47D cell lines by resazurin assay.

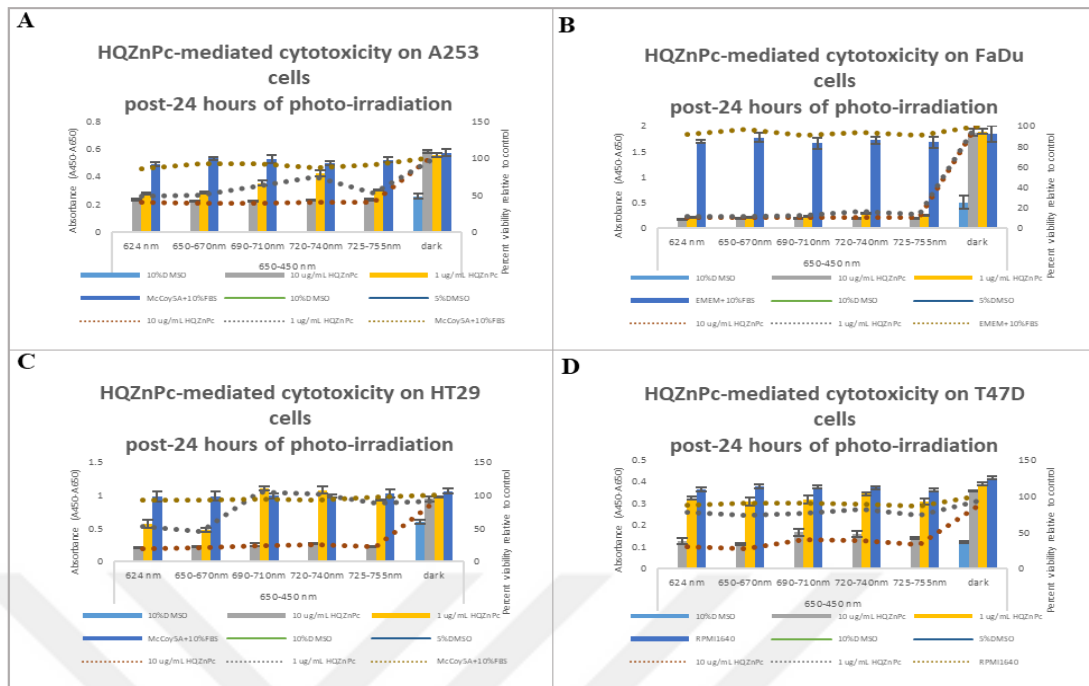


Figure 41 Dose dependent photo-induced cytotoxicity of HQZnPc phthalocyanine on A. Salivary gland carcinoma, A253, B. Pharynx carcinoma, FaDu, C. Colorectal adenocarcinoma, HT29, D. Breast carcinoma, T47D cell lines by WST-1 assay.

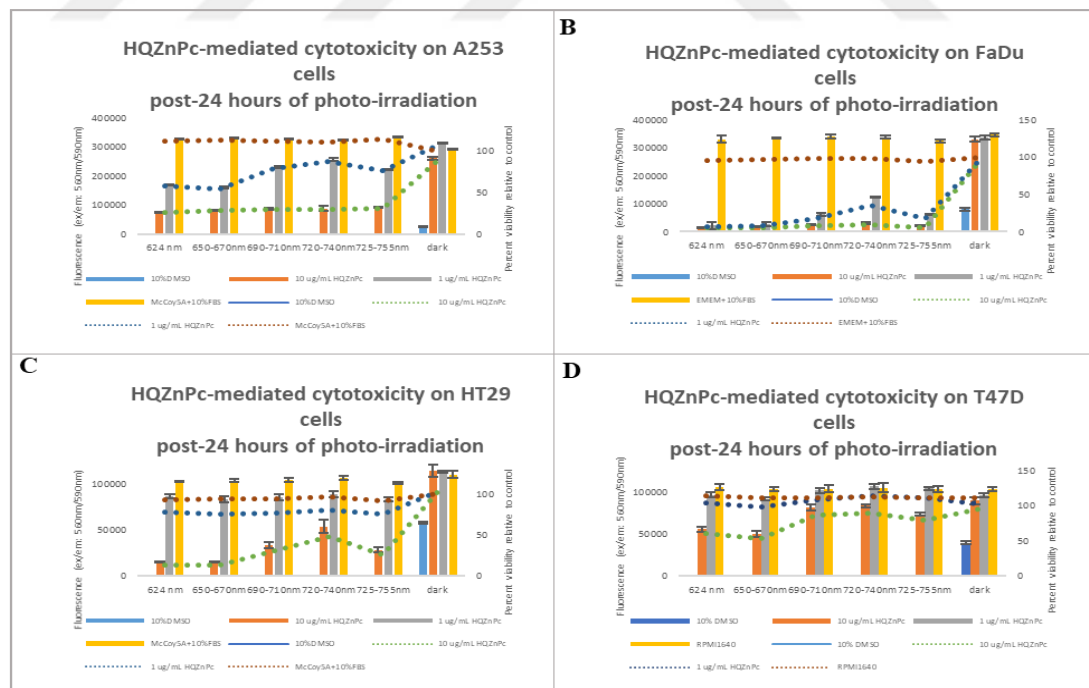


Figure 42 Dose dependent photo-induced cytotoxicity of HQZnPc phthalocyanine on A. Salivary gland carcinoma, A253, B. Pharynx carcinoma, FaDu, C. Colorectal adenocarcinoma, HT29, D. Breast carcinoma, T47D cell lines by resazurin assay.

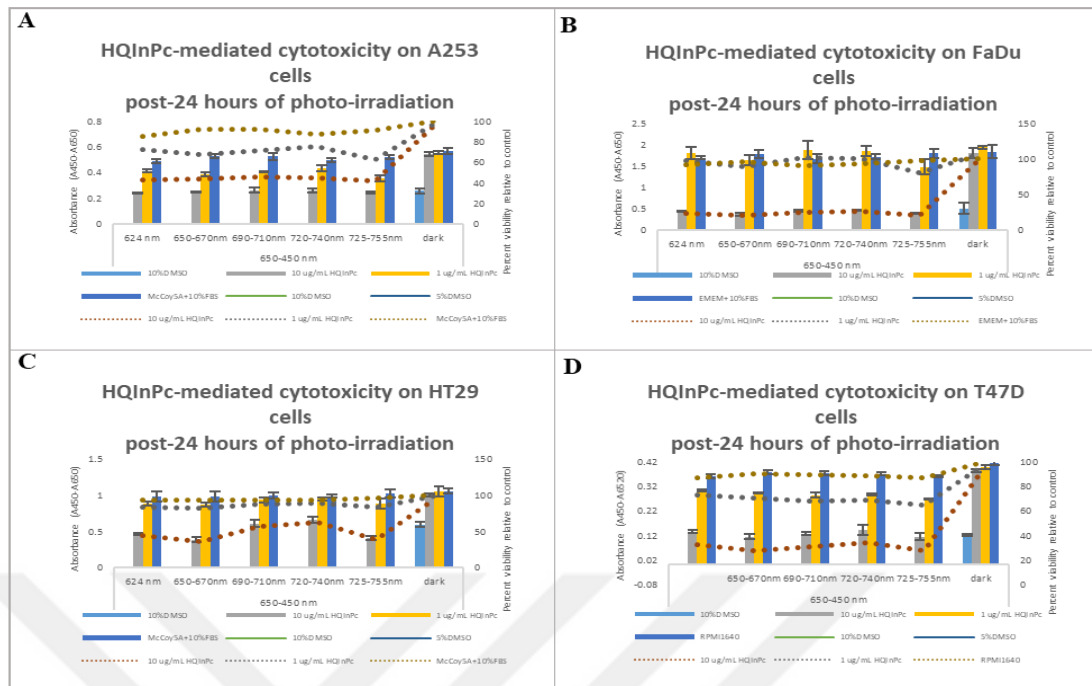


Figure 43 Dose dependent photo-induced cytotoxicity of HQInPc phthalocyanine on A. Salivary gland carcinoma, A253, B. Pharynx carcinoma, FaDu, C. Colorectal adenocarcinoma, HT29, D. Breast carcinoma, T47D cell lines by WST-1 assay.

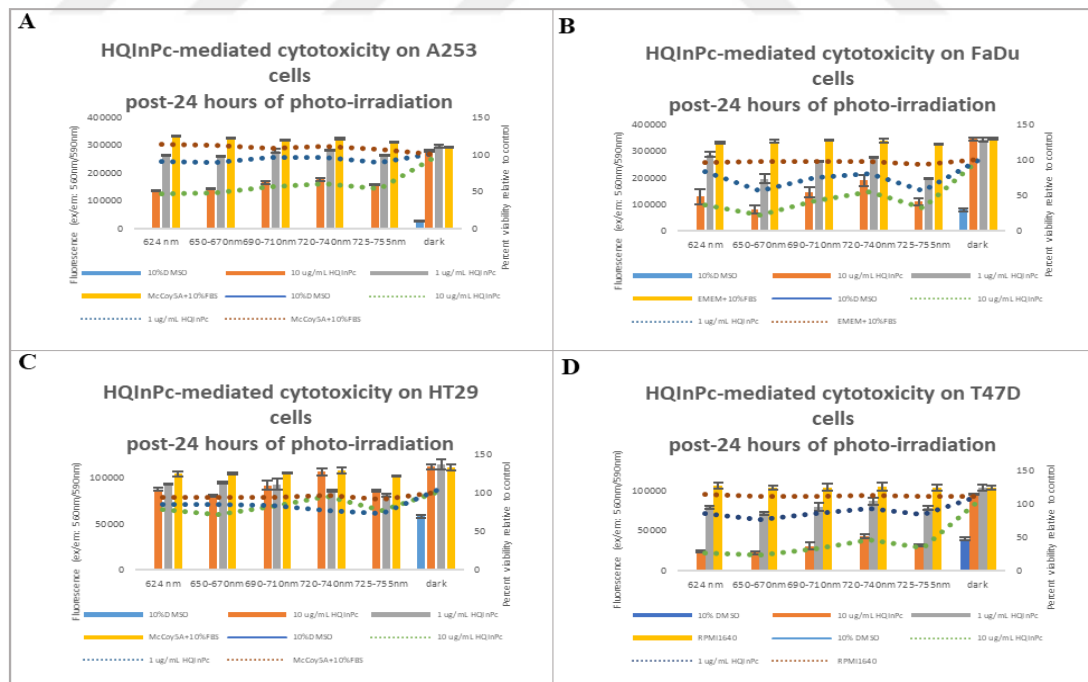


Figure 44 Dose dependent photo-induced cytotoxicity of HQInPc phthalocyanine on A. Salivary gland carcinoma, A253, B. Pharynx carcinoma, FaDu, C. Colorectal adenocarcinoma, HT29, D. Breast carcinoma, T47D cell lines by resazurin assay.

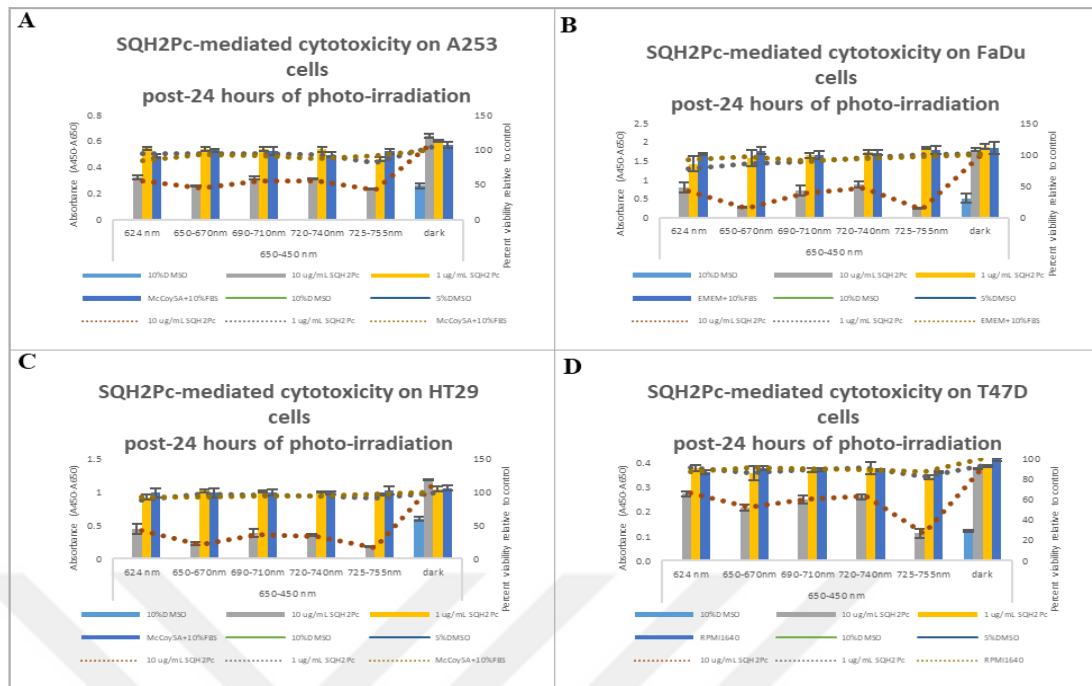


Figure 45 Dose dependent photo-induced cytotoxicity of SQH₂Pc phthalocyanine on A. Salivary gland carcinoma, A253, B. Pharynx carcinoma, FaDu, C. Colorectal adenocarcinoma, HT29, D. Breast carcinoma, T47D cell lines by WST-1 assay.

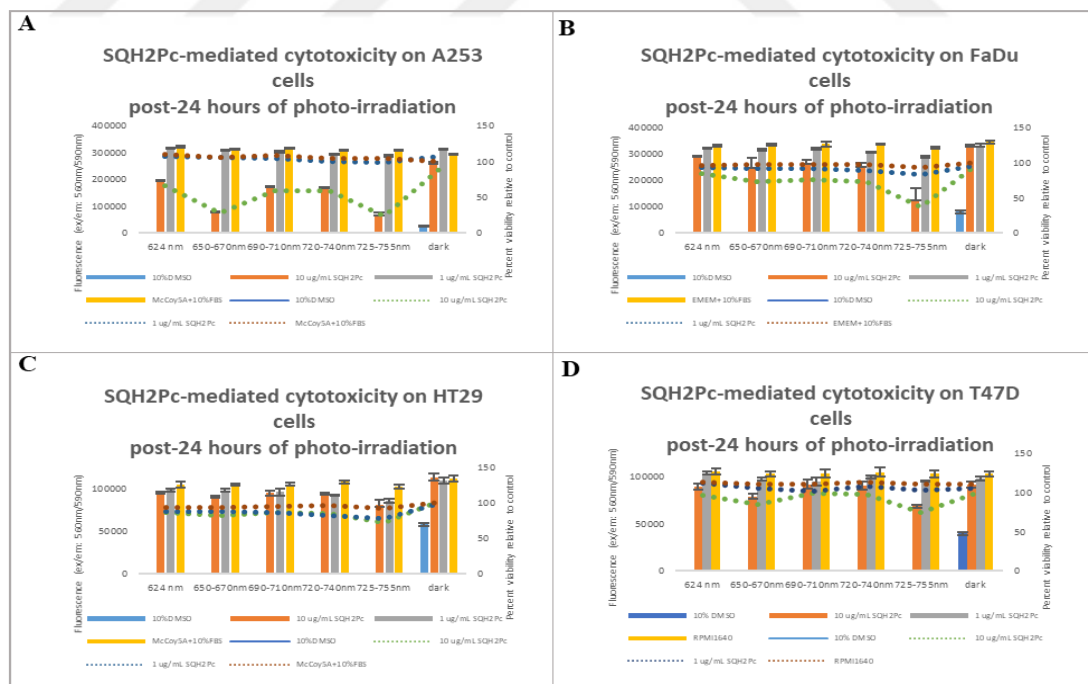


Figure 46 Dose dependent photo-induced cytotoxicity of SQH₂Pc phthalocyanine on A. Salivary gland carcinoma, A253, B. Pharynx carcinoma, FaDu, C. Colorectal adenocarcinoma, HT29, D. Breast carcinoma, T47D cell lines by resazurin assay.

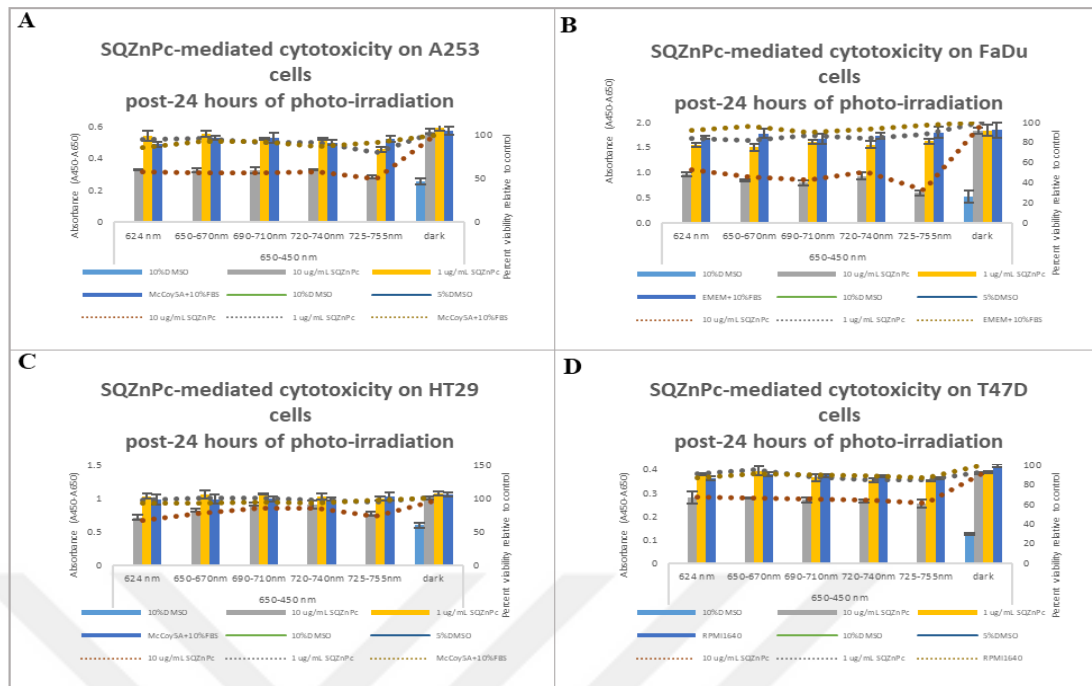


Figure 47 Dose dependent photo-induced cytotoxicity of SQZnPc phthalocyanine on A. Salivary gland carcinoma, A253, B. Pharynx carcinoma, FaDu, C. Colorectal adenocarcinoma, HT29, D. Breast carcinoma, T47D cell lines by WST-1 assay.

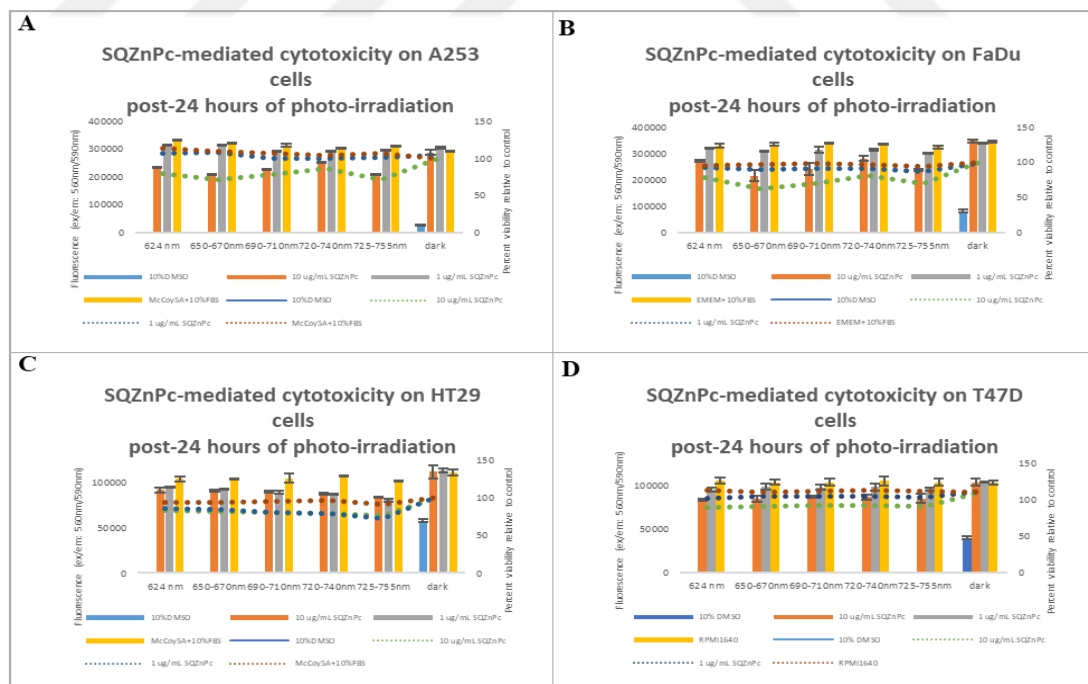


Figure 48 Dose dependent photo-induced cytotoxicity of SQZnPc phthalocyanine on A. Salivary gland carcinoma, A253, B. Pharynx carcinoma, FaDu, C. Colorectal adenocarcinoma, HT29, D. Breast carcinoma, T47D cell lines by resazurin assay.

47. PDT-mediated Oxidative Stress Evaluation

In photodynamic therapy, cellular damage mostly occurs due to reactive oxygen species formation through energy transfer from Pc molecules to nearby molecular oxygen. To link the reason for the cell PDT-induced cell damage, ROS evaluation following post-30 minutes (immediate) and post-24 hours (late) of PDT was carried out using non-fluorescent DCFDA that forms fluorescent DCF in presence of ROS.

Following 30 minutes and 24 hours of PDT with an hour drug administration at 37 C° and 5% CO₂ humidified environment, the relative ROS amount was measured by DCFDA that yields fluorescent DCF. At the different range of wavelength and constant light fluence was applied for each group. The temperature during light treatment was kept constant to 37 C° to avoid temperature-related oxidative stress. Values are shown as the mean±SD of three independent experimental replicates.

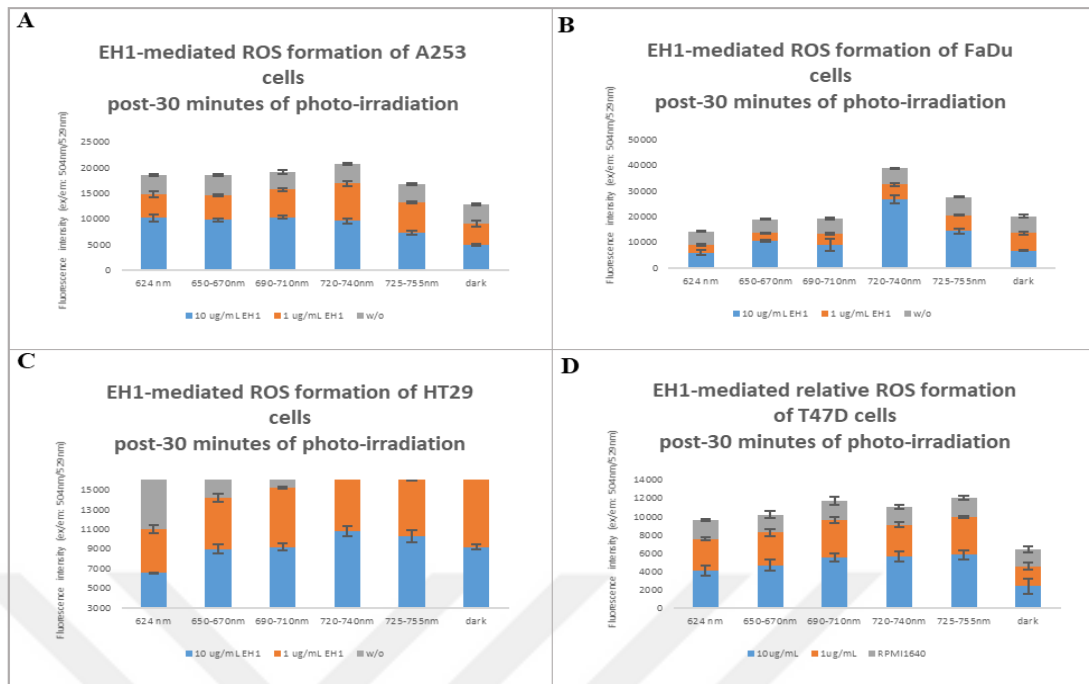


Figure 49 Dose dependent post-30 minutes photo-induced ROS formation of EH1 phthalocyanine on A. Salivary gland carcinoma, A253, B. Pharynx carcinoma, FaDu, C. Colorectal adenocarcinoma, HT29, D. Breast carcinoma, T47D cell lines.

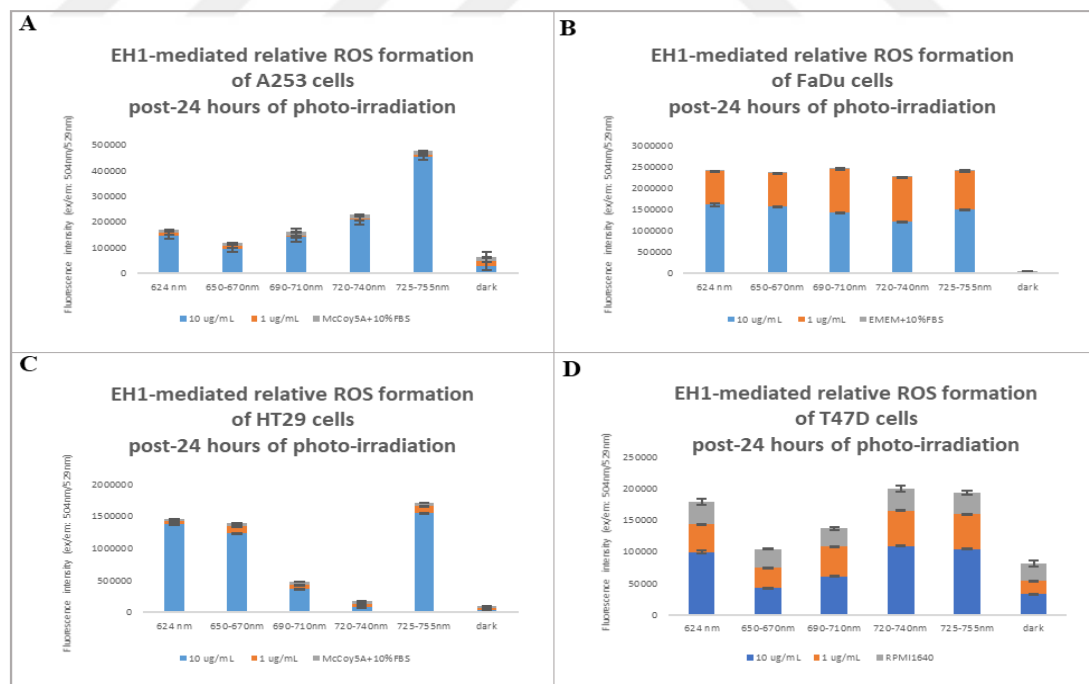


Figure 50 Dose dependent post-24 hours photo-induced ROS formation of EH1 phthalocyanine on A. Salivary gland carcinoma, A253, B. Pharynx carcinoma, FaDu, C. Colorectal adenocarcinoma, HT29, D. Breast carcinoma, T47D cell lines.

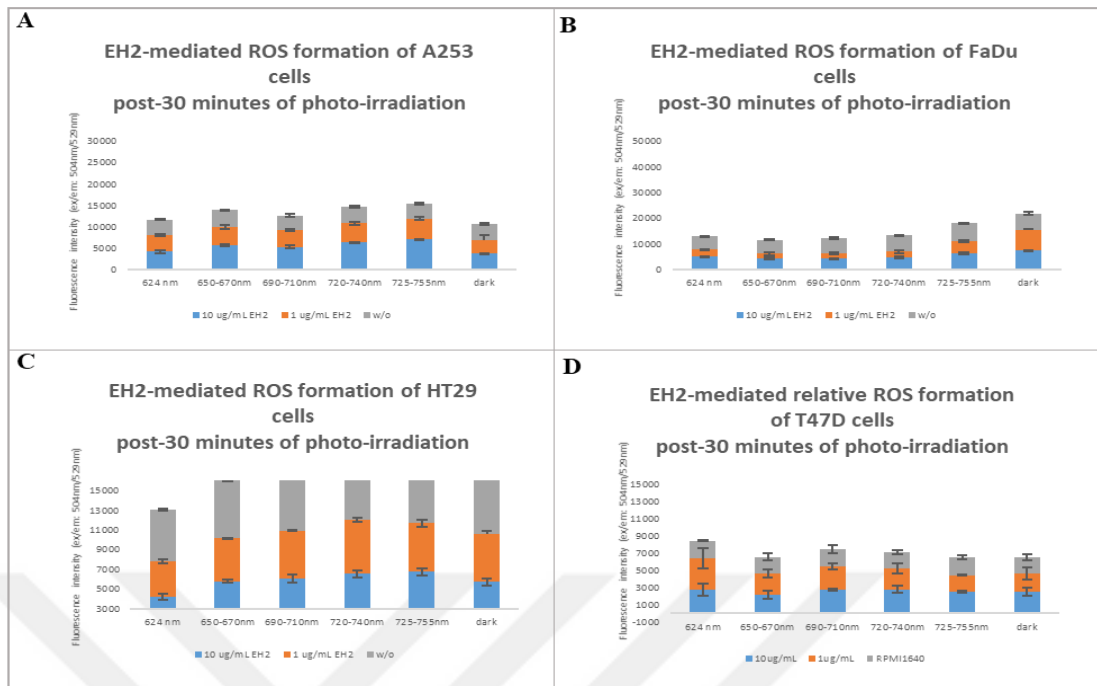


Figure 51 Dose dependent post-30 minutes photo-induced ROS formation of EH2 phthalocyanine on A. Salivary gland carcinoma, A253, B. Pharynx carcinoma, FaDu, C. Colorectal adenocarcinoma, HT29, D. Breast carcinoma, T47D cell lines.

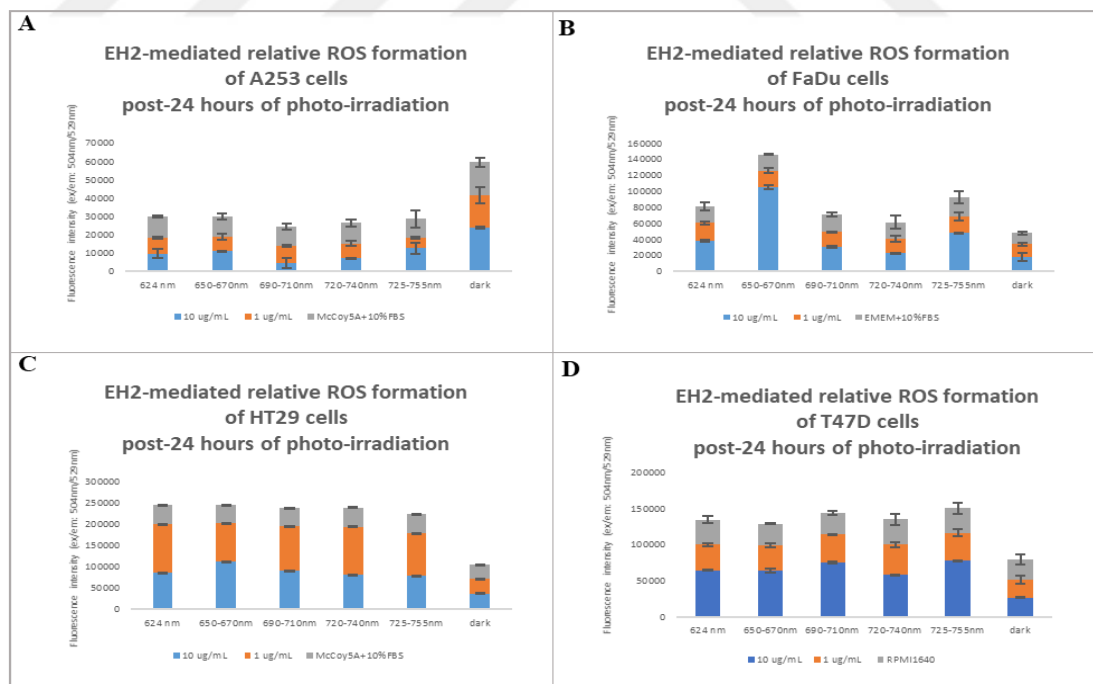


Figure 52 Dose dependent post-24 hours photo-induced ROS formation of EH2 phthalocyanine on A. Salivary gland carcinoma, A253, B. Pharynx carcinoma, FaDu, C. Colorectal adenocarcinoma, HT29, D. Breast carcinoma, T47D cell lines.

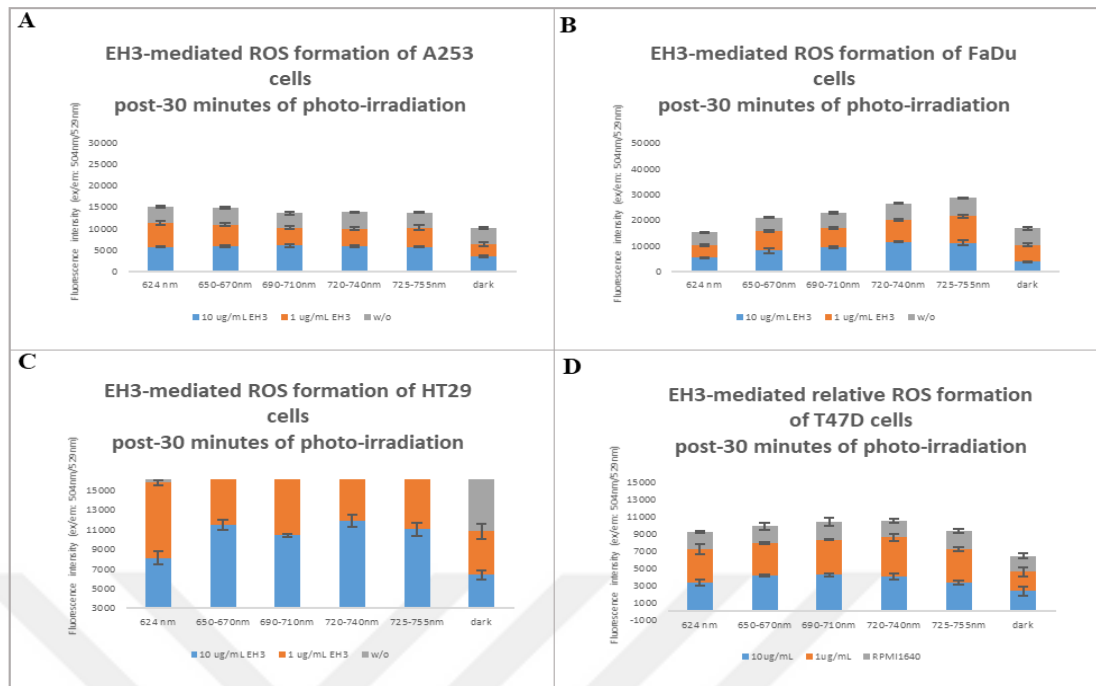


Figure 53 Dose dependent post-30 minutes photo-induced ROS formation of EH3 phthalocyanine on A. Salivary gland carcinoma, A253, B. Pharynx carcinoma, FaDu, C. Colorectal adenocarcinoma, HT29, D. Breast carcinoma, T47D cell lines.

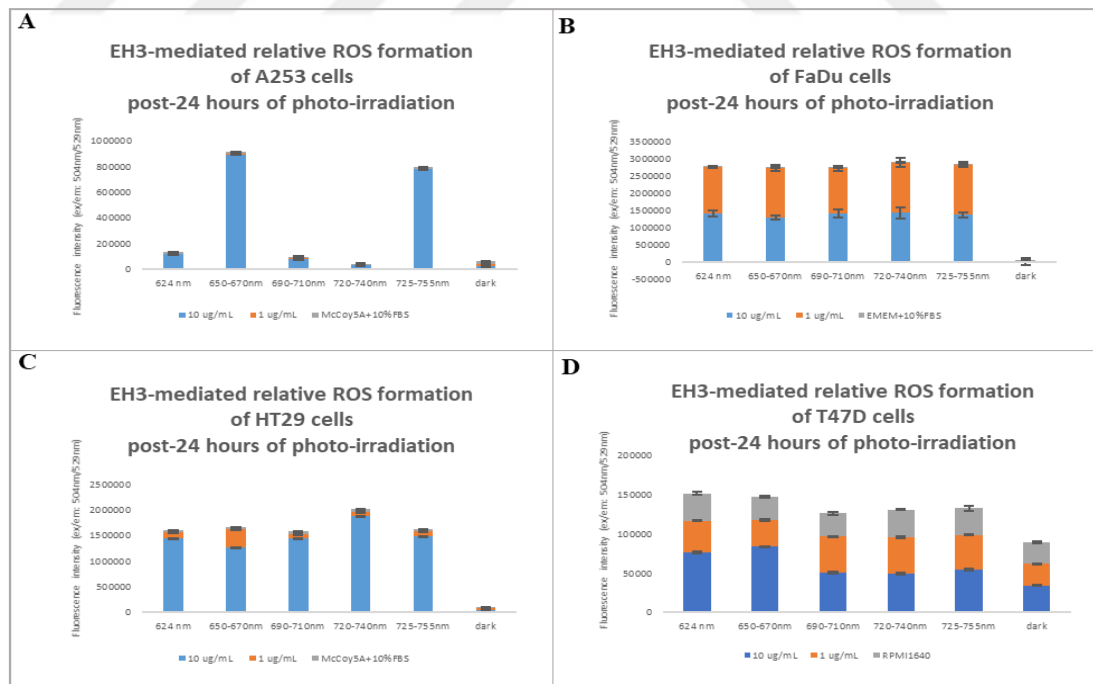


Figure 54 Dose dependent post-24 hours photo-induced ROS formation of EH3 phthalocyanine on A. Salivary gland carcinoma, A253, B. Pharynx carcinoma, FaDu, C. Colorectal adenocarcinoma, HT29, D. Breast carcinoma, T47D cell lines.

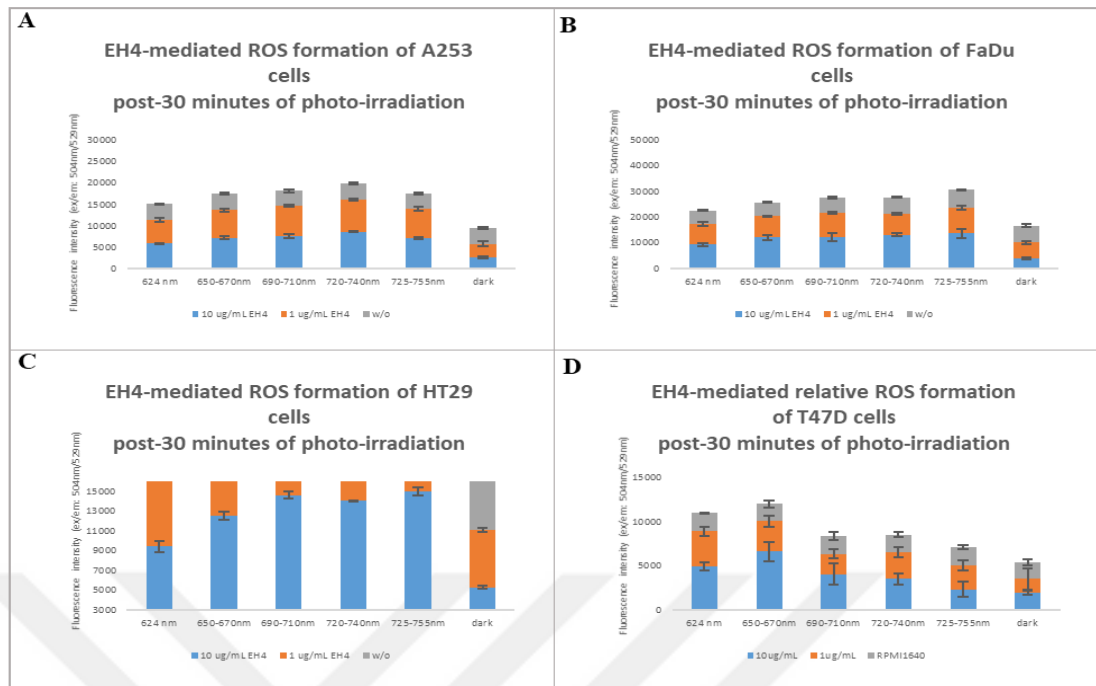


Figure 55 Dose dependent post-30 minutes photo-induced ROS formation of EH4 phthalocyanine on A. Salivary gland carcinoma, A253, B. Pharynx carcinoma, FaDu, C. Colorectal adenocarcinoma, HT29, D. Breast carcinoma, T47D cell lines.

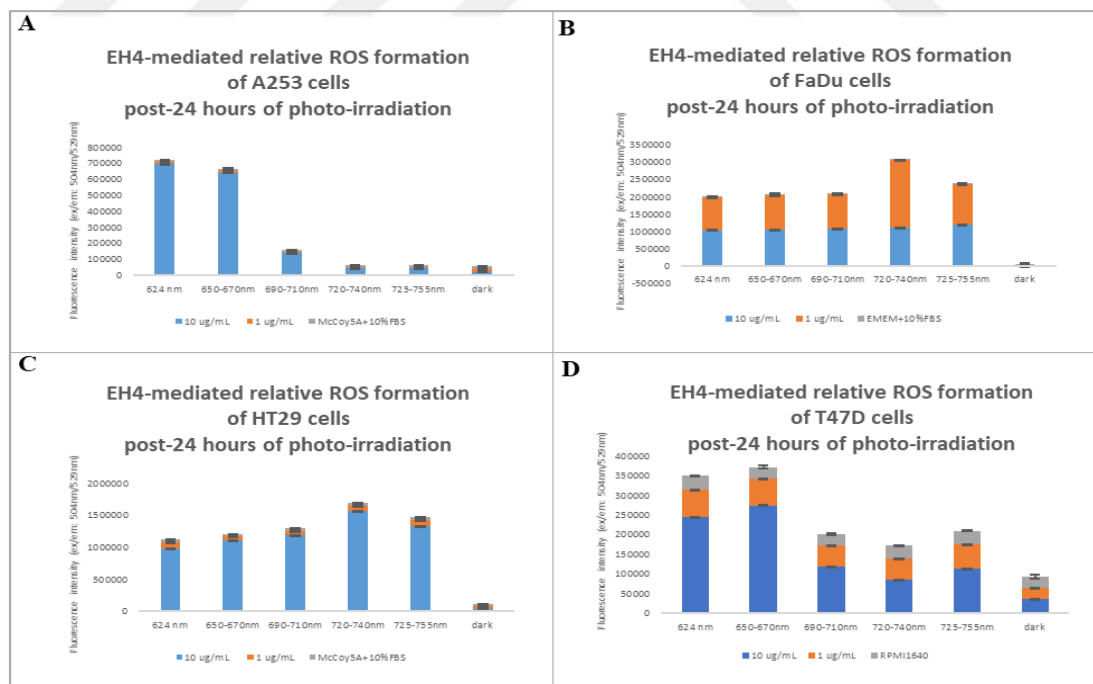


Figure 56 Dose dependent post-24 hours photo-induced ROS formation of EH4 phthalocyanine on A. Salivary gland carcinoma, A253, B. Pharynx carcinoma, FaDu, C. Colorectal adenocarcinoma, HT29, D. Breast carcinoma, T47D cell lines.

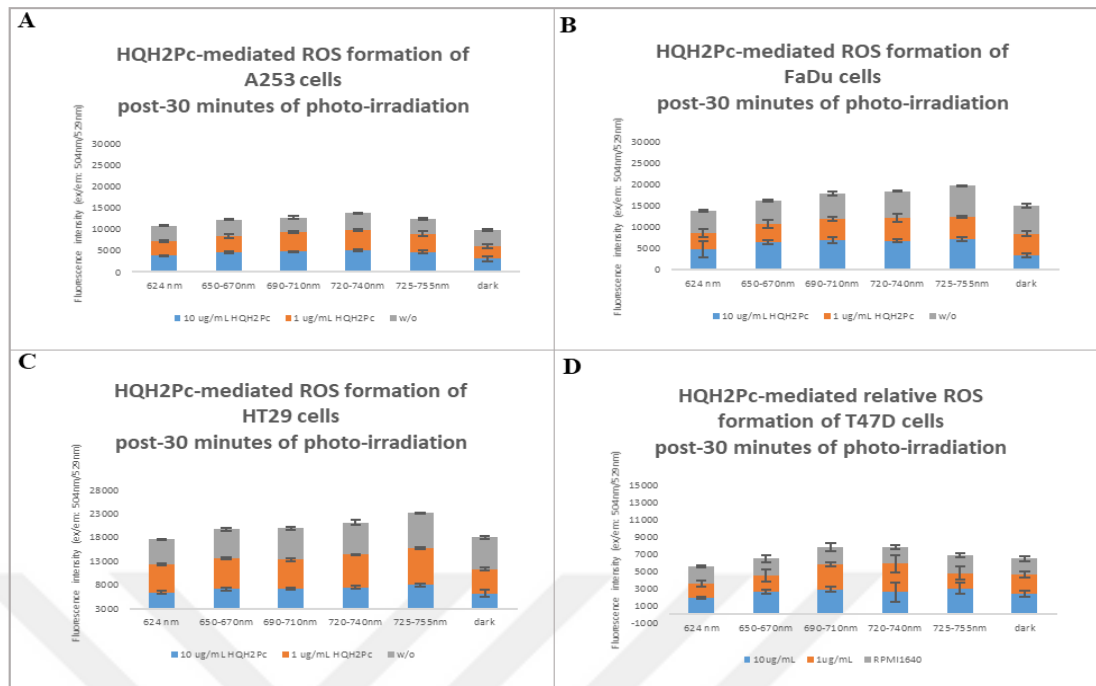


Figure 57 Dose dependent post-30 minutes photo-induced ROS formation of HQH₂Pc phthalocyanine on A. Salivary gland carcinoma, A253, B. Pharynx carcinoma, FaDu, C. Colorectal adenocarcinoma, HT29, D. Breast carcinoma, T47D cell lines.

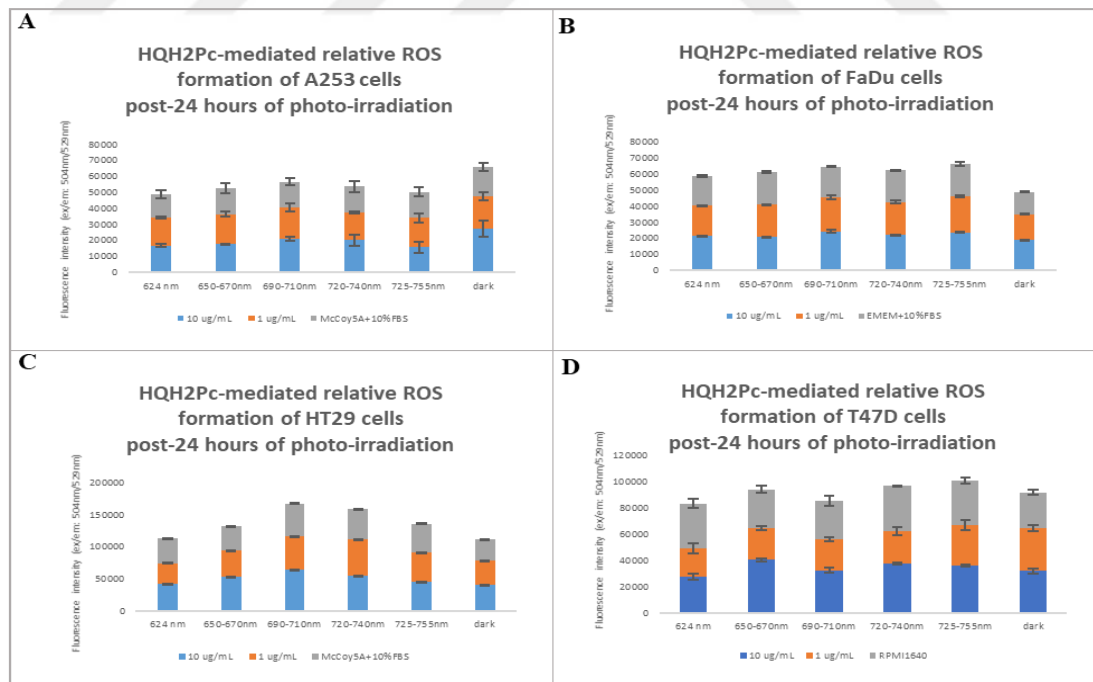


Figure 58 Dose dependent post-24 hours photo-induced ROS formation of HQH₂Pc phthalocyanine on A. Salivary gland carcinoma, A253, B. Pharynx carcinoma, FaDu, C. Colorectal adenocarcinoma, HT29, D. Breast carcinoma, T47D cell lines.

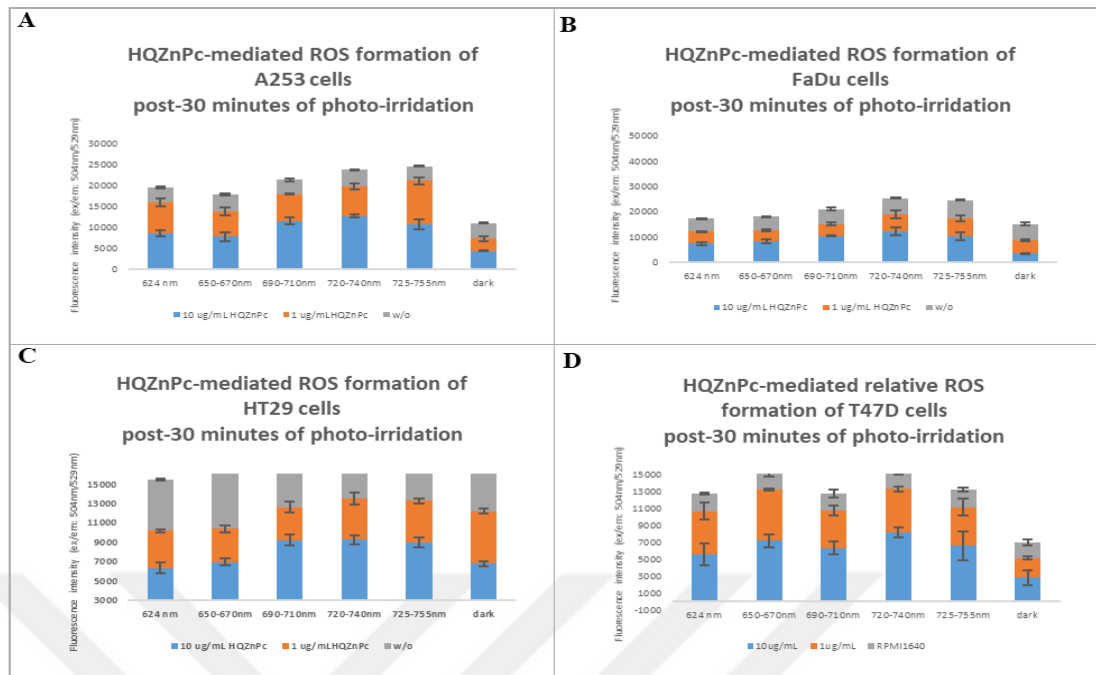


Figure 59 Dose dependent post-30 minutes photo-induced ROS formation of HQZnPc phthalocyanine on A. Salivary gland carcinoma, A253, B. Pharynx carcinoma, FaDu, C. Colorectal adenocarcinoma, HT29, D. Breast carcinoma, T47D cell lines.

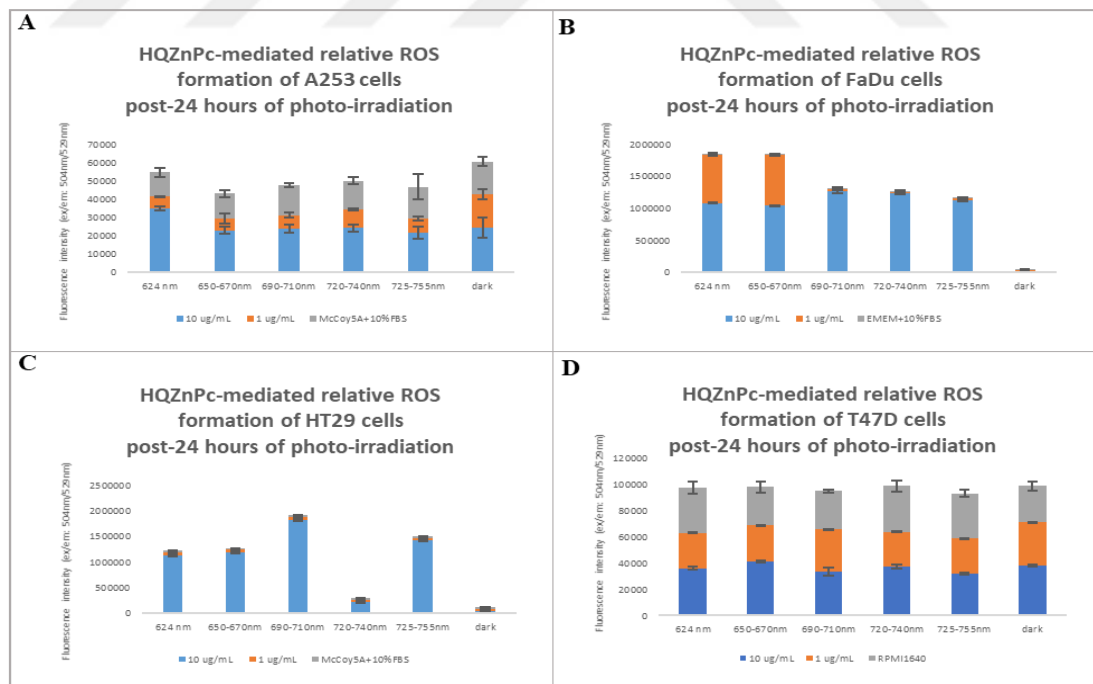


Figure 60 Dose dependent post-24 hours photo-induced ROS formation of HQZnPc phthalocyanine on A. Salivary gland carcinoma, A253, B. Pharynx carcinoma, FaDu, C. Colorectal adenocarcinoma, HT29, D. Breast carcinoma, T47D cell lines.

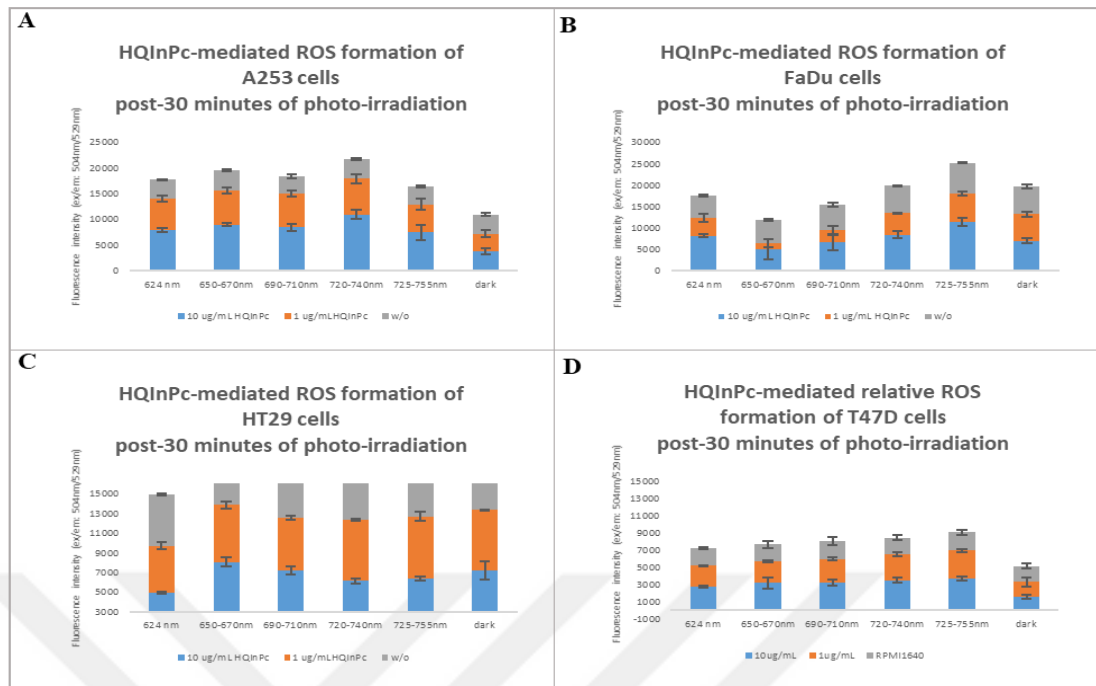


Figure 61 Dose dependent post-30 minutes photo-induced ROS formation of HQInPc phthalocyanine on A. Salivary gland carcinoma, A253, B. Pharynx carcinoma, FaDu, C. Colorectal adenocarcinoma, HT29, D. Breast carcinoma, T47D cell lines.

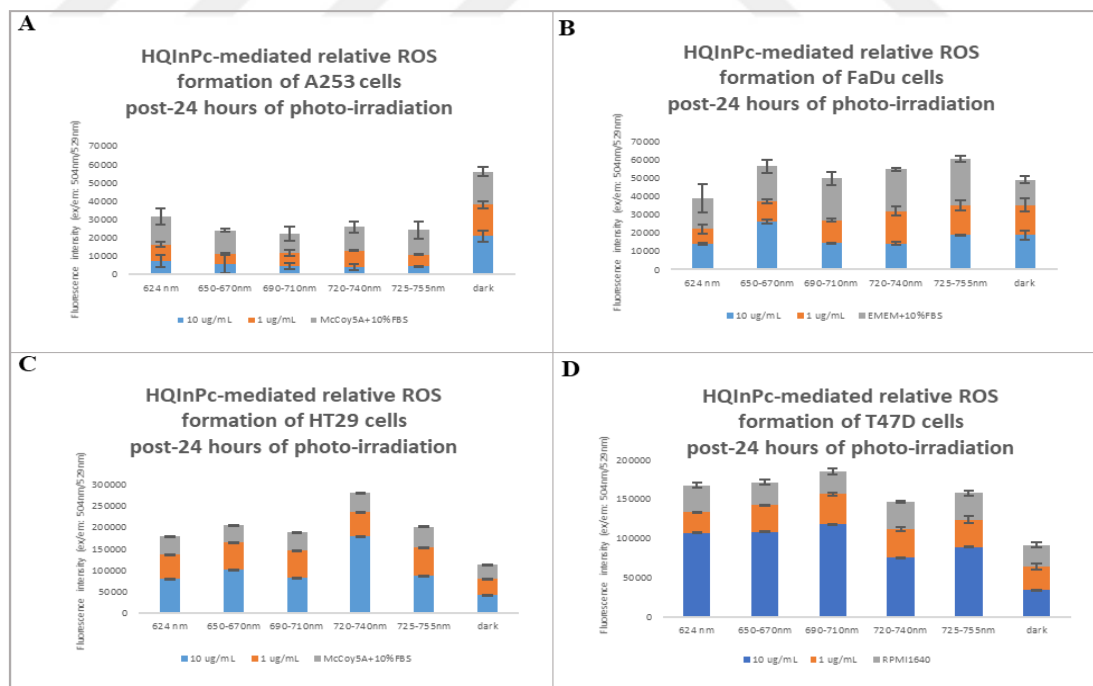


Figure 62 Dose dependent post-24 hours photo-induced ROS formation of HQInPc phthalocyanine on A. Salivary gland carcinoma, A253, B. Pharynx carcinoma, FaDu, C. Colorectal adenocarcinoma, HT29, D. Breast carcinoma, T47D cell lines.

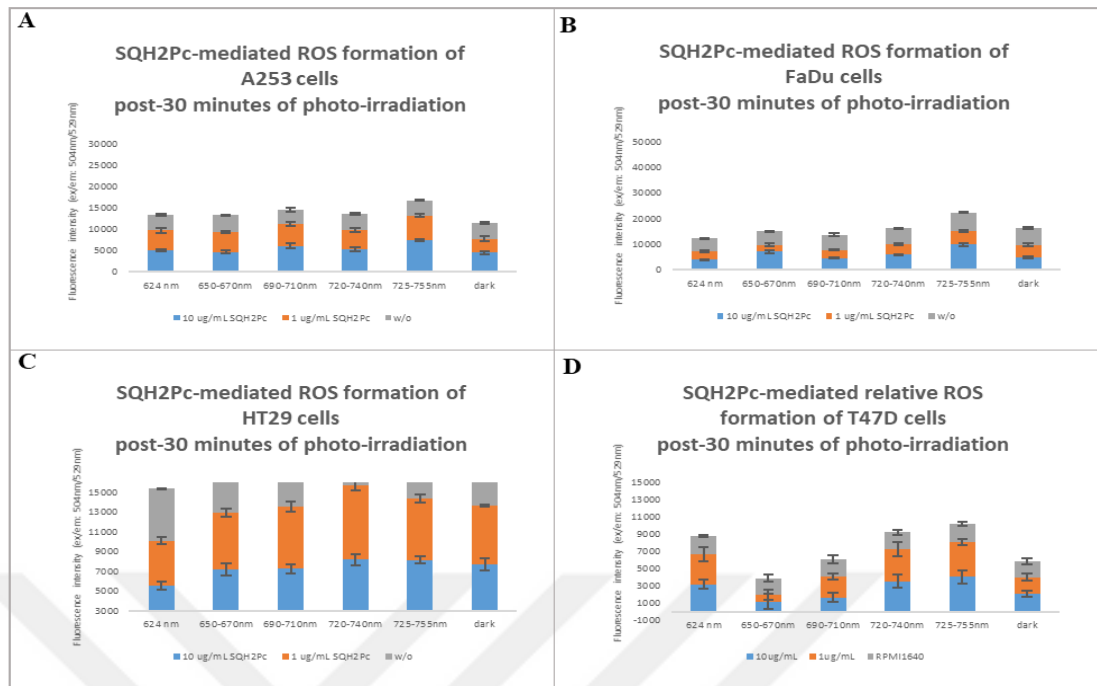


Figure 63 Dose dependent post-30 minutes photo-induced ROS formation of SQH₂Pc phthalocyanine on A. Salivary gland carcinoma, A253, B. Pharynx carcinoma, FaDu, C. Colorectal adenocarcinoma, HT29, D. Breast carcinoma, T47D cell lines.

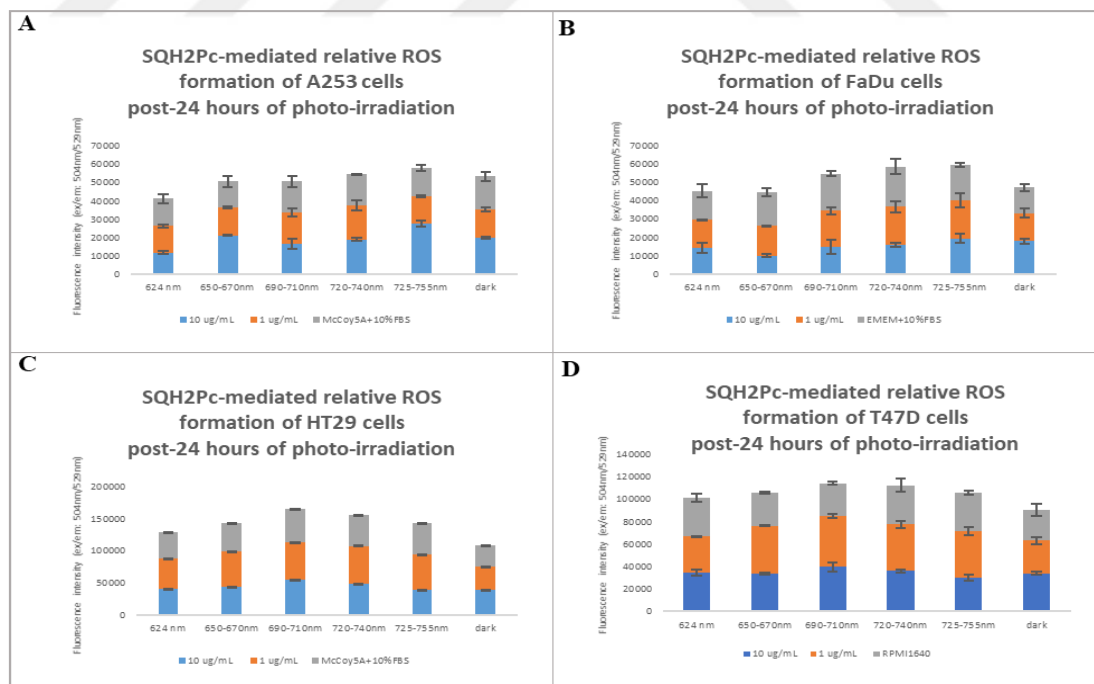


Figure 64 Dose dependent post-24 hours photo-induced ROS formation of SQH₂Pc phthalocyanine on A. Salivary gland carcinoma, A253, B. Pharynx carcinoma, FaDu, C. Colorectal adenocarcinoma, HT29, D. Breast carcinoma, T47D cell lines.

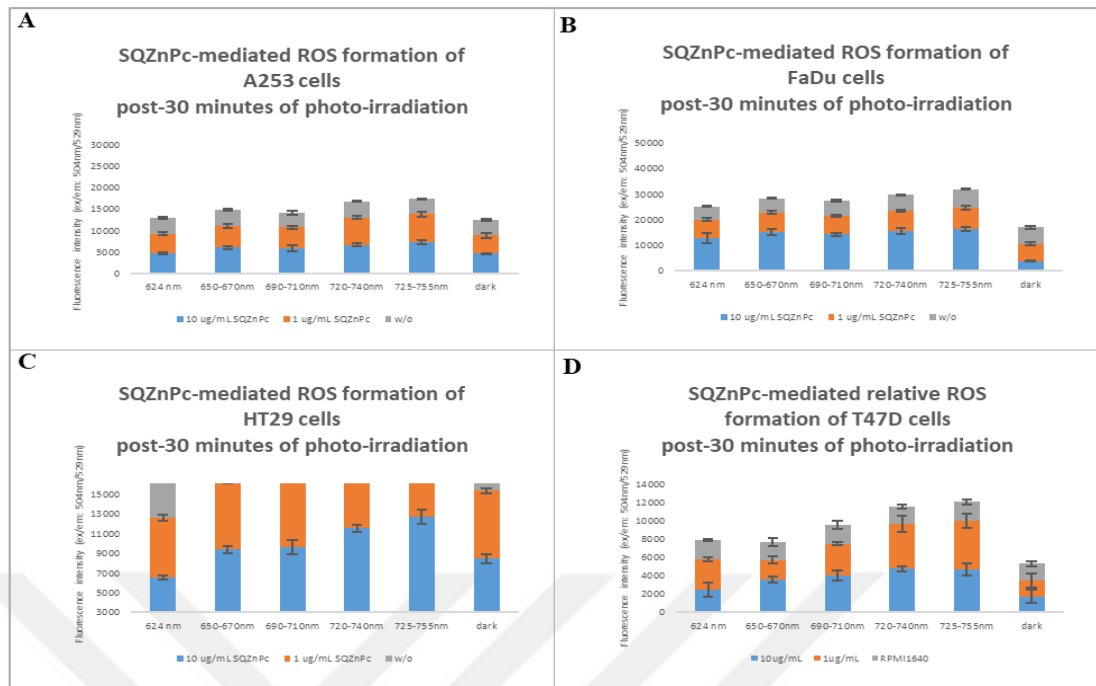


Figure 65 Dose dependent post-30 minutes photo-induced ROS formation of SQZnPc phthalocyanine on A. Salivary gland carcinoma, A253, B. Pharynx carcinoma, FaDu, C. Colorectal adenocarcinoma, HT29, D. Breast carcinoma, T47D cell lines.

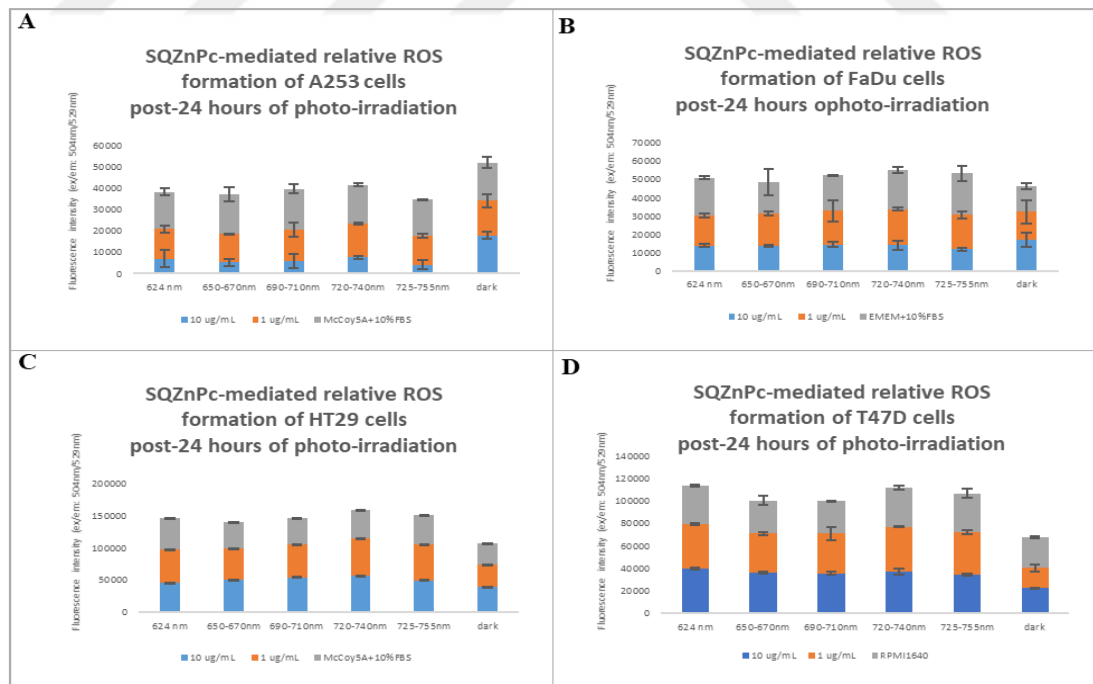


Figure 66 Dose dependent post-24 hours photo-induced ROS formation of SQZnPc phthalocyanine on A. Salivary gland carcinoma, A253, B. Pharynx carcinoma, FaDu, C. Colorectal adenocarcinoma, HT29, D. Breast carcinoma, T47D cell lines.

48. Comparison of PDT-induced Cytotoxicity of Nine Phthalocyanine Molecules on Cancer Cell Lines

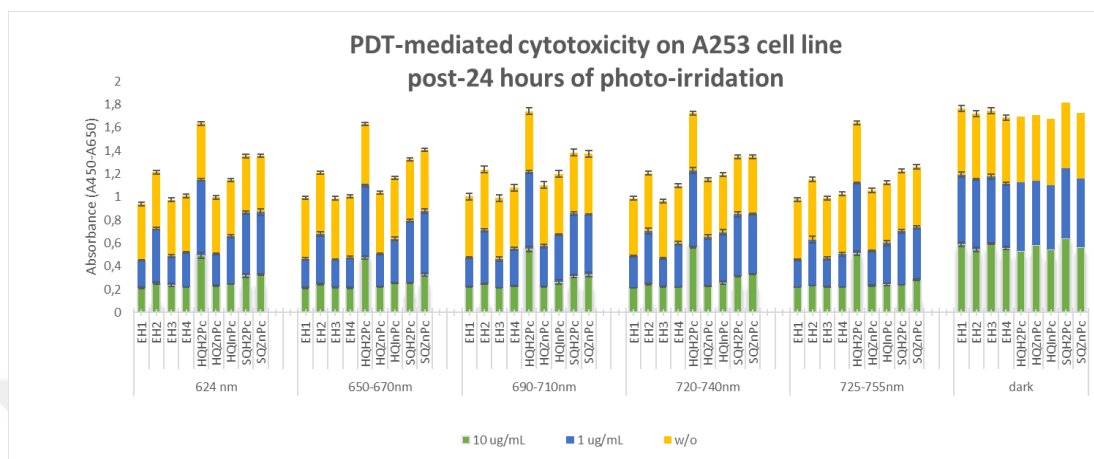


Figure 67 PDT-mediated cytotoxicity of nine phthalocyanine molecules on A253 cell line.

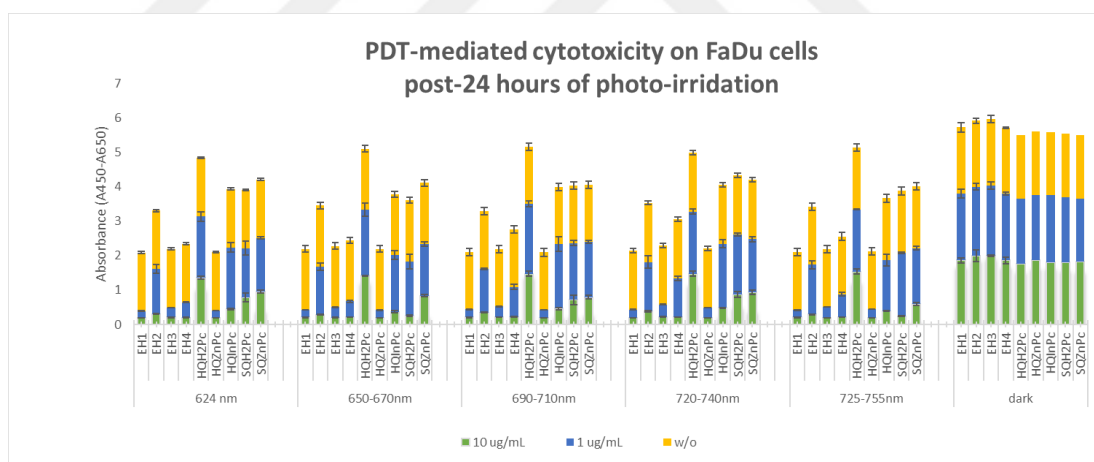


Figure 68 PDT-mediated cytotoxicity of nine phthalocyanine molecules on FaDu cell line.

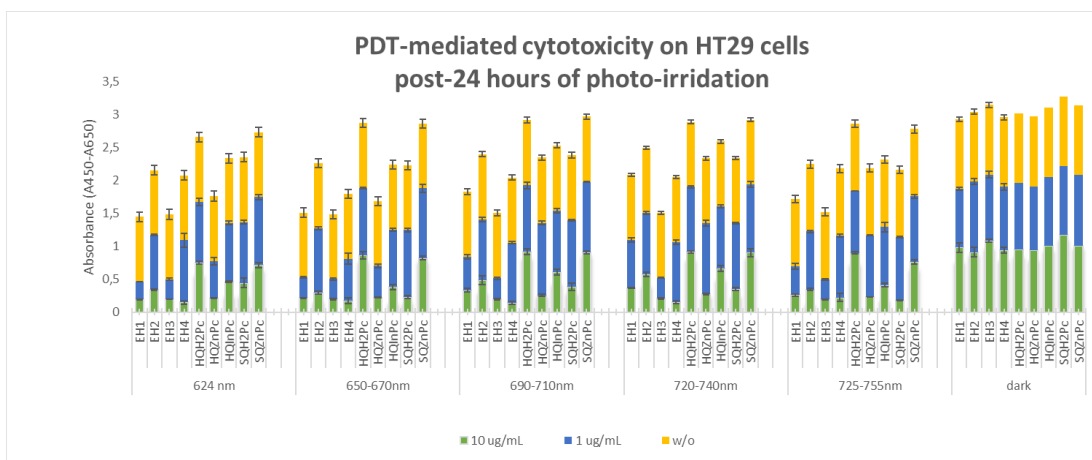


Figure 69 PDT-mediated cytotoxicity of nine phthalocyanine molecules on HT29 cell line.

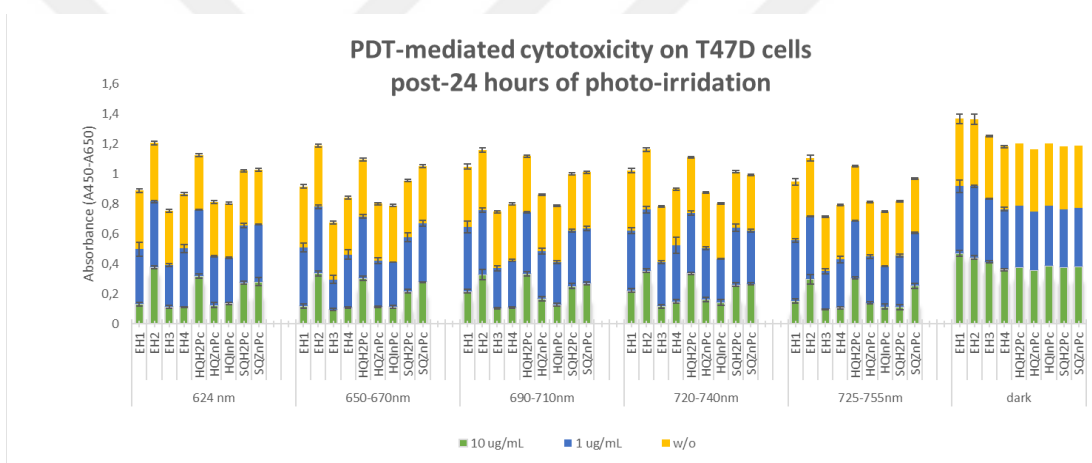


Figure 70 PDT-mediated cytotoxicity of nine phthalocyanine molecules on T47D cell line.

Comparison of PDT-mediated cytotoxicity among nine phthalocyanine molecules revealed that the least cytotoxic response was obtained from the T47D cell line, and the highest cytotoxic response was obtained from FaDu cell line. When overall cytotoxicity after PDT was compared, from the highest to lowest cytotoxicity was orderly on FaDu, HT29, A253, T47D cell lines.

On the A253, FaDu, HT29 and T47D cell lines, EH1, EH3, EH4, and HQZnPc that was applied with a concentration of 10 $\mu\text{g/mL}$ showed the highest cytotoxicity

followed by EH2, HQInPc, SQH₂Pc, and SQZnPc molecules. On T47D cell lines, different from the other cell lines, EH2 showed the lowest cytotoxicity. HQH₂Pc-mediated PDT did not show any cytotoxic response on the cell lines when it was applied with a concentration of 10 µg/ml.

EH1, EH3, EH4, and HQZnPc molecules when they were applied with a concentration of 1 µg/mL showed significant cytotoxicity on FaDu cell line, moderate cytotoxicity on A253 cell lines, whereas the other molecules did not show any cytotoxicity. EH1 and EH3 molecules when they were applied with a concentration of 1 µg/mL showed moderate cytotoxicity on HT29 cell line, whereas the other molecules did not show any cytotoxicity. On T47D cell line, the molecules did not show any cytotoxicity when they were applied with a concentration of 1 µg/ml. HQH₂Pc-mediated PDT did not show any cytotoxic response on the cell lines when it was applied with a concentration of 1 µg/ml.

49. Comparison of PDT-induced Immediate and Late ROS Production of Nine Phthalocyanine Molecules on Cancer Cell Lines

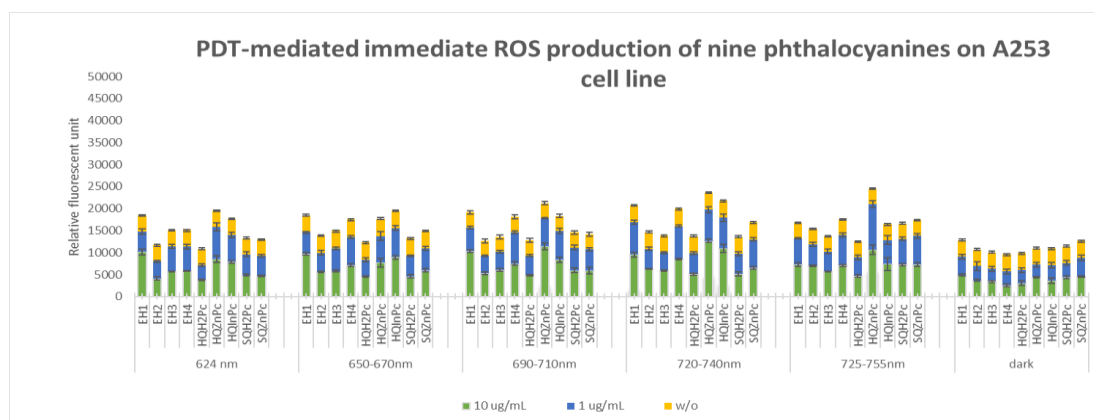


Figure 71 PDT-mediated immediate ROS production of nine phthalocyanine molecules on A253 cell line

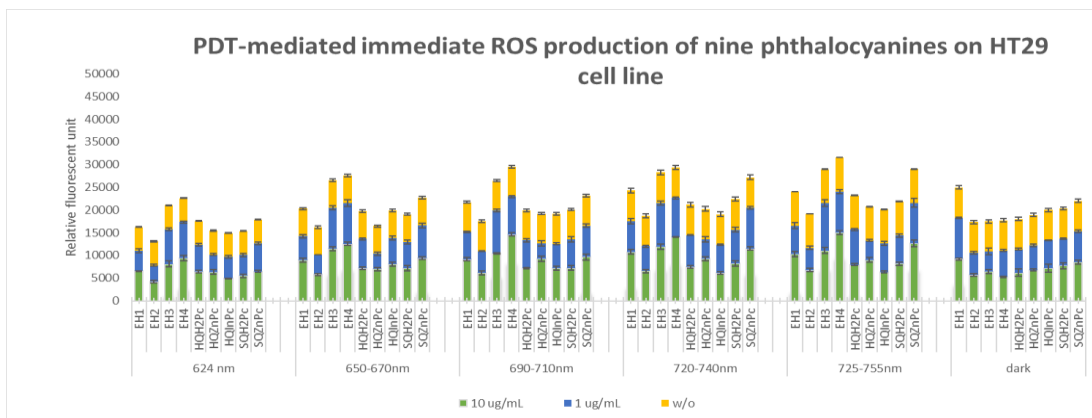


Figure 75 PDT-mediated immediate ROS production of nine phthalocyanine molecules on HT29 cell line

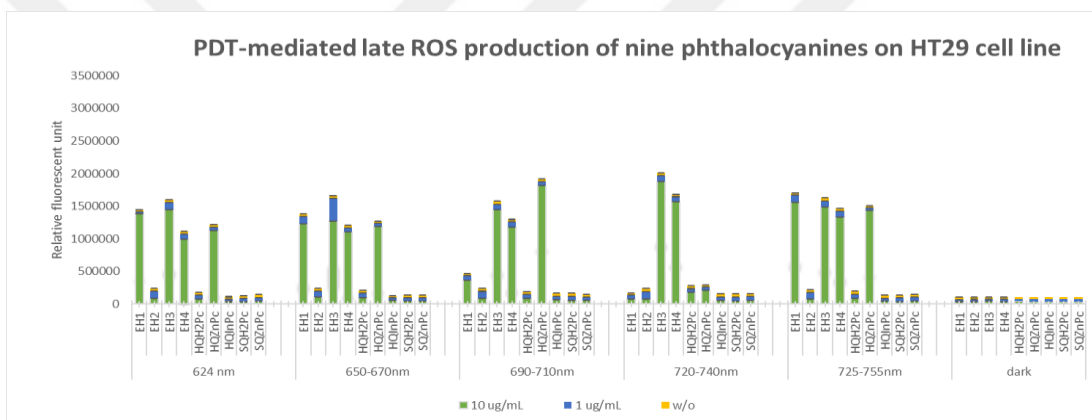


Figure 76 PDT-mediated late ROS production of nine phthalocyanine molecules on HT29 cell line

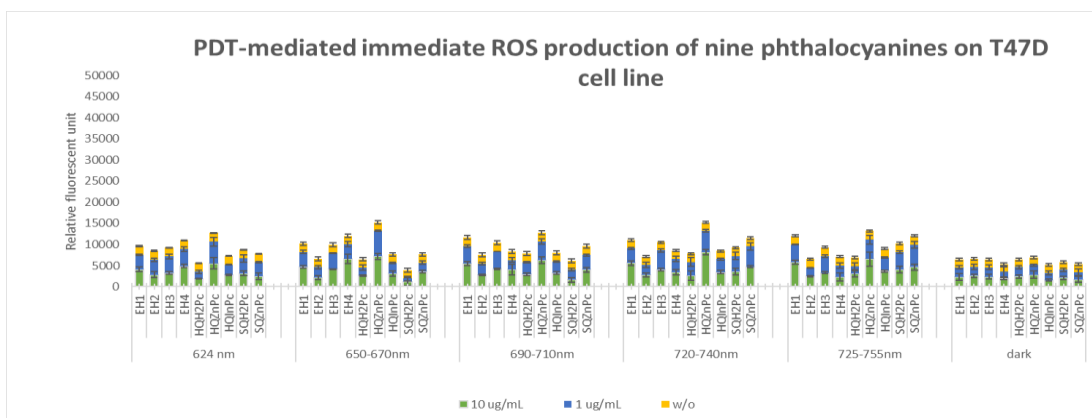


Figure 77 PDT-mediated immediate ROS production of nine phthalocyanine molecules on T47D cell line

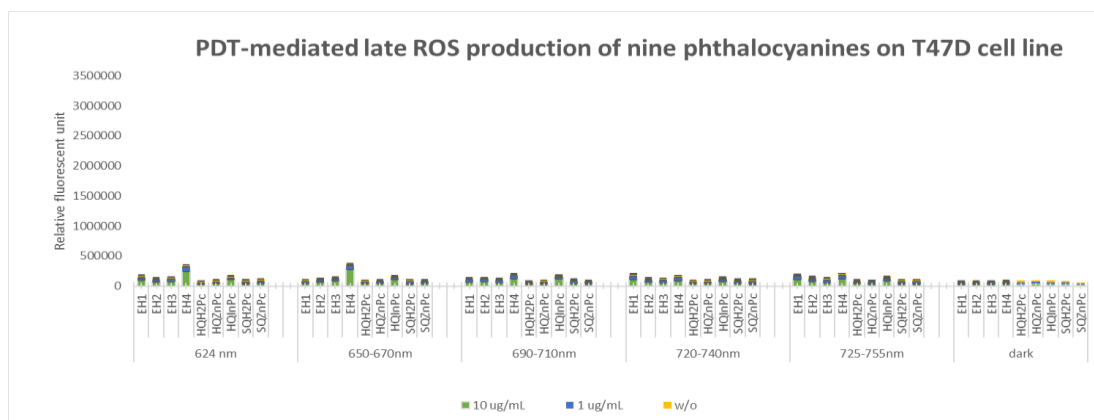


Figure 78 PDT-mediated late ROS production of nine phthalocyanine molecules on T47D cell line

Comparison of PDT-mediated immediate ROS production among nine phthalocyanine molecules revealed that the least ROS production in terms of relative fluorescence unit was obtained from the T47D cell line, and the highest ROS production was obtained from FaDu cell line when it was applied with Pc concentration of 10 $\mu\text{g}/\text{mL}$. On the HT29 cell line, PDT of the molecules did not lead to immediate ROS production since yielding similar RFU values compared to dark control groups.

Comparison of PDT-mediated late ROS production among nine phthalocyanine molecules revealed that the least ROS production in terms of relative fluorescence unit was obtained from the T47D cell line, and the highest ROS production was obtained from FaDu cell line.

When overall ROS production after PDT was compared, from the highest to the lowest ROS production was orderly on FaDu, HT29, A253, T47D cell lines. ROS amount produced through all cancer cell lines in the dark was very low compared to the PDT-mediated ROS amount following 24 hours of light irradiation.

PDT-induced late ROS production of A253 cell lines varied across different wavelengths. Following 24 hours of PDT, the highest amount of ROS produced at 624 nm by EH4 molecule, at 650-670 nm by EH3 and EH4 molecules, and at 725-755 nm by EH2 and EH3 molecule when 10 $\mu\text{g} / \text{ml}$ concentrations of the molecules were applied.

On the FaDu cell line, EH1, EH3, EH4, and HQZnPc molecules triggered the highest ROS production following 24 hours of PDT at all wavelengths that were applied. However, PDT with both concentration of HQZnPc molecule had a certain increase in ROS at 624 nm and 650-670 nm, while reducing ROS production at 690-710 nm, 720-740 nm, and 725-755nm when it was applied with a concentration of 1 $\mu\text{g}/\text{ml}$.

On the HT29 cell line, EH1, EH3, EH4, and HQZnPc molecules triggered the highest ROS production following 24 hours of PDT at all wavelengths that were applied.

On the T47D cell line, EH4 molecule triggered the highest ROS production following 24 hours of PDT when it was applied with a concentration of 10 $\mu\text{g}/\text{ml}$. However, among cell lines, the lowest ROS production was obtained from the T47D cell line.

4.10. Tables of Results

4.10.1. Tables of dark cytotoxicity

In this section, cytotoxic effects of the Pc molecules on the cell lines at dark conditions were revealed as percentage value relative to non-treated controls.

Table 11 Relative percentage cell viability of cancer cell lines following 24 hours of EH1 phthalocyanine administrations at dark.

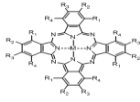
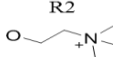
EH1	Concentration	A253	FaDu	HT29	T47D
	100 µg/ml	89	83	109	65
	10 µg/ml	109	79	103	79
Center metal Zn	1 µg/ml	102	78	107	91
R2 	0,1 µg/ml	102	84	93	87

Table 12 Relative percentage cell viability of cancer cell lines following 24 hours of EH2 phthalocyanine administrations at dark.

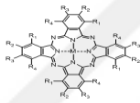
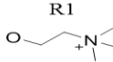
EH2	Concentration	A253	FaDu	HT29	T47D
	100 µg/ml	83	83	86	62
	10 µg/ml	91	83	89	71
Center metal Zn	1 µg/ml	98	75	85	70
R1 	0,1 µg/ml	102	81	88	74

Table 13 Relative percentage cell viability of cancer cell lines following 24 hours of EH3 phthalocyanine administrations at dark.

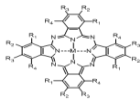
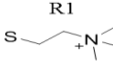
EH3	Concentration	A253	FaDu	HT29	T47D
	100 µg/ml	95	83	93	93
	10 µg/ml	94	79	81	106
Center metal Zn	1 µg/ml	98	82	87	103
R1 	0,1 µg/ml	92	83	74	111

Table 14 Relative percentage cell viability of cancer cell lines following 24 hours of EH4 phthalocyanine administrations at dark.

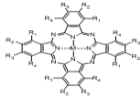
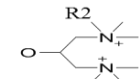
EH4	Concentration	A253	FaDu	HT29	T47D
	100 µg/ml	89	74	80	61
	10 µg/ml	97	74	77	74
Center metal Zn	1 µg/ml	96	72	76	71
	0,1 µg/ml	95	75	74	78

Table 15 Relative percentage cell viability of cancer cell lines following 24 hours of HQH₂Pc phthalocyanine administrations at dark.

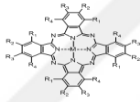
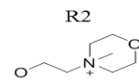
HQH ₂ Pc	Concentration	A253	FaDu	HT29	T47D
	100 µg/ml	69	83	83	53
	10 µg/ml	80	81	96	72
Center metal 2H	1 µg/ml	102	76	102	70
	0,1 µg/ml	98	79	98	80

Table 16 Relative percentage cell viability of cancer cell lines following 24 hours of HQZnPc phthalocyanine administrations at dark.

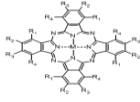
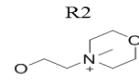
HQZnPc	Concentration	A253	FaDu	HT29	T47D
	100 µg/ml	69	72	73	75
	10 µg/ml	87	74	89	78
Center metal Zn	1 µg/ml	90	74	81	89
	0,1 µg/ml	94	82	90	78

Table 17 Relative percentage cell viability of cancer cell lines following 24 hours of HQInPc phthalocyanine administrations at dark.

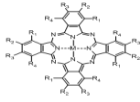
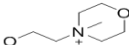
HQInPc	Concentration	A253	FaDu	HT29	T47D
	100 µg/ml	90	88	83	112
	10 µg/ml	95	91	82	119
Center metal InCl	1 µg/ml	97	93	100	107
R2 	0,1 µg/ml	96	92	121	98

Table 18 Relative percentage cell viability of cancer cell lines following 24 hours of SQH₂Pc phthalocyanine administrations at dark.

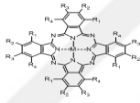
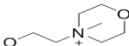
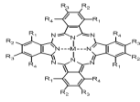
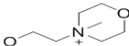
SQH ₂ Pc	Concentration	A253	FaDu	HT29	T47D
	10 µg/ml 1 µg/ml	100	65	93	75
	10 µg/ml 1 µg/ml	98	71	71	80
Center metal 2H	10 µg/ml 1 µg/ml	100	72	88	80
R1 	10 µg/ml 1 µg/ml	97	75	84	89

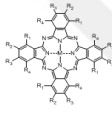
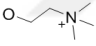
Table 19 Relative percentage cell viability of cancer cell lines following 24 hours of SQZnPc phthalocyanine administrations at dark.

SQZnPc	Concentration	A253	FaDu	HT29	T47D
	100 µg/ml	93	87	113	79
	10 µg/ml	94	89	102	90
Center metal Zn	1 µg/ml	102	91	107	90
R1 	0,1 µg/ml	104	92	106	84

4.10.2. Comparative table of experiments with EH1 phthalocyanine

In this section, overall results obtained from EH1-mediated PDT with five different wavelengths were revealed as percentage value relative to non-treated controls.

Table 20 Relative percentage cell viability and ROS formation of cancer cell lines after photodynamic therapy with EH1 phthalocyanine at 624 nm (light fluence of 2 joules/cm²).

EH1	Assay	Wavelength	Concentration	A253	FaDu	HT29	T47D
	Cytotoxicity (WST-1)	624 nm	10 µg/ml	37	10	18	30
			1 µg/ml	42	11	26	81
	Cytotoxicity (Resazurin)		10 µg/ml	25	7	28	22
			1 µg/ml	44	5	70	64
	Center metal Zn ROS (30 minutes)		10 µg/ml	269	157	98	220
			1 µg/ml	123	81	67	185
R2 	ROS (24 hours)	10 µg/ml	821	11492	4091	361	
		1 µg/ml	48	5624	112	164	

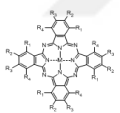
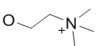
At wavelength of 624 nm with 2 joules/cm² light fluence, photo-induced cellular damage caused by the EH1 molecule was measured in each cancer cell line but in different degrees. According to WST-1 assay, the most affected cell line was FaDu cell line where both high and low doses of EH1 molecule lead to appx. 90% cell death relative to the non-treated control. Other cell lines, HT29 and A253 cell lines were significantly affected by photodynamic therapy of both high and low doses of EH1 molecule, while the T47D cell line only affected from photodynamic therapy of high dose of EH1 molecule, and not affected from low dose.

Considering 10 percent difference is acceptable, there were some differences above this limit between WST-1 and resazurin assay. However, according to general

trends of viability depend on the Pc concentration, the resazurin assay results mostly supported the WST-1 assay.

EH-1 induced immediate ROS production was seen by both high and low dose of the molecule on A253 and T47D cell line, only high dose on FaDu cell line, and there were not ROS production of HT29 cell line. When to look at the late ROS production following PDT, EH1-induced PDT triggered ROS production on each cell line, except A253 cell line when applied low dose of the molecule. The highest ROS production was measured from the FaDu cell line, followed by HT29, T47D and A253 cell lines, respectively.

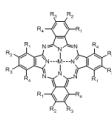
Table 21 Relative percentage cell viability and ROS formation of cancer cell lines after photodynamic therapy with EH1 phthalocyanine at 650-670 nm (light fluence of 2 joules/cm²).

EH1	Assay	Wavelength	Concentration	A253	FaDu	HT29	T47D
	Cytotoxicity (WST-1)	650-670 nm	10 µg/ml	37	11	20	26
			1 µg/ml	44	12	30	87
Cytotoxicity (Resazurin)	10 µg/ml		25	7	25	48	
	1 µg/ml		42	5	58	92	
Center metal Zn	ROS (30 minutes)		10 µg/ml	259	278	134	251
			1 µg/ml	128	79	78	194
R2 	ROS (24 hours)		10 µg/ml	533	11162	3641	154
			1 µg/ml	52	5631	354	118

At wavelength of 650-670 nm with 2 joules/cm² light fluence, photo-induced cellular damage caused by the EH1 molecule was measured in each cancer cell line except T47D cell line when it was applied with low dose of the molecule. According to the assays, the most affected cell line was FaDu cell line where both high and low doses of EH1 molecule lead to appx. 90% cell death relative to the non-treated control. Other cell lines, HT29 and A253 cell lines were significantly affected by photodynamic therapy of both high and low doses of EH1 molecule, while the T47D

cell line only affected from photodynamic therapy of high dose of EH1 molecule, and not affected from low dose. Considering 10 percent difference is acceptable, there were some differences above this limit between WST-1 and resazurin assay. However, according to general trends of viability depend on the Pc concentration, the resazurin assay results mostly supported the WST-1 assay. EH-1 induced immediate ROS production was seen on each cell line in different degrees except FaDu and HT29 cell line when it was applied by low dose of the molecule. The highest amount of ROS was seen on the FaDu cell line caused by high dose of the molecule, it was followed by A253, T47D and HT29 cell lines, respectively. When to look at the late ROS production following PDT, EH1-induced PDT triggered ROS production on each cell line except A253 and T47D cell lines when were applied by low dose of the molecule. The highest ROS production was measured from the FaDu cell line, also HT29, A253, and T47D cell lines, respectively.

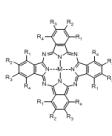
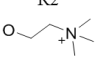
Table 22 Relative percentage cell viability and ROS formation of cancer cell lines after photodynamic therapy with EH1 phthalocyanine at 690-710 nm (light fluence of 2 joules/cm²).

EH1	Assay	Wavelength	Concentration	A253	FaDu	HT29	T47D
	Cytotoxicity (WST-1)	690-710 nm	10 µg/ml	39	11	32	48
			1 µg/ml	44	13	48	96
Cytotoxicity (Resazurin)	10 µg/ml		26	12	56	40	
	1 µg/ml		56	10	76	87	
Center metal Zn	ROS (30 minutes)		10 µg/ml	273	237	137	298
			1 µg/ml	143	114	90	222
R2	ROS (24 hours)		10 µg/ml	787	10216	1083	222
			1 µg/ml	34	7318	204	172

At wavelength of 690-710 nm with 2 joules/cm² light fluence, photo-induced cellular damage caused by the EH1 molecule was measured in each cancer cell line except T47D cell line when it was applied by low dose of the molecule. According to both WST-1 and resazurin assays, the most affected cell line was FaDu cell line where both high and low doses of EH1 molecule lead to appx. 90% cell death relative to the

non-treated control. Other cell lines, HT29 and A253 cell lines were significantly affected by photodynamic therapy of both high and low doses of EH1 molecule, while the T47D cell line only affected from photodynamic therapy of high dose of EH1 molecule, and not affected from low dose. Considering 10 percent difference is acceptable, there were some differences above this limit between WST-1 and resazurin assay. However, according to general trends of viability depend on the Pc concentration, the resazurin assay results mostly supported the WST-1 assay. EH-1 induced immediate ROS production was seen on each cell line when applied by high dose of the molecule. The highest amount of ROS was seen on the T47D cell line, it was followed by A253, FaDu, and HT29 cell lines, respectively. When to look at the late ROS production following PDT, EH1-induced PDT triggered ROS production on each cell line. The highest ROS production was measured from the FaDu cell line, also, HT29, A253 and T47D cell lines, respectively. The least ROS production was seen on the A253 cell line, even a low dose of EH1 did not trigger ROS on the A253 cell line.

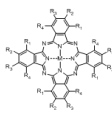
Table 23 Relative percentage cell viability and ROS formation of cancer cell lines after photodynamic therapy with EH1 phthalocyanine at 720-740 nm (light fluence of 2 joules/cm²).

EH1	Assay	Wavelength	Concentration	A253	FaDu	HT29	T47D
	Cytotoxicity (WST-1)	720-740 nm	10 µg/ml	37	11	35	49
			1 µg/ml	48	13	69	89
Cytotoxicity (Resazurin)	10 µg/ml		24	12	71	25	
	1 µg/ml		66	15	82	73	
Center metal Zn	ROS (30 minutes)		10 µg/ml	253	793	161	302
			1 µg/ml	194	159	101	189
	ROS (24 hours)		10 µg/ml	1160	8640	241	396
			1 µg/ml	32	7469	163	204

At wavelength of 720-740 nm with 2 joules/cm² light fluence, photo-induced cellular damage caused by the EH1 molecule was measured in each cancer cell line but in different degrees. According to both WST-1 and resazurin assay, the most

affected cell line was FaDu cell line where both high and low doses of EH1 molecule lead to appx. 90% cell death relative to the non-treated control. Other cell lines, A253, HT29, and T47D cell lines were significantly affected by photodynamic therapy of only high dose of EH1 molecule, while they were not affected from PDT with low of the molecule. Considering 10 percent difference is acceptable, there were some differences above this limit between WST-1 and resazurin assay. However, according to general trends of viability depend on the Pc concentration, the resazurin assay results mostly supported the WST-1 assay. EH-1 induced immediate ROS production was seen on each cell line in different degrees. The highest amount of ROS was seen on the FaDu cell line, it was followed by T47D, A253, and HT29 cell lines, respectively. Low dose of the molecule did not trigger HT29 cell line to produce ROS immediately. When to look at the late ROS production following PDT, EH1-induced PDT triggered ROS production on each cell line. The highest ROS production was measured from the FaDu cell line, also A253, T47D and HT29 cell lines, respectively. The least ROS production was seen on the A253 cell line, even a low dose of EH1 did not trigger ROS on the A253 cell line.

Table 24 Relative percentage cell viability and ROS formation of cancer cell lines after photodynamic therapy with EH1 phthalocyanine at 725-755 nm (light fluence of 2 joules/cm²).

EH1	Assay	Wavelength	Concentration	A253	FaDu	HT29	T47D
	Cytotoxicity (WST-1)	725-755 nm	10 µg/ml	38	11	25	34
			1 µg/ml	41	12	41	90
	Cytotoxicity (Resazurin)		10 µg/ml	25	9	40	23
			1 µg/ml	51	8	76	72
Center metal Zn	ROS (30 minutes)		10 µg/ml	194	466	154	313
			1 µg/ml	156	166	94	223
R2	ROS (24 hours)		10 µg/ml	2522	10718	4616	378
			1 µg/ml	45	6441	332	205

At wavelength of 725-755 nm with 2 joules/cm² light fluence, photo-induced cellular damage caused by the EH1 molecule was measured in each cancer cell line

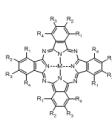
but in different degrees. According to WST-1 assay, the most affected cell line was FaDu cell line where both high and low doses of EH1 molecule lead to appx. 90% cell death relative to the non-treated control. Other cell lines, HT29 and A253 cell lines were significantly affected by photodynamic therapy of both high and low doses of EH1 molecule, while the T47D cell line only affected from photodynamic therapy of high dose of EH1 molecule, and not affected from low dose. Considering 10 percent difference is acceptable, there were some differences above this limit between WST-1 and resazurin assay. However, according to general trends of viability depend on the Pc concentration, the resazurin assay results mostly supported the WST-1 assay.

EH-1 induced immediate ROS production was seen on each cell line in different degrees. The highest amount of ROS was seen on the FaDu cell line, it was followed by T47D, A253, and HT29 cell lines, respectively. When to look at the late ROS production following PDT, EH1-induced PDT triggered ROS production on each cell line. The highest ROS production was measured from the FaDu cell line, also T47D, HT29, and A253 cell lines, respectively. The least Ros production was seen on the A253 cell line, even a low dose of EH1 did not trigger ROS on the A253 cell line.

4.10.3. Comparative table of experiments with EH2 phthalocyanine

In this section, overall results obtained from EH2-mediated PDT with five different wavelengths were collected as percentage relative to non-treated control. Each data was revealed as % value.

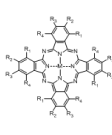
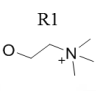
Table 25 Relative percentage cell viability and ROS formation of cancer cell lines after photodynamic therapy with EH2 phthalocyanine at 624 nm (light fluence of 2 joules/cm²).

EH2	Assay	Wavelength	Concentration	A253	FaDu	HT29	T47D
	Cytotoxicity (WST-1)	624 nm	10 µg/ml	44	17	32	84
			1 µg/ml	83	71	79	98
	Cytotoxicity (Resazurin)		10 µg/ml	42	28	75	41
			1 µg/ml	99	78	71	88
Center metal Zn	ROS (30 minutes)		10 µg/ml	110	132	63	151
			1 µg/ml	102	72	54	195
R1	ROS (24 hours)		10 µg/ml	52	270	253	235
			1 µg/ml	49	163	341	129

At wavelength of 624 nm with 2 joules/cm² light fluence, photo-induced cellular damage caused by the EH2 molecule was measured in each cancer cell line except T47D cell line for the high dose of EH2 molecule, and there was no effect was shown for the low dose of the molecule. According to WST-1 assay, the most affected cell line was FaDu cell line, followed by HT29, and A253 cell lines. Considering 10 percent difference is acceptable, there were some differences above this limit between WST-1 and resazurin assay. However, according to general trends of viability depend on the Pc concentration, the resazurin assay results mostly supported the WST-1 assay.

Right after PDT, either high or low doses of EH2 molecule did not trigger ROS formation on the A253, FaDu, and HT29 cell lines. However, high dose of the molecule triggered immediate ROS formation on T47D cell line. Following PDT, late ROS formation was triggered with PDT of both doses of EH2 molecule on each cell line except A253 cell line. Compared to the results, it can be said that the cytotoxic responses of FaDu, HT29, and T47D cell lines were ROS dependent, however cytotoxic response of A253 cell line was not ROS-dependent.

Table 26 Relative percentage cell viability and ROS formation of cancer cell lines after photodynamic therapy with EH2 phthalocyanine at 650-670 nm (light fluence of 2 joules/cm²).

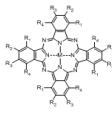
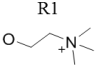
EH2	Assay	Wavelength	Concentration	A253	FaDu	HT29	T47D
 Center metal Zn	Cytotoxicity (WST-1)	650-670 nm	10 µg/ml	43	15	28	75
			1 µg/ml	76	76	92	99
	Cytotoxicity (Resazurin)		10 µg/ml	37	18	70	36
			1 µg/ml	98	82	75	82
	ROS (30 minutes)		10 µg/ml	149	115	86	116
			1 µg/ml	115	49	65	133
 R1	ROS (24 hours)	10 µg/ml	61	754	331	232	
		1 µg/ml	43	145	271	128	

At wavelength of 650-670 nm with 2 joules/cm² light fluence, photo-induced cellular damage caused by the EH2 molecule was measured on A253, FaDu, and HT29 cell lines for the high dose of EH2 molecule, and there was no effect was shown for the low dose of the molecule. According to WST-1 assay, the most affected cell line from EH2-mediated PDT was FaDu cell line, followed by HT29, and A253 cell lines.

Considering 10 percent difference is acceptable, there were some differences above this limit between WST-1 and resazurin assay. However, according to general trends of viability depend on the Pc concentration, the resazurin assay results mostly supported the WST-1 assay.

Right after PDT, high dose of EH2 molecule triggered ROS formation on the A253, FaDu, and both high and low dose triggered ROS formation on T47D cell lines. Following PDT, late ROS formation was triggered with PDT of both doses of EH2 molecule on each cell line except A253 cell line. Compared to the results, it can be said that the cytotoxic responses of FaDu, HT29, and T47D cell lines were ROS dependent, however cytotoxic response of A253 cell line was not ROS-dependent.

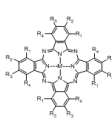
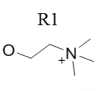
Table 27 Relative percentage cell viability and ROS formation of cancer cell lines after photodynamic therapy with EH2 phthalocyanine at 690-710 nm (light fluence of 2 joules/cm²).

EH2	Assay	Wavelength	Concentration	A253	FaDu	HT29	T47D
 Center metal Zn	Cytotoxicity (WST-1)	690-710 nm	10 µg/ml	43	19	46	73
			1 µg/ml	81	69	87	96
	Cytotoxicity (Resazurin)		10 µg/ml	46	31	78	37
			1 µg/ml	89	88	76	86
	ROS (30 minutes)		10 µg/ml	140	110	91	149
			1 µg/ml	104	56	72	146
 R1	ROS (24 hours)	10 µg/ml	25	219	268	274	
		1 µg/ml	52	135	311	141	

At wavelength of 690-710 nm with 2 joules/cm² light fluence, photo-induced cellular damage caused by the EH2 molecule was measured in each cancer cell line except T47D cell line for the high dose of EH2 molecule, and there was no effect was shown for the low dose of the molecule. According to WST-1 assay, the most affected cell line was FaDu cell line, followed by HT29, and A253 cell lines. Considering 10 percent difference is acceptable, there were some differences above this limit between WST-1 and resazurin assay. However, according to general trends of viability depend on the Pc concentration, the resazurin assay results mostly supported the WST-1 assay.

Right after PDT, high doses of EH2 molecule triggered immediate ROS formation on the A253, FaDu, and both dose of the molecule triggered ROS formation on T47D cell lines. However, neither low nor high dose of the molecule did not trigger immediate ROS formation on HT29 cell line. Following PDT, late ROS formation was triggered with PDT of both doses of EH2 molecule on each cell line except A253 cell line. Compared to the results, it can be said that the cytotoxic responses of FaDu, HT29, and T47D cell lines were ROS dependent, however cytotoxic response of A253 cell line was not ROS-dependent.

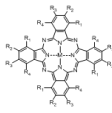
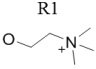
Table 28 Relative percentage cell viability and ROS formation of cancer cell lines after photodynamic therapy with EH2 phthalocyanine at 720-740nm (light fluence of 2 joules/cm²).

EH2	Assay	Wavelength	Concentration	A253	FaDu	HT29	T47D
 Center metal Zn	Cytotoxicity (WST-1)	720-740 nm	10 µg/ml	43	21	54	79
			1 µg/ml	81	78	88	91
	Cytotoxicity (Resazurin)		10 µg/ml	48	44	82	50
			1 µg/ml	101	86	76	86
	ROS (30 minutes)		10 µg/ml	167	123	98	152
			1 µg/ml	120	62	82	129
 R1	ROS (24 hours)	10 µg/ml	40	161	238	214	
		1 µg/ml	44	128	337	151	

At wavelength of 720-740 nm with 2 joules/cm² light fluence, photo-induced cellular damage caused by the EH2 molecule was measured in each cancer cell line except T47D cell line for the high dose of EH2 molecule, and there was no effect was shown for the low dose of the molecule. According to WST-1 assay, the most affected cell line was FaDu cell line, followed by HT29, and A253 cell lines. Considering 10 percent difference is acceptable, there were some differences above this limit between WST-1 and resazurin assay. However, according to general trends of viability depend on the Pc concentration, the resazurin assay results mostly supported the WST-1 assay.

Right after PDT, high doses of EH2 molecule triggered immediate ROS formation on the FaDu cell line, and both dose of the molecule triggered ROS formation on A253 and T47D cell lines. However, neither low nor high dose of the molecule did not trigger immediate ROS formation on HT29 cell line. Following PDT, late ROS formation was triggered with PDT of both doses of EH2 molecule on each cell line except A253 cell line. Compared to the results, it can be said that the cytotoxic responses of FaDu, HT29, and T47D cell lines were ROS dependent, however cytotoxic response of A253 cell line was not ROS-dependent.

Table 29 Relative percentage cell viability and ROS formation of cancer cell lines after photodynamic therapy with EH2 phthalocyanine at 725-755 nm (light fluence of 2 joules/cm²).

EH2	Assay	Wavelength	Concentration	A253	FaDu	HT29	T47D
 Center metal Zn	Cytotoxicity (WST-1)	725-755 nm	10 µg/ml	41	16	32	66
			1 µg/ml	70	79	83	93
	Cytotoxicity (Resazurin)		10 µg/ml	36	25	77	31
			1 µg/ml	98	82	78	82
	ROS (30 minutes)		10 µg/ml	187	168	101	135
			1 µg/ml	129	121	74	105
 R1	ROS (24 hours)	10 µg/ml	69	344	237	281	
		1 µg/ml	32	148	294	140	

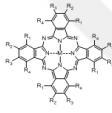
At wavelength of 725-755 nm with 2 joules/cm² light fluence, photo-induced cellular damage caused by the EH2 molecule was measured in each cancer cell line for the high dose of EH2 molecule, and there was no effect was shown for the low dose of the molecule. According to WST-1 assay, the most affected cell line was FaDu cell line, followed by HT29, A253, and T47D cell lines. Considering 10 percent difference is acceptable, there were some differences above this limit between WST-1 and resazurin assay. However, according to general trends of viability depend on the Pc concentration, the resazurin assay results mostly supported the WST-1 assay.

Right after PDT, either high or low doses of EH2 molecule did not trigger ROS formation on the cell lines. Following PDT, low dose of EH2 did not lead to late ROS formation, while high dose of EH2 induced late ROS production on each cell line in different degrees. The highest amount of ROS was seen on the T47D cell line, it was followed by FaDu, HT29, and A253 cell lines, respectively. Compared to the results, it can be said that the cytotoxic responses of each cell line were ROS dependent.

4.10.4. Comparative table of experiments with EH3 phthalocyanine

In this section, overall results obtained from EH3-mediated PDT with five different wavelengths were collected as percentage relative to non-treated control. Each data was revealed as % value.

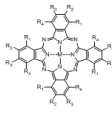
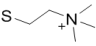
Table 30 Relative percentage cell viability and ROS formation of cancer cell lines after photodynamic therapy with EH3 phthalocyanine at 624 nm (light fluence of 2 joules/cm²).

EH3	Assay	Wavelength	Concentration	A253	FaDu	HT29	T47D	
	Cytotoxicity (WST-1)	624 nm	10 µg/ml	41	11	19	28	
			1 µg/ml	44	16	29	66	
	Cytotoxicity (Resazurin)		10 µg/ml	22	8	24	30	
			1 µg/ml	57	11	64	84	
	Center metal Zn		ROS (30 minutes)	10 µg/ml	151	141	121	178
				1 µg/ml	151	124	114	207
R1	ROS (24 hours)	10 µg/ml	644	10073	4276	277		
		1 µg/ml	33	9579	343	147		

At wavelength of 624 nm with 2 joules/cm² light fluence, photo-induced cellular damage caused by the EH3 molecule was measured in each cancer cell line but in different degrees. According to both WST-1 and resazurin assays, the most affected cell line was FaDu cell line where both high and low doses of EH1 molecule lead to appx. 90% cell death relative to the non-treated control. Other cell lines, HT29 and A253 cell lines were significantly affected by photodynamic therapy of both high and low doses of EH1 molecule, while the T47D cell line only affected from photodynamic therapy with high dose of EH3 molecule. Considering 10 percent difference is acceptable, there were some differences above this limit between WST-1 and resazurin assay. However, according to general trends of viability depend on the Pc concentration, the resazurin assay results mostly supported the WST-1 assay.

PDT-induced immediate ROS production was seen moderately on each cell line for both low and high doses of the molecule. Following PDT, both low and high doses EH3 molecule lead to late ROS formation, except that low dose of the molecule did not trigger late ROS formation on A253 cell line. The highest amount of ROS was seen on the FaDu cell line, it was followed by HT29, A253, and T74D cell lines, respectively. It can be said that PDT-mediated cytotoxic response on the cell lines was ROS dependent.

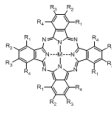
Table 31 Relative percentage cell viability and ROS formation of cancer cell lines after photodynamic therapy with EH3 phthalocyanine at 650-670 nm (light fluence of 2 joules/cm²).

EH3	Assay	Wavelength	Concentration	A253	FaDu	HT29	T47D
	Cytotoxicity (WST-1)	650-670 nm	10 µg/ml	38	11	18	23
			1 µg/ml	42	16	29	48
	Cytotoxicity (Resazurin)		10 µg/ml	17	7	25	25
			1 µg/ml	56	10	53	81
Center metal Zn	ROS (30 minutes)	10 µg/ml	155	215	171	225	
		1 µg/ml	136	199	135	204	
R1	ROS (24 hours)	10 µg/ml	4991	9281	3760	305	
		1 µg/ml	31	10245	1040	122	

At wavelength of 650-670 nm with 2 joules/cm² light fluence, photo-induced cellular damage caused by the EH3 molecule was measured in each cancer cell line but in different degrees. According to both WST-1 and resazurin assays, the most affected cell line was FaDu cell line where both high and low doses of EH1 molecule lead to appx. 90% cell death relative to the non-treated control. Other cell lines, HT29 and A253 cell lines were significantly affected by photodynamic therapy of both high and low doses of EH1 molecule, while the T47D cell line only affected from photodynamic therapy with high dose of EH3 molecule. Considering 10 percent difference is acceptable, there were some differences above this limit between WST-1 and resazurin assay. However, according to general trends of viability depend on the Pc concentration, the resazurin assay results mostly supported the WST-1 assay.

PDT-induced immediate ROS production was seen moderately on each cell line for both low and high doses of the molecule. Following PDT, both low and high doses EH3 molecule lead to late ROS formation, except that low dose of the molecule did not trigger late ROS formation on A253 cell line. The highest amount of ROS was seen on the FaDu cell line, it was followed by HT29, A253, and T74D cell lines, respectively. It can be said that PDT-mediated cytotoxic response on the cell lines was ROS dependent.

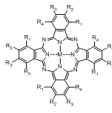
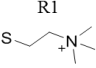
Table 32 Relative percentage cell viability and ROS formation of cancer cell lines after photodynamic therapy with EH3 phthalocyanine at 690-710 nm (light fluence of 2 joules/cm²).

EH3	Assay	Wavelength	Concentration	A253	FaDu	HT29	T47D
	Cytotoxicity (WST-1)	690-710 nm	10 µg/ml	37	12	19	25
			1 µg/ml	44	17	30	64
	Cytotoxicity (Resazurin)		10 µg/ml	21	8	30	45
			1 µg/ml	59	13	72	82
Center metal Zn	ROS (30 minutes)	10 µg/ml	160	249	155	227	
	1 µg/ml	110	196	141	222		
R1	ROS (24 hours)	10 µg/ml	429	10091	4282	184	
		1 µg/ml	32	9339	254	167	

At wavelength of 690-710 nm with 2 joules/cm² light fluence, photo-induced cellular damage caused by the EH3 molecule was measured in each cancer cell line but in different degrees. According to both WST-1 and resazurin assays, the most affected cell line was FaDu cell line where both high and low doses of EH1 molecule lead to appx. 90% cell death relative to the non-treated control. Other cell lines, HT29 and A253 cell lines were significantly affected by photodynamic therapy of both high and low doses of EH1 molecule, while the T47D cell line only affected from photodynamic therapy with high dose of EH3 molecule. Considering 10 percent difference is acceptable, there were some differences above this limit between WST-1 and resazurin assay. However, according to general trends of viability depend on the Pc concentration, the resazurin assay results mostly supported the WST-1 assay.

PDT-induced immediate ROS production was seen moderately on each cell line for both low and high doses of the molecule. Following PDT, both low and high doses EH3 molecule lead to late ROS formation, except that low dose of the molecule did not trigger late ROS formation on A253 cell line. The highest amount of ROS was seen on the FaDu cell line, it was followed by HT29, A253, and T74D cell lines, respectively. It can be said that PDT-mediated cytotoxic response on the cell lines was ROS dependent.

Table 33 Relative percentage cell viability and ROS formation of cancer cell lines after photodynamic therapy with EH3 phthalocyanine at 720-740nm (light fluence of 2 joules/cm²).

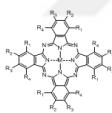
EH3	Assay	Wavelength	Concentration	A253	FaDu	HT29	T47D
	Cytotoxicity (WST-1)	720-740 nm	10 µg/ml	39	12	20	28
			1 µg/ml	43	20	30	71
	Cytotoxicity (Resazurin)		10 µg/ml	28	9	34	54
			1 µg/ml	60	16	73	85
Center metal Zn	ROS (30 minutes)	10 µg/ml	156	305	177	218	
		1 µg/ml	108	227	145	245	
	ROS (24 hours)	10 µg/ml	153	10202	5559	180	
		1 µg/ml	25	10442	275	168	

At wavelength of 720-740 nm with 2 joules/cm² light fluence, photo-induced cellular damage caused by the EH3 molecule was measured in each cancer cell line except T47D cell line when applied by low dose of the molecule. According to both WST-1 and resazurin assays, the most affected cell line was FaDu cell line where both high and low doses of EH1 molecule lead to appx. 90% cell death relative to the non-treated control. Other cell lines, HT29 and A253 cell lines were significantly affected by photodynamic therapy of both high and low doses of EH1 molecule, while the T47D cell line only affected from photodynamic therapy with high dose of EH3 molecule. Considering 10 percent difference is acceptable, there were some differences above this limit between WST-1 and resazurin assay. However, according to general trends

of viability depend on the Pc concentration, the resazurin assay results mostly supported the WST-1 assay.

PDT-induced immediate ROS production was seen moderately on each cell line for both low and high doses of the molecule. Following PDT, both low and high doses EH3 molecule lead to late ROS formation, except that low dose of the molecule did not trigger late ROS formation on A253 cell line. The highest amount of ROS was seen on the FaDu cell line, it was followed by HT29, and T74D cell lines, respectively. It can be said that PDT-mediated cytotoxic response on the cell lines was ROS dependent.

Table 34 Relative percentage cell viability and ROS formation of cancer cell lines after photodynamic therapy with EH3 phthalocyanine at 725-755 nm (light fluence of 2 joules/cm²).

EH3	Assay	Wavelength	Concentration	A253	FaDu	HT29	T47D
	Cytotoxicity (WST-1)	725-755 nm	10 µg/ml	39	11	18	23
			1 µg/ml	43	17	29	61
Cytotoxicity (Resazurin)	10 µg/ml		18	7	29	42	
	1 µg/ml		60	12	70	84	
Center metal Zn	ROS (30 minutes)		10 µg/ml	151	293	165	177
			1 µg/ml	120	275	156	212
R1	ROS (24 hours)		10 µg/ml	4344	9815	4424	198
			1 µg/ml	25	10421	270	160

At wavelength of 725-755 nm with 2 joules/cm² light fluence, photo-induced cellular damage caused by the EH3 molecule was measured in each cancer cell line but in different degrees.

According to WST-1 assay, the most affected cell line was FaDu cell line where both high and low doses of EH1 molecule lead to appx. 90% cell death relative to the

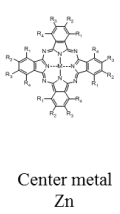
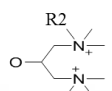
non-treated control. Other cell lines, HT29 and A253 cell lines were significantly affected by photodynamic therapy of both high and low doses of EH1 molecule, while the T47D cell line only affected from photodynamic therapy of high dose of EH3 molecule, and moderately affected from low dose. Considering 10 percent difference is acceptable, there were some differences above this limit between WST-1 and resazurin assay. However, according to general trends of viability depend on the Pc concentration, the resazurin assay results mostly supported the WST-1 assay.

PDT-induced immediate ROS production was seen moderately on each cell line, however, there were significant ROS amount was measured triggered by PDT lately for each cell line except on A253 and HT29 cell line when treated with the low dose of the molecule. It can be said that PDT-mediated cytotoxic response on the cell lines was ROS dependent.

4.10.5. Comparative table of experiments with EH4 phthalocyanine

In this section, overall results obtained from EH4-mediated PDT with five different wavelengths were collected as percentage relative to non-treated control. Each data was revealed as % value.

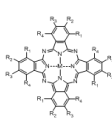
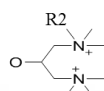
Table 35 Relative percentage cell viability and ROS formation of cancer cell lines after photodynamic therapy with EH4 phthalocyanine at 624 nm (light fluence of 2 joules/cm²).

EH4	Assay	Wavelength	Concentration	A253	FaDu	HT29	T47D
	Cytotoxicity (WST-1)	624 nm	10 µg/ml	38	11	14	27
			1 µg/ml	53	24	89	94
	Cytotoxicity (Resazurin)		10 µg/ml	14	4	12	15
			1 µg/ml	33	4	63	50
	ROS (30 minutes)		10 µg/ml	153	245	140	264
			1 µg/ml	148	211	119	216
	ROS (24 hours)	10 µg/ml	3865	7379	2932	889	
		1 µg/ml	64	6788	263	254	

At wavelength of 624 nm with 2 joules/cm² light fluence, photo-induced cellular damage caused by EH4 molecule was measured in each cancer cell line except HT29 and T47D cell lines when it was applied by low dose of the molecule. According to WST-1 assay, the most affected cell line was FaDu cell line where both high and low doses of EH1 molecule lead to significant cell death relative to the non-treated control. Other cell lines, HT29 A253, and T47D cell lines were significantly affected by photodynamic therapy of high EH1 molecule, while the low dose of EH4 molecule did not trigger significant cell death. Considering 10 percent difference is acceptable, there were some differences above this limit between WST-1 and resazurin assay. However, according to general trends of viability depend on the Pc concentration, the resazurin assay results mostly supported the WST-1 assay.

EH4 induced immediate ROS production was moderately seen on each cell line. The highest amount of ROS was seen on the T47D cell line, it was followed by FaDu, A253, and HT29 cell lines, respectively. The EH4-induced PDT triggered late ROS production on each cell line. The higher ROS production was measured from the FaDu cell line, followed by A253, HT29, and T47D cell lines, respectively. The least ROS production was seen on the A253 cell line, even the low dose of EH4 did not trigger ROS on the A253 cell line.

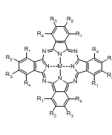
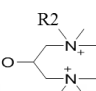
Table 36 Relative percentage cell viability and ROS formation of cancer cell lines after photodynamic therapy with EH4 phthalocyanine at 650-670 nm (light fluence of 2 joules/cm²).

EH4	Assay	Wavelength	Concentration	A253	FaDu	HT29	T47D
 Center metal Zn	Cytotoxicity (WST-1)	650-670 nm	10 µg/ml	37	12	17	26
			1 µg/ml	46	25	60	85
	Cytotoxicity (Resazurin)		10 µg/ml	11	4	12	14
			1 µg/ml	28	4	73	45
	ROS (30 minutes)		10 µg/ml	190	317	188	356
			1 µg/ml	170	219	134	187
 R2	ROS (24 hours)	10 µg/ml	3570	7537	3290	993	
		1 µg/ml	72	7103	177	248	

At wavelength of 650-670 nm with 2 joules/cm² light fluence, photo-induced cellular damage caused by EH4 molecule was measured in each cancer cell line except HT29 and T47D cell lines when it was applied by low dose of the molecule. According to WST-1 assay, the most affected cell line was FaDu cell line where both high and low doses of EH1 molecule lead to significant cell death relative to the non-treated control. Other cell lines, HT29 A253, and T47D cell lines were significantly affected by photodynamic therapy with high dose of EH4 molecule, while the low dose of EH4 molecule did not trigger significant cell death. Considering 10 percent difference is acceptable, there were some differences above this limit between WST-1 and resazurin assay. However, according to general trends of viability depend on the Pc concentration, the resazurin assay results mostly supported the WST-1 assay.

EH4-induced immediate ROS production was moderately seen on each cell line. The highest amount of ROS was seen on the T47D cell line, it was followed by FaDu, A253, and HT29 cell lines, respectively. The EH4-induced PDT triggered late ROS production on each cell line. The higher ROS production was measured from the FaDu cell line, followed by A253, HT29, and T47D cell lines, respectively. The least ROS production was seen on the A253 cell line, even the low dose of EH4 did not trigger ROS on the A253 cell line.

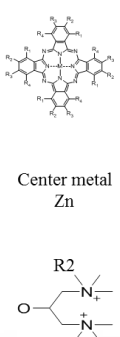
Table 37 Relative percentage cell viability and ROS formation of cancer cell lines after photodynamic therapy with EH4 phthalocyanine at 690-710 nm (light fluence of 2 joules/cm²).

EH4	Assay	Wavelength	Concentration	A253	FaDu	HT29	T47D
 Center metal Zn	Cytotoxicity (WST-1)	690-710 nm	10 µg/ml	40	12	13	26
			1 µg/ml	57	47	87	75
	Cytotoxicity (Resazurin)		10 µg/ml	16	5	17	34
			1 µg/ml	54	8	76	71
	ROS (30 minutes)		10 µg/ml	199	324	218	218
			1 µg/ml	191	249	125	123
 R2	ROS (24 hours)	10 µg/ml	771	7730	3508	427	
		1 µg/ml	24	7064	216	199	

At wavelength of 690-710 nm with 2 joules/cm² light fluence, photo-induced cellular damage caused by EH4 molecule was measured in each cancer cell line except HT29 and T47D cell lines when it was applied by low dose of the molecule. According to WST-1 assay, the most affected cell line was FaDu and HT29 cell line where high dose of EH1 molecule lead to significant cell death relative to the non-treated control. Other cell lines, A253, and T47D cell lines were significantly affected by photodynamic therapy of high EH4 molecule. PDT with low dose of the molecule did not lead to significant cellular death according to WST-1 assay. Considering 10 percent difference is acceptable, there were some differences above this limit between WST-1 and resazurin assay. However, according to general trends of viability depend on the Pc concentration, the resazurin assay results mostly supported the WST-1 assay.

EH4 induced immediate ROS production was moderately seen on each cell line. The highest amount of ROS was seen on the FaDu cell line, it was followed by HT29, T47D, and A253 cell lines, respectively. The EH4-induced PDT triggered late ROS production on each cell line. The higher ROS production was measured from the FaDu cell line, followed by HT29, A253 and T47D cell lines, respectively. The least ROS production was seen on the A253 cell line, even the low dose of EH4 did not trigger ROS on the A253 cell line.

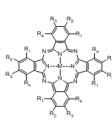
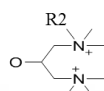
Table 38 Relative percentage cell viability and ROS formation of cancer cell lines after photodynamic therapy with EH4 phthalocyanine at 720-740 nm (light fluence of 2 joules/cm²).

EH4	Assay	Wavelength	Concentration	A253	FaDu	HT29	T47D
 Center metal Zn	Cytotoxicity (WST-1)	720-740 nm	10 µg/ml	38	12	15	36
			1 µg/ml	66	61	86	90
	Cytotoxicity (Resazurin)		10 µg/ml	25	6	39	51
			1 µg/ml	68	22	76	78
	ROS (30 minutes)		10 µg/ml	227	346	209	188
			1 µg/ml	199	218	129	167
	ROS (24 hours)		10 µg/ml	237	7820	4660	309
			1 µg/ml	37	14053	223	191

At wavelength of 720-740 nm with 2 joules/cm² light fluence, photo-induced cellular damage caused by EH4 molecule was measured in each cancer cell line except HT29 and T47D cell lines when it was applied by low dose of the molecule. According to WST-1 assay, the most affected cell line was FaDu cell line where both high and low doses of EH1 molecule lead to significant cell death relative to the non-treated control. Other cell lines, HT29 A253, and T47D cell lines were significantly affected by photodynamic therapy of high EH1 molecule, while the low dose of EH4 molecule did not trigger significant cell death. Considering 10 percent difference is acceptable, there were some differences above this limit between WST-1 and resazurin assay. However, according to general trends of viability depend on the Pc concentration, the resazurin assay results mostly supported the WST-1 assay.

EH4 induced immediate ROS production was moderately seen on each cell line. The highest amount of ROS was seen on the T47D cell line, it was followed by FaDu, A253, and HT29 cell lines, respectively. The EH4-induced PDT triggered late ROS production on each cell line. The higher ROS production was measured from the FaDu cell line, followed by A253, HT29, and T47D cell lines, respectively. The least ROS production was seen on the A253 cell line, even the low dose of EH4 did not trigger ROS on the A253 cell line.

Table 39 Relative percentage cell viability and ROS formation of cancer cell lines after photodynamic therapy with EH4 phthalocyanine at 725-755 nm (light fluence of 2 joules/cm²).

EH4	Assay	Wavelength	Concentration	A253	FaDu	HT29	T47D
 Center metal Zn	Cytotoxicity (WST-1)	725-755 nm	10 µg/ml	38	12	21	26
			1 µg/ml	50	36	89	78
	Cytotoxicity (Resazurin)		10 µg/ml	19	5	20	36
			1 µg/ml	52	8	73	77
	ROS (30 minutes)		10 µg/ml	188	362	224	126
			1 µg/ml	183	261	136	145
 ROS (24 hours)	10 µg/ml	245	8447	3945	413		
	1 µg/ml	28	8436	268	221		

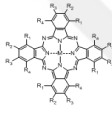
At wavelength of 725-755 nm with 2 joules/cm² light fluence, photo-induced cellular damage caused by EH4 molecule was measured in each cancer cell line, but in different degrees. According to WST-1 assay, the most affected cell line was FaDu cell line where both high and low doses of EH1 molecule lead to significant cell death relative to the non-treated control. Other cell lines, HT29, A253, and T47D cell lines were significantly affected by photodynamic therapy of both high EH1 molecule, while the low dose of EH4 molecule did not trigger significant cell death. Considering 10 percent difference is acceptable, there were some differences above this limit between WST-1 and resazurin assay. However, according to general trends of viability depend on the Pc concentration, the resazurin assay results mostly supported the WST-1 assay.

EH4 induced immediate ROS production was moderately seen on each cell line. The highest amount of ROS was seen on the FaDu cell line, it was followed by HT29, A253, and T47D cell lines, respectively. The EH4-induced PDT triggered late ROS production on each cell line. The highest ROS production was measured from the FaDu cell line, also T47D, HT29, and A253 cell lines, respectively. The least ROS production was seen on the A253 cell line, even the low dose of EH1 did not trigger ROS on the A253 cell line.

4.10.6. Comparative table of experiments with HQH₂Pc phthalocyanine

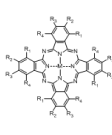
In this section, overall results obtained from HQH₂Pc-mediated PDT with five different wavelengths were collected as percentage relative to non-treated control. Each data was revealed as % value.

Table 40 Relative percentage cell viability and ROS formation of cancer cell lines after photodynamic therapy with HQH₂Pc phthalocyanine at 624 nm (light fluence of 2 joules/cm²).

HQH ₂ Pc	Assay	Wavelength	Concentration	A253	FaDu	HT29	T47D
	Cytotoxicity (WST-1)	624 nm	10 µg/ml	87	74	71	77
			1 µg/ml	114	97	87	106
	Cytotoxicity (Resazurin)		10 µg/ml	81	94	91	102
			1 µg/ml	105	94	101	108
Center metal 2H	ROS (30 minutes)		10 µg/ml	101	125	96	103
			1 µg/ml	90	103	89	87
R2	ROS (24 hours)		10 µg/ml	93	152	237	100
			1 µg/ml	97	136	172	78

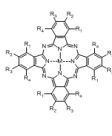
At wavelength of 624 nm with 2 joules/cm² light fluence, photo-induced cellular damage caused by the HQH₂Pc molecule was not measured in the cancer cell line. Both WST-1 and resazurin assays had supported each other. Neither immediate nor late PDT-induced ROS was not formed. HQH₂Pc molecule is not suitable for PDT.

Table 41 Relative percentage cell viability and ROS formation of cancer cell lines after photodynamic therapy with HQH₂Pc phthalocyanine at 650-670 nm (light fluence of 2 joules/cm²).

HQH ₂ Pc	Assay	Wavelength	Concentration	A253	FaDu	HT29	T47D
	Cytotoxicity (WST-1)	650-670 nm	10 µg/ml	83	77	82	73
			1 µg/ml	109	104	97	99
	Cytotoxicity (Resazurin)		10 µg/ml	79	93	94	91
			1 µg/ml	106	95	100	113
	Center metal 2H ROS (30 minutes)		10 µg/ml	121	171	107	141
			1 µg/ml	100	114	97	103
R2 ROS (24 hours)	10 µg/ml	97	148	301	146		
	1 µg/ml	104	147	189	88		

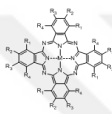
At wavelength of 650-670 nm with 2 joules/cm² light fluence, photo-induced cellular damage caused by the HQH₂Pc molecule was not measured in the cancer cell line. Both WST-1 and resazurin assays had supported each other. Neither immediate nor late PDT-induced ROS was not formed. HQH₂Pc molecule is not suitable for PDT.

Table 42 Relative percentage cell viability and ROS formation of cancer cell lines after photodynamic therapy with HQH₂Pc phthalocyanine at 690-710 nm (light fluence of 2 joules/cm²).

HQH ₂ Pc	Assay	Wavelength	Concentration	A253	FaDu	HT29	T47D
	Cytotoxicity (WST-1)	690-710 nm	10 µg/ml	96	80	87	80
			1 µg/ml	116	110	95	98
	Cytotoxicity (Resazurin)		10 µg/ml	87	94	93	92
			1 µg/ml	107	96	97	112
Center metal 2H ROS (30 minutes)	10 µg/ml	129	182	107	156		
	1 µg/ml	119	134	92	157		
R2 ROS (24 hours)	10 µg/ml	117	174	246	117		
	1 µg/ml	108	151	188	87		

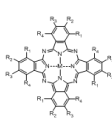
At wavelength of 690-710 nm with 2 joules/cm² light fluence, photo-induced cellular damage caused by the HQH₂Pc molecule was not measured in the cancer cell line. Both WST-1 and resazurin assays had supported each other. Neither immediate nor late PDT-induced ROS was not formed. HQH₂Pc molecule is not suitable for PDT.

Table 43 Relative percentage cell viability and ROS formation of cancer cell lines after photodynamic therapy with HQH₂Pc phthalocyanine at 720-740 nm (light fluence of 2 joules/cm²).

HQH ₂ Pc	Assay	Wavelength	Concentration	A253	FaDu	HT29	T47D
	Cytotoxicity (WST-1)	720-740 nm	10 µg/ml	99	80	87	81
			1 µg/ml	116	98	93	96
Cytotoxicity (Resazurin)	10 µg/ml		88	96	96	94	
	1 µg/ml		104	93	101	111	
Center metal 2H	ROS (30 minutes)		10 µg/ml	136	180	112	139
			1 µg/ml	127	140	104	178
R2	ROS (24 hours)		10 µg/ml	112	158	530	135
			1 µg/ml	96	148	172	90

At wavelength of 720-740 nm with 2 joules/cm² light fluence, photo-induced cellular damage caused by the HQH₂Pc molecule was not measured in the cancer cell line. Both WST-1 and resazurin assays had supported each other. Neither immediate nor late PDT-induced ROS was not formed. HQH₂Pc molecule is not suitable for PDT.

Table 44 Relative percentage cell viability and ROS formation of cancer cell lines after photodynamic therapy with HQH₂Pc phthalocyanine at 725-755 nm (light fluence of 2 joules/cm²).

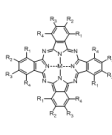
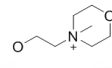
HQH ₂ Pc	Assay	Wavelength	Concentration	A253	FaDu	HT29	T47D	
	Cytotoxicity (WST-1)	725-755 nm	10 µg/ml	90	83	85	74	
			1 µg/ml	106	98	89	91	
	Cytotoxicity (Resazurin)		10 µg/ml	85	93	90	99	
			1 µg/ml	103	98	94	113	
	Center metal 2H		ROS (30 minutes)	10 µg/ml	124	189	119	163
			1 µg/ml	113	141	116	96	
R2	ROS (24 hours)	10 µg/ml	86	170	258	131		
		1 µg/ml	103	161	195	111		

At wavelength of 725-755 nm with 2 joules/cm² light fluence, photo-induced cellular damage caused by the HQH₂Pc molecule was not measured in the cancer cell line. Both WST-1 and resazurin assays had supported each other. Neither immediate nor late PDT-induced ROS was not formed. HQH₂Pc molecule is not suitable for PDT.

4.10.7. Comparative table of experiments with HQZnPc phthalocyanine

In this section, overall results obtained from HQZnPc-mediated PDT with five different wavelengths were collected as percentage relative to non-treated control. Each data was revealed as % value.

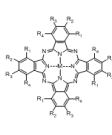
Table 45 Relative percentage cell viability and ROS formation of cancer cell lines after photodynamic therapy with HQZnPc phthalocyanine at 624 nm (light fluence of 2 joules/cm²).

HQZnPc	Assay	Wavelength	Concentration	A253	FaDu	HT29	T47D
 Center metal Zn R2	Cytotoxicity (WST-1)	624 nm	10 µg/ml	41	10	20	30
			1 µg/ml	48	12	54	78
	Cytotoxicity (Resazurin)		10 µg/ml	26	5	14	54
			1 µg/ml	58	7	78	93
	ROS (30 minutes)		10 µg/ml	225	193	95	299
			1 µg/ml	194	128	58	275
 ROS (24 hours)	10 µg/ml	197	7788	3355	131		
	1 µg/ml	34	5413	153	98		

At wavelength of 624 nm with 2 joules/cm² light fluence, photo-induced cellular damage caused by the HQZnPc molecule was measured in each cancer cell line but different degrees. According to WST-1 assay, the most affected cell line was FaDu cell line where both high and low doses of EH1 molecule lead to appx. 90% cell death relative to the non-treated control. Other cell lines, A253, HT29, and T47D cell lines were significantly affected by photodynamic therapy of high HQZnPc molecule, and not affected by low dose. Considering 10 percent difference is acceptable, there were some differences above this limit between WST-1 and resazurin assay. However, according to general trends of viability depend on the Pc concentration, the resazurin assay results mostly supported the WST-1 assay.

HQZnPc induced immediate ROS production was seen on each cell lines except HT29 cell line. The highest amount of ROS was seen on the T47D cell line, it was followed by A253, and FaDu cell lines, respectively. PDT mediated late ROS production was significantly seen on FaDu when applied by both high and low doses of the molecule, on HT29 when applied only high dose of the molecule. Only high dose of the molecule triggered late ROS production on A253 and T47D cell lines, moderately. However, low dose of the molecule did not lead to ROS production on A253 and T47D cell lines.

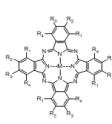
Table 46 Relative percentage cell viability and ROS formation of cancer cell lines after photodynamic therapy with HQZnPc phthalocyanine at 650-670 nm (light fluence of 2 joules/cm²).

HQZnPc	Assay	Wavelength	Concentration	A253	FaDu	HT29	T47D	
	Cytotoxicity (WST-1)	650-670 nm	10 µg/ml	39	11	21	27	
			1 µg/ml	50	12	45	74	
	Cytotoxicity (Resazurin)		10 µg/ml	28	5	14	49	
			1 µg/ml	55	8	75	89	
	Center metal Zn		ROS (30 minutes)	10 µg/ml	204	217	104	387
			1 µg/ml	161	119	51	327	
R2	ROS (24 hours)	10 µg/ml	128	7465	3524	150		
		1 µg/ml	37	5646	152	99		

At wavelength of 650-670 nm with 2 joules/cm² light fluence, photo-induced cellular damage caused by the HQZnPc molecule was measured in each cancer cell line but different degrees. According to WST-1 assay, the most affected cell line was FaDu cell line where both high and low doses of EH1 molecule lead to appx. 90% cell death relative to the non-treated control. Other cell lines, A253, HT29, and T47D cell lines were significantly affected by photodynamic therapy of high HQZnPc molecule, and not affected by low dose. Considering 10 percent difference is acceptable, there were some differences above this limit between WST-1 and resazurin assay. However, according to general trends of viability depend on the Pc concentration, the resazurin assay results mostly supported the WST-1 assay.

HQZnPc induced immediate ROS production was seen on each cell lines except HT29 cell line. The highest amount of ROS was seen on the T47D cell line, it was followed by FaDu, and A253 cell lines, respectively. PDT mediated late ROS production was significantly seen on FaDu when applied by both high and low doses of the molecule, on HT29 when applied only high dose of the molecule. Only high dose of the molecule triggered late ROS production on A253 and T47D cell lines, moderately. However, low dose of the molecule did not lead to ROS production on A253 and T47D cell lines.

Table 47 Relative percentage cell viability and ROS formation of cancer cell lines after photodynamic therapy with HQZnPc phthalocyanine at 690-710 nm (light fluence of 2 joules/cm²).

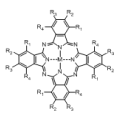
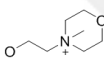
HQZnPc	Assay	Wavelength	Concentration	A253	FaDu	HT29	T47D
	Cytotoxicity (WST-1)	690-710 nm	10 µg/ml	39	10	24	40
			1 µg/ml	62	13	104	76
	Cytotoxicity (Resazurin)		10 µg/ml	30	8	31	79
			1 µg/ml	79	18	77	98
Center metal Zn	ROS (30 minutes)		10 µg/ml	304	274	138	338
			1 µg/ml	169	128	51	241
R2	ROS (24 hours)		10 µg/ml	132	9102	5381	121
			1 µg/ml	42	211	181	118

At wavelength of 690-710 nm with 2 joules/cm² light fluence, photo-induced cellular damage caused by the HQZnPc molecule was measured in each cancer cell line but different degrees. According to WST-1 assay, the most affected cell line was FaDu cell line where both high and low doses of EH1 molecule lead to appx. 90% cell death relative to the non-treated control. Other cell lines, A253, HT29, and T47D cell lines were significantly affected by photodynamic therapy of high HQZnPc molecule, and not affected by low dose. Considering 10 percent difference is acceptable, there were some differences above this limit between WST-1 and resazurin assay. However, according to general trends of viability depend on the Pc concentration, the resazurin assay results mostly supported the WST-1 assay.

HQZnPc induced immediate ROS production was seen on each cell lines except HT29 cell line when it was applied by low dose of the molecule. The highest amount of ROS was seen on the T47D cell line, it was followed by A253, and FaDu cell lines, respectively. PDT mediated late ROS production was significantly seen on FaDu and HT29 when applied by both high dose of the molecule. Low dose of the molecule triggered late ROS production on FaDu and HT29 cell lines, moderately. Only high dose of the molecule triggered late ROS production on A253 and T47D cell lines,

moderately. However, low dose of the molecule did not lead to ROS production on A253 and T47D cell lines.

Table 48 Relative percentage cell viability and ROS formation of cancer cell lines after photodynamic therapy with HQZnPc phthalocyanine at 720-740 nm (light fluence of 2 joules/cm²).

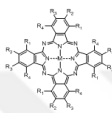
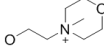
HQZnPc	Assay	Wavelength	Concentration	A253	FaDu	HT29	T47D
 Center metal Zn R2 	Cytotoxicity (WST-1)	720-740 nm	10 µg/ml	40	11	26	38
			1 µg/ml	74	16	102	82
	Cytotoxicity (Resazurin)		10 µg/ml	30	9	48	81
			1 µg/ml	88	36	81	103
	ROS (30 minutes)		10 µg/ml	336	292	138	441
			1 µg/ml	188	177	64	275
ROS (24 hours)	10 µg/ml	135	8905	628	136		
	1 µg/ml	57	84	139	96		

At wavelength of 720-740 nm with 2 joules/cm² light fluence, photo-induced cellular damage caused by the HQZnPc molecule was measured in each cancer cell line but different degrees. According to WST-1 assay, the most affected cell line was FaDu cell line where both high and low doses of EH1 molecule lead to appx. 90% cell death relative to the non-treated control. Other cell lines, A253, HT29, and T47D cell lines were significantly affected by photodynamic therapy of high HQZnPc molecule, and not affected by low dose. Considering 10 percent difference is acceptable, there were some differences above this limit between WST-1 and resazurin assay. However, according to general trends of viability depend on the Pc concentration, the resazurin assay results mostly supported the WST-1 assay.

HQZnPc induced immediate ROS production was seen on each cell lines except HT29 cell line when it was applied by low dose of the molecule. The highest amount of ROS was seen on the T47D cell line, it was followed by A253, and FaDu cell lines, respectively. PDT mediated late ROS production was significantly seen on FaDu when

applied by high dose of the molecule, also it moderately triggered ROS production on HT29, T47D and A253 cell lines. However, low dose of the molecule did not lead to ROS production on the cell lines.

Table 49 Relative percentage cell viability and ROS formation of cancer cell lines after photodynamic therapy with HQZnPc phthalocyanine at 725-755 nm (light fluence of 2 joules/cm²).

HQZnPc	Assay	Wavelength	Concentration	A253	FaDu	HT29	T47D
 Center metal Zn R2 	Cytotoxicity (WST-1)	725-755 nm	10 µg/ml	40	10	22	34
			1 µg/ml	53	14	88	74
	Cytotoxicity (Resazurin)		10 µg/ml	32	6	25	71
			1 µg/ml	76	18	75	101
	ROS (30 minutes)		10 µg/ml	283	272	134	353
			1 µg/ml	274	189	64	247
ROS (24 hours)	10 µg/ml	122	8035	4245	115		
	1 µg/ml	43	213	130	99		

At wavelength of 725-755 nm with 2 joules/cm² light fluence, photo-induced cellular damage caused by the HQZnPc molecule was measured in each cancer cell line but different degrees. According to WST-1 assay, the most affected cell line was FaDu cell line where both high and low doses of EH1 molecule lead to appx. 90% cell death relative to the non-treated control. Other cell lines, A253, HT29, and T47D cell lines were significantly affected by photodynamic therapy of high HQZnPc molecule, and not affected by low dose. Considering 10 percent difference is acceptable, there were some differences above this limit between WST-1 and resazurin assay. However, according to general trends of viability depend on the Pc concentration, the resazurin assay results mostly supported the WST-1 assay.

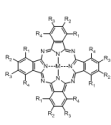
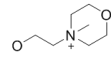
HQZnPc induced immediate ROS production was seen on each cell line in different degrees. The highest amount of ROS was seen on the T47D cell line, it was followed by A253, FaDu, and HT29 cell lines, respectively. At the light of proper

wavelengths, PDT mediated late ROS production was significantly seen FaDu, T47D, and HT29 cell lines when treated with the high dose of the molecule, and there was no significant ROS measured right after PDT with the low dose of HQZnPc molecule. However, the light with higher energy induced ROS production on FaDu, HT29 and T47D cell lines even low HQZnPc dose.

4.10.8. Comparative table of experiments with HQInPc phthalocyanine

In this section, overall results obtained from HQInPc-mediated PDT with five different wavelengths were collected as percentage relative to non-treated control. Each data was revealed as % value.

Table 50 Relative percentage cell viability and ROS formation of cancer cell lines after photodynamic therapy with HQInPc phthalocyanine at 624 nm (light fluence of 2 joules/cm²).

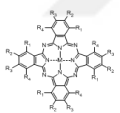
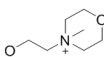
HQInPc	Assay	Wavelength	Concentration	A253	FaDu	HT29	T47D
	Cytotoxicity (WST-1)	624 nm	10 µg/ml	43	24	44	33
			1 µg/ml	72	98	84	73
	Cytotoxicity (Resazurin)		10 µg/ml	47	37	79	24
			1 µg/ml	90	83	84	76
Center metal InCl	ROS (30 minutes)	10 µg/ml	208	216	73	150	
		1 µg/ml	163	111	71	130	
R2 	ROS (24 hours)	10 µg/ml	40	101	123	389	
		1 µg/ml	51	59	98	94	

At wavelength of 624 nm with 2 joules/cm² light fluence, photo -induced cellular damage caused by the high dose HQInPc molecule was measured in each cancer cell line, but not by the low dose of the molecule. According to WST-1 assay, the most affected cell line was FaDu, followed by T47D, HT29, and A253 cell lines. Considering 10 percent difference is acceptable, there were some differences above

this limit between WST-1 and resazurin assay. However, according to general trends of viability depend on the Pc concentration, the resazurin assay results mostly supported the WST-1 assay.

HQInPc induced immediate ROS production was seen on each cell line except the HT29 cell line. The highest amount of ROS was seen on the FaDu cell line, it was followed by A253 and T47D cell lines, respectively. HQInPc-induced PDT triggered late ROS production on only T47D cell line when it was applied by high dose of the molecule. There was no significant late ROS formation triggered following PDT on the cell lines.

Table 51 Relative percentage cell viability and ROS formation of cancer cell lines after photodynamic therapy with HQInPc phthalocyanine at 650-670 nm (light fluence of 2 joules/cm²).

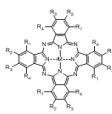
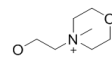
HQInPc	Assay	Wavelength	Concentration	A253	FaDu	HT29	T47D
	Cytotoxicity (WST-1)	650-670 nm	10 µg/ml	44	20	36	28
			1 µg/ml	67	89	82	71
	Cytotoxicity (Resazurin)		10 µg/ml	48	23	72	21
			1 µg/ml	89	57	85	69
Center metal InCl	ROS (30 minutes)		10 µg/ml	237	131	120	170
			1 µg/ml	176	39	86	135
R2 	ROS (24 hours)		10 µg/ml	30	188	157	393
			1 µg/ml	32	79	122	122

At wavelength of 650-670 nm with 2 joules/cm² light fluence, photo -induced cellular damage caused by the high dose HQInPc molecule was measured in each cancer cell line, but not by the low dose of the molecule. According to WST-1 assay, the most affected cell line was FaDu, followed by T47D, HT29, and A253 cell lines. Considering 10 percent difference is acceptable, there were some differences above this limit between WST-1 and resazurin assay. However, according to general trends

of viability depend on the Pc concentration, the resazurin assay results mostly supported the WST-1 assay.

HQInPc induced immediate ROS production was seen on each cell lines except FaDu and HT29 cell lines when it was applied by low dose of the molecule. The highest amount of ROS was seen on the A253, it was followed by T74D, FaDu and HT29 cell lines, respectively. HQInPc-induced PDT triggered late ROS production on T47D cell line, when it was applied by high dose of the molecule. It was followed by FaDu, and HT29 cell lines. There was no late ROS formation triggered following PDT on A253 cell line when it was applied by both doses, and FaDu when it was applied low dose of the molecule.

Table 52 Relative percentage cell viability and ROS formation of cancer cell lines after photodynamic therapy with HQInPc phthalocyanine at 690-710 nm (light fluence of 2 joules/cm²).

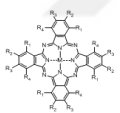
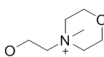
HQInPc	Assay	Wavelength	Concentration	A253	FaDu	HT29	T47D
	Cytotoxicity (WST-1)	690-710 nm	10 µg/ml	46	25	57	31
			1 µg/ml	71	102	88	68
	Cytotoxicity (Resazurin)		10 µg/ml	57	42	82	30
			1 µg/ml	95	75	83	77
Center metal InCl	ROS (30 minutes)		10 µg/ml	222	173	107	174
			1 µg/ml	173	77	80	148
R2 	ROS (24 hours)		10 µg/ml	26	104	191	428
			1 µg/ml	38	89	154	139

At wavelength of 690-710 nm with 2 joules/cm² light fluence, photo -induced cellular damage caused by the high dose HQInPc molecule was measured in each cancer cell line, but not by the low dose of the molecule. According to WST-1 assay, the most affected cell line was FaDu, followed by T47D, HT29, and A253 cell lines. Considering 10 percent difference is acceptable, there were some differences above this limit between WST-1 and resazurin assay. However, according to general trends

of viability depend on the Pc concentration, the resazurin assay results mostly supported the WST-1 assay.

HQInPc induced immediate ROS production was seen on each cell line except FaDu and HT29 cell lines when it was applied by low dose of the molecule. The highest amount of ROS was seen on A253 cell line, it was followed by T47D and FaDu cell lines, respectively. HQInPc-induced PDT triggered late ROS production on T47D and HT29 cell lines when it was applied by both low and high dose of the molecule. There was no significant late ROS formation triggered following PDT on A253 and FaDu cell lines.

Table 53 Relative percentage cell viability and ROS formation of cancer cell lines after photodynamic therapy with HQInPc phthalocyanine at 720-740 nm (light fluence of 2 joules/cm²).

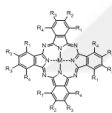
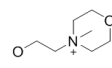
HQInPc	Assay	Wavelength	Concentration	A253	FaDu	HT29	T47D
	Cytotoxicity (WST-1)	720-740 nm	10 µg/ml	45	26	62	34
			1 µg/ml	76	101	90	69
	Cytotoxicity (Resazurin)		10 µg/ml	60	55	77	41
			1 µg/ml	96	80	96	84
Center metal InCl	ROS (30 minutes)	10 µg/ml	289	222	92	188	
		1 µg/ml	186	135	92	163	
R2 	ROS (24 hours)	10 µg/ml	22	103	162	274	
		1 µg/ml	50	127	169	131	

At wavelength of 624 nm with 2 joules/cm² light fluence, photo-induced cellular damage caused by the high dose HQInPc molecule was measured in each cancer cell line except HT29 cell line. Low dose of the molecule did not lead to cytotoxic response on any cell lines. According to WST-1 assay, the most affected cell line was FaDu, followed by T47D, and A253 cell lines. Considering 10 percent difference is acceptable, there were some differences above this limit between WST-1 and resazurin

assay. However, according to general trends of viability depend on the Pc concentration, the resazurin assay results mostly supported the WST-1 assay.

HQInPc-induced immediate ROS production was seen on each cell line except the HT29 cell line. The highest amount of ROS was seen on the A253 cell line, it was followed by FaDu and T47D cell lines, respectively. HQInPc-induced PDT triggered late ROS production on T47D and HT29 cell line when it was applied by high dose of the molecule. There was no significant late ROS formation triggered following PDT on A253 and FaDu cell line.

Table 54 Relative percentage cell viability and ROS formation of cancer cell lines after photodynamic therapy with HQInPc phthalocyanine at 725-755 nm (light fluence of 2 joules/cm²).

HQInPc	Assay	Wavelength	Concentration	A253	FaDu	HT29	T47D
	Cytotoxicity (WST-1)	725-755 nm	10 µg/ml	42	21	39	28
			1 µg/ml	63	81	83	65
	Cytotoxicity (Resazurin)		10 µg/ml	54	32	77	30
			1 µg/ml	90	57	73	76
Center metal InCl	ROS (30 minutes)		10 µg/ml	196	303	95	197
			1 µg/ml	145	175	95	178
R2 	ROS (24 hours)		10 µg/ml	25	136	136	323
			1 µg/ml	35	115	137	125

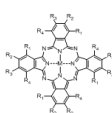
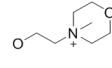
At wavelength of 624 nm with 2 joules/cm² light fluence, photo-induced cellular damage caused by the high dose HQInPc molecule was measured in each cancer cell line, but not by the low dose of the molecule. According to WST-1 assay, the most affected cell line was FaDu, followed by T47D, HT29, and A253 cell lines. Considering 10 percent difference is acceptable, there were some differences above this limit between WST-1 and resazurin assay. However, according to general trends of viability depend on the Pc concentration, the resazurin assay results mostly supported the WST-1 assay.

HQInPc-induced immediate ROS production was seen on each cell line except the HT29 cell line. The highest amount of ROS was seen on the FaDu cell line, it was followed by T47D and A253 cell lines, respectively. HQInPc-induced PDT triggered late ROS production on the only T47D cell line. The high dose of HQInPc molecule triggered a significant amount of ROS, while the low dose of the molecule leads to only moderately ROS formation on the T47D cell line. There was no significant amount of ROS formed lately following PDT on A253, FaDu, and HT29 cell line.

4.10.9. Comparative table of experiments with SQH₂Pc phthalocyanine

In this section, overall results obtained from SQH₂Pc-mediated PDT with five different wavelengths were collected as percentage relative to non-treated control. Each data was revealed as % value.

Table 55 Relative percentage cell viability and ROS formation of cancer cell lines after photodynamic therapy with SQH₂Pc phthalocyanine at 624 nm (light fluence of 2 joules/cm²).

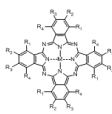
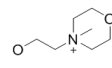
SQH ₂ Pc	Assay	Wavelength	Concentration	A253	FaDu	HT29	T47D
	Cytotoxicity (WSI-1)	624 nm	10 µg/ml	56	43	42	66
			1 µg/ml	95	77	87	91
	Cytotoxicity (Resazurin)		10 µg/ml	67	84	86	87
			1 µg/ml	108	94	88	101
Center metal 2H	ROS (30 minutes)		10 µg/ml	130	107	83	171
			1 µg/ml	125	80	68	190
R1 	ROS (24 hours)		10 µg/ml	65	101	121	126
			1 µg/ml	81	112	138	116

At wavelength of 624 nm with 2 joules/cm² light fluence, photo-induced cellular damage caused by the SQH₂Pc molecule was measured in each cancer cell line moderately only when were applied by high dose of the molecule. Considering 10

percent difference is acceptable, there were some differences above this limit between WST-1 and resazurin assay. However, according to general trends of viability depend on the Pc concentration, the resazurin assay results mostly supported the WST-1 assay.

Right after PDT, high doses of SQH₂Pc molecule triggered immediate ROS formation on the T47D and A253 cell lines when applied both dose of the molecule. However, neither low nor high dose of the molecule did not trigger immediate ROS formation on FaDu and HT29 cell lines. Following PDT, late ROS formation was triggered with PDT of both doses of SQH₂Pc molecule on A253 and T47D cell lines. PDT with neither dose of SQH₂Pc molecule did not triggered late ROS formation on A253 and FaDu cell line.

Table 56 Relative percentage cell viability and ROS formation of cancer cell lines after photodynamic therapy with SQH₂Pc phthalocyanine at 650-670 nm (light fluence of 2 joules/cm²).

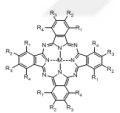
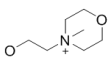
SQH ₂ Pc	Assay	Wavelength	Concentration	A253	FaDu	HT29	T47D
	Cytotoxicity (WST-1)	650-670 nm	10 µg/ml	45	14	22	52
			1 µg/ml	95	85	96	86
Cytotoxicity (Resazurin)	10 µg/ml		27	72	82	77	
	1 µg/ml		105	92	88	95	
Center metal 2H	ROS (30 minutes)		10 µg/ml	121	186	107	64
			1 µg/ml	124	70	87	40
R1 	ROS (24 hours)		10 µg/ml	117	71	130	120
			1 µg/ml	86	116	162	156

At wavelength of 650-670 nm with 2 joules/cm² light fluence, photo-induced cellular damage caused by the SQH₂Pc molecule was measured in each cancer cell line only when were applied by high dose of the molecule. The most cytotoxic response was taken from FaDu cell line, followed by HT29, A253 and T47D cell lines, respectively. Considering 10 percent difference is acceptable, there were some differences above this limit between WST-1 and resazurin assay. However, according

to general trends of viability depend on the Pc concentration, the resazurin assay results mostly supported the WST-1 assay.

Right after PDT, high doses of SQH₂Pc molecule triggered immediate ROS formation on A253 and FaDu cell lines when applied both dose of the molecule. However, neither low nor high dose of the molecule did not trigger immediate ROS formation on HT29 and T47D cell lines. Following PDT, late ROS formation was moderately triggered with PDT of both doses of SQH₂Pc molecule on HT29 and T47D cell lines, high dose of the molecule on A253 cell line. PDT with neither dose of SQH₂Pc molecule did not triggered late ROS formation on FaDu cell line.

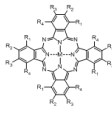
Table 57 Relative percentage cell viability and ROS formation of cancer cell lines after photodynamic therapy with SQH₂Pc phthalocyanine at 690-710 nm (light fluence of 2 joules/cm²).

SQH ₂ Pc	Assay	Wavelength	Concentration	A253	FaDu	HT29	T47D
	Cytotoxicity (WST-1)	690-710 nm	10 µg/ml	55	39	36	60
			1 µg/ml	95	90	96	89
	Cytotoxicity (Resazurin)		10 µg/ml	59	76	86	89
			1 µg/ml	104	92	86	92
Center metal 2H	ROS (30 minutes)		10 µg/ml	159	120	108	89
			1 µg/ml	136	86	94	130
R1 	ROS (24 hours)		10 µg/ml	92	106	161	144
			1 µg/ml	95	140	176	165

At wavelength of 690-710 nm with 2 joules/cm² light fluence, photo-induced cellular damage caused by the SQH₂Pc molecule was measured in each cancer cell line moderately only when were applied by high dose of the molecule. Considering 10 percent difference is acceptable, there were some differences above this limit between WST-1 and resazurin assay. However, according to general trends of viability depend on the Pc concentration, the resazurin assay results mostly supported the WST-1 assay.

Right after PDT, high doses of SQH₂Pc molecule triggered immediate ROS formation on the FaDu and A253 cell lines when applied both dose of the molecule. However, neither low nor high dose of the molecule did not trigger immediate ROS formation on HT29 and T47D cell lines. Following PDT, late ROS formation was triggered with PDT of both doses of SQH₂Pc molecule on HT29 and T47D cell lines. PDT with neither dose of SQH₂Pc molecule did not triggered late ROS formation on A253 and FaDu cell line.

Table 58 Relative percentage cell viability and ROS formation of cancer cell lines after photodynamic therapy with SQH₂Pc phthalocyanine at 720-740 nm (light fluence of 2 joules/cm²).

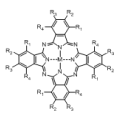
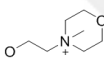
SQH ₂ Pc	Assay	Wavelength	Concentration	A253	FaDu	HT29	T47D
	Cytotoxicity (WST-1)	720-740 nm	10 µg/ml	42	47	33	63
			1 µg/ml	81	95	94	91
	Cytotoxicity (Resazurin)		10 µg/ml	58	73	84	88
			1 µg/ml	100	89	82	97
Center metal 2H	ROS (30 minutes)		10 µg/ml	136	156	122	190
			1 µg/ml	123	105	112	202
R1	ROS (24 hours)		10 µg/ml	105	113	142	130
			1 µg/ml	103	150	177	151

At wavelength of 720-740 nm with 2 joules/cm² light fluence, photo-induced cellular damage caused by the SQH₂Pc molecule was measured in each cancer cell line moderately only when were applied by high dose of the molecule. Considering 10 percent difference is acceptable, there were some differences above this limit between WST-1 and resazurin assay. However, according to general trends of viability depend on the Pc concentration, the resazurin assay results mostly supported the WST-1 assay.

Right after PDT, both doses of SQH₂Pc molecule moderately triggered immediate ROS formation on each cell lines. Following PDT, late ROS formation was triggered with PDT of both doses of SQH₂Pc molecule on HT29 and T47D cell lines. PDT with

neither dose of SQH₂Pc molecule did not triggered late ROS formation on A253 and FaDu cell line.

Table 59 Relative percentage cell viability and ROS formation of cancer cell lines after photodynamic therapy with SQH₂Pc phthalocyanine at 725-755 nm (light fluence of 2 joules/cm²).

SQH ₂ Pc	Assay	Wavelength	Concentration	A253	FaDu	HT29	T47D
 Center metal 2H R1 	Cytotoxicity (WST-1)	725-755 nm	10 µg/ml	56	13	17	27
			1 µg/ml	95	100	91	82
	Cytotoxicity (Resazurin)		10 µg/ml	23	37	73	67
			1 µg/ml	98	84	77	93
	ROS (30 minutes)		10 µg/ml	192	262	122	217
			1 µg/ml	156	139	93	222
ROS (24 hours)	10 µg/ml	154	139	116	109		
	1 µg/ml	82	150	164	150		

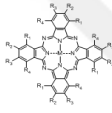
At wavelength of 725-755 nm with 2 joules/cm² light fluence, photo-induced cellular damage caused by the high dose SQH₂Pc molecule was measured in each cancer cell line but in different degrees. The low dose of the molecule did not have any cytotoxic effects on the cell lines. SQH₂Pc molecule was most effective on FaDu and HT29 cell lines, followed by T47D and A253 cell lines, respectively. Considering 10 percent difference is acceptable, there were some differences above this limit between WST-1 and resazurin assay. However, according to general trends of viability depend on the Pc concentration, the resazurin assay results mostly supported the WST-1 assay.

Right after PDT, both doses of SQH₂Pc molecule moderately triggered immediate ROS formation on each cell lines except HT29 cell line when it was applied by low dose of the molecule. Following PDT, late ROS formation was triggered with PDT of both doses of SQH₂Pc molecule on FaDu, HT29, and T47D cell line. SQH₂Pc molecule only lead to late ROS formation when it was applied by high dose.

4.10.10. Comparative table of experiments with SQZnPc phthalocyanine

In this section, overall results obtained from SQZnPc-mediated PDT with five different wavelengths were collected as percentage relative to non-treated control. Each data was revealed as % value.

Table 60 Relative percentage cell viability and ROS formation of cancer cell lines after photodynamic therapy with SQZnPc phthalocyanine at 624 nm (light fluence of 2 joules/cm²).

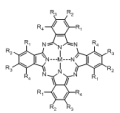
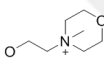
SQZnPc	Assay	Wavelength	Concentration	A253	FaDu	HT29	T47D
	Cytotoxicity (WST-1)	624 nm	10 µg/ml	57	52	68	68
			1 µg/ml	95	84	98	91
	Cytotoxicity (Resazurin)		10 µg/ml	80	79	83	81
			1 µg/ml	107	93	86	92
Center metal Zn	ROS (30 minutes)		10 µg/ml	124	338	97	131
			1 µg/ml	121	191	91	180
R1	ROS (24 hours)		10 µg/ml	39	99	135	144
			1 µg/ml	77	118	156	143

At wavelength of 624 nm with 2 joules/cm² light fluence, photo-induced cellular damage caused by the high dose of the SQZnPc molecule was moderately measured in A253 and FaDu cell lines, but not on HT29 and T47D cell lines. Considering 10 percent difference is acceptable, there were some differences above this limit between WST-1 and resazurin assay. However, according to general trends of viability depend on the Pc concentration, the resazurin assay results mostly supported the WST-1 assay.

SQZnPc-induced immediate ROS production was seen on each cell line in different degrees. The highest amount of ROS was seen on the FaDu cell line, it was followed by T47D, A253, and HT29 cell lines, respectively. Following PDT, late ROS formation was triggered with PDT of both doses of SQZnPc molecule on HT29, And

T47D cell line. SQZnPc molecule did not lead to late ROS formation on A253 and FaDu cell lines.

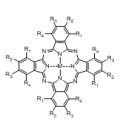
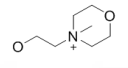
Table 61 Relative percentage cell viability and ROS formation of cancer cell lines after photodynamic therapy with SQZnPc phthalocyanine at 650-670 nm (light fluence of 2 joules/cm²).

SQZnPc	Assay	Wavelength	Concentration	A253	FaDu	HT29	T47D
 Center metal Zn R1	Cytotoxicity (WST-1)	650-670 nm	10 µg/ml	57	45	78	67
			1 µg/ml	96	81	100	95
	Cytotoxicity (Resazurin)		10 µg/ml	72	63	82	82
			1 µg/ml	108	89	84	95
	ROS (30 minutes)		10 µg/ml	158	401	140	193
			1 µg/ml	133	204	108	114
 R1	ROS (24 hours)	10 µg/ml	29	99	147	131	
		1 µg/ml	74	125	150	126	

At wavelength of 650-670 nm with 2 joules/cm² light fluence, photo-induced cellular damage caused by the high dose of the SQZnPc molecule was moderately measured in A253 and FaDu cell lines, but not on HT29 and T47D cell lines. Considering 10 percent difference is acceptable, there were some differences above this limit between WST-1 and resazurin assay. However, according to general trends of viability depend on the Pc concentration, the resazurin assay results mostly supported the WST-1 assay.

SQZnPc-induced immediate ROS production was seen on each cell line in different degrees. The highest amount of ROS was seen on the FaDu cell line, it was followed by T47D, A253, and HT29 cell lines, respectively. Following PDT, late ROS formation was triggered with PDT of both doses of SQZnPc molecule on HT29, And T47D cell line. SQZnPc molecule did not lead to late ROS formation on A253 and FaDu cell lines.

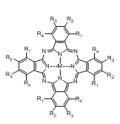
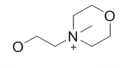
Table 62 Relative percentage cell viability and ROS formation of cancer cell lines after photodynamic therapy with SQZnPc phthalocyanine at 690-710 nm (light fluence of 2 joules/cm²).

SQZnPc	Assay	Wavelength	Concentration	A253	FaDu	HT29	T47D
 Center metal Zn R1 	Cytotoxicity (WST-1)	690-710 nm	10 µg/ml	57	43	86	65
			1 µg/ml	91	87	101	88
	Cytotoxicity (Resazurin)		10 µg/ml	78	70	81	84
			1 µg/ml	100	91	80	95
	ROS (30 minutes)		10 µg/ml	157	376	144	216
			1 µg/ml	128	193	104	187
ROS (24 hours)	10 µg/ml	34	103	160	128		
	1 µg/ml	82	132	152	129		

At wavelength of 670-710 nm with 2 joules/cm² light fluence, photo-induced cellular damage caused by the high dose of the SQZnPc molecule was moderately measured in A253 and FaDu cell lines, but not on HT29 and T47D cell lines. Considering 10 percent difference is acceptable, there were some differences above this limit between WST-1 and resazurin assay. However, according to general trends of viability depend on the Pc concentration, the resazurin assay results mostly supported the WST-1 assay.

SQZnPc-induced immediate ROS production was seen on each cell line in different degrees. The highest amount of ROS was seen on the FaDu cell line, it was followed by T47D, A253, and HT29 cell lines, respectively. Following PDT, late ROS formation was triggered with PDT of both doses of SQZnPc molecule on HT29, And T47D cell line. SQZnPc molecule did not lead to late ROS formation on A253 and FaDu cell lines.

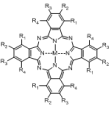
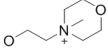
Table 63 Relative percentage cell viability and ROS formation of cancer cell lines after photodynamic therapy with SQZnPc phthalocyanine at 720-740 nm (light fluence of 2 joules/cm²).

SQZnPc	Assay	Wavelength	Concentration	A253	FaDu	HT29	T47D
 Center metal Zn R1 	Cytotoxicity (WST-1)	720-740 nm	10 µg/ml	58	50	85	64
			1 µg/ml	91	84	98	85
	Cytotoxicity (Resazurin)		10 µg/ml	86	81	79	84
			1 µg/ml	101	91	78	95
	ROS (30 minutes)		10 µg/ml	174	411	172	256
			1 µg/ml	171	208	134	261
ROS (24 hours)	10 µg/ml	42	102	166	134		
	1 µg/ml	88	141	175	145		

At wavelength of 720-740 nm with 2 joules/cm² light fluence, photo-induced cellular damage caused by the high dose of the SQZnPc molecule was moderately measured in A253 and FaDu cell lines, but not on HT29 and T47D cell lines. Considering 10 percent difference is acceptable, there were some differences above this limit between WST-1 and resazurin assay. However, according to general trends of viability depend on the Pc concentration, the resazurin assay results mostly supported the WST-1 assay.

SQZnPc-induced immediate ROS production was seen on each cell line in different degrees. The highest amount of ROS was seen on the FaDu cell line, it was followed by T47D, A253, and HT29 cell lines, respectively. Following PDT, late ROS formation was triggered with PDT of both doses of SQZnPc molecule on HT29, And T47D cell line. SQZnPc molecule did not lead to late ROS formation on A253 and FaDu cell lines.

Table 64 Relative percentage cell viability and ROS formation of cancer cell lines after photodynamic therapy with SQZnPc phthalocyanine at 725-755 nm (light fluence of 2 joules/cm²).

SQZnPc	Assay	Wavelength	Concentration	A253	FaDu	HT29	T47D
 Center metal Zn R1 	Cytotoxicity (WST-1)	725-755 nm	10 µg/ml	49	32	73	61
			1 µg/ml	80	88	94	85
	Cytotoxicity (Resazurin)		10 µg/ml	72	69	76	82
			1 µg/ml	101	87	73	93
	ROS (30 minutes)		10 µg/ml	194	435	190	249
			1 µg/ml	173	219	132	287
ROS (24 hours)	10 µg/ml	22	85	147	126		
	1 µg/ml	77	135	168	136		

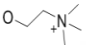
At wavelength of 725-755 nm with 2 joules/cm² light fluence, photo-induced cellular damage caused by the high dose of the SQZnPc molecule was moderately measured in A253 and FaDu cell lines, but not on HT29 and T47D cell lines. Considering 10 percent difference is acceptable, there were some differences above this limit between WST-1 and resazurin assay. However, according to general trends of viability depend on the Pc concentration, the resazurin assay results mostly supported the WST-1 assay.

SQZnPc-induced immediate ROS production was seen on each cell line in different degrees. The highest amount of ROS was seen on the FaDu cell line, it was followed by T47D, A253, and HT29 cell lines, respectively. Following PDT, late ROS formation was triggered with PDT of both doses of SQZnPc molecule on HT29, And T47D cell line. SQZnPc molecule did not lead to late ROS formation on A253 and FaDu cell lines.

4.1.1. Statistical Analysis

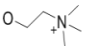
For each assay, data were represented as mean \pm SD of 3 independent experimental repeats. Statistical analysis for comparison of the data relative to the non-treated control was done using the two-way ANOVA. The statistic studies of cytotoxic response to the molecule was carried out based on WST-1 assay results.

Table 65 Significance of EH1-mediated PDT (at 624 nm with light fluence 2 joules/cm²), two-way ANOVA results.

EH1	Assay	Wavelength	Concentration	A253	FaDu	HT29	T47D
Center metal Zn	Cytotoxicity	624 nm	10 μ g/ml	***	***	**	**
			1 μ g/ml	***	***	**	ns
R2	ROS (30 minutes)		10 μ g/ml	**	*	ns	**
			1 μ g/ml	ns	**	*	ns
	ROS (24 hours)		10 μ g/ml	*	**	ns	**
			1 μ g/ml	**	***	**	ns

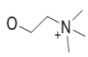
p-value is less than 0.05, marked with one star (*), p-value is less than 0.01, marked with two stars (**), p-value is less than 0.001, marked with three stars (***), ns for not significant.

Table 66 Significance of EH1-mediated PDT (at 650-670 nm with light fluence 2 joules/cm²), two-way ANOVA results.

EH1	Assay	Wavelength	Concentration	A253	FaDu	HT29	T47D
Center metal Zn	Cytotoxicity	650-670 nm	10 μ g/ml	***	***	**	**
			1 μ g/ml	**	***	**	*
R2	ROS (30 minutes)		10 μ g/ml	***	*	*	**
			1 μ g/ml	ns	ns	*	*
	ROS (24 hours)		10 μ g/ml	ns	***	ns	**
			1 μ g/ml	*	***	**	*

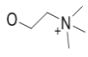
p-value is less than 0.05, marked with one star (*), p-value is less than 0.01, marked with two stars (**), p-value is less than 0.001, marked with three stars (***), ns for not significant.

Table 67 Significance of EH1-mediated PDT (at 690-710 nm with light fluence 2 joules/cm²), two-way ANOVA results.

EH1	Assay	Wavelength	Concentration	A253	FaDu	HT29	T47D
Center metal Zn	Cytotoxicity	690-710 nm	10 µg/ml	***	***	**	**
			1 µg/ml	***	***	*	ns
R2	ROS (30 minutes)		10 µg/ml	***	ns	*	**
			1 µg/ml	*	*	*	ns
	ROS (24 hours)		10 µg/ml	**	***	*	**
			1 µg/ml	ns	***	ns	ns

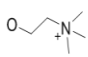
p-value is less than 0.05, marked with one star (*), p-value is less than 0.01, marked with two stars (**), p-value is less than 0.001, marked with three stars (***), ns for not significant.

Table 68 Significance of EH1-mediated PDT (at 720-740 nm with light fluence 2 joules/cm²), two-way ANOVA results.

EH1	Assay	Wavelength	Concentration	A253	FaDu	HT29	T47D
Center metal Zn	Cytotoxicity	720-740 nm	10 µg/ml	***	***	**	**
			1 µg/ml	***	***	*	**
R2	ROS (30 minutes)		10 µg/ml	**	**	*	**
			1 µg/ml	*	ns	ns	**
	ROS (24 hours)		10 µg/ml	**	**	*	**
			1 µg/ml	ns	*	*	**

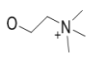
p-value is less than 0.05, marked with one star (*), p-value is less than 0.01, marked with two stars (**), p-value is less than 0.001, marked with three stars (***), ns for not significant.

Table 69 Significance of EH1-mediated PDT (at 725-755 nm with light fluence 2 joules/cm²), two-way ANOVA results.

EH1	Assay	Wavelength	Concentration	A253	FaDu	HT29	T47D
Center metal Zn	Cytotoxicity	725-755 nm	10 µg/ml	***	***	**	***
			1 µg/ml	***	***	*	ns
R2	ROS (30 minutes)		10 µg/ml	**	**	**	***
			1 µg/ml	**	ns	ns	ns
	ROS (24 hours)		10 µg/ml	*	**	ns	***
			1 µg/ml	*	***	*	ns

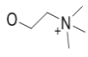
p-value is less than 0.05, marked with one star (*), p-value is less than 0.01, marked with two stars (**), p-value is less than 0.001, marked with three stars (***), ns for not significant.

Table 73 Significance of EH2-mediated PDT (at 720-740 nm with light fluence 2 joules/cm²), two-way ANOVA results.

EH2	Assay	Wavelength	Concentration	A253	FaDu	HT29	T47D
Center metal Zn	Cytotoxicity	720-740 nm	10 µg/ml	***	***	**	*
			1 µg/ml	*	ns	ns	***
R1	ROS (30 minutes)		10 µg/ml	**	ns	ns	*
			1 µg/ml	*	ns	ns	***
	ROS (24 hours)		10 µg/ml	**	*	ns	*
			1 µg/ml	*	**	ns	***

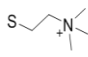
p-value is less than 0.05, marked with one star (*), p-value is less than 0.01, marked with two stars (**), p-value is less than 0.001, marked with three stars (***), ns for not significant.

Table 74 Significance of EH2-mediated PDT (at 725-755 nm with light fluence 2 joules/cm²), two-way ANOVA results.

EH2	Assay	Wavelength	Concentration	A253	FaDu	HT29	T47D
Center metal Zn	Cytotoxicity	725-755 nm	10 µg/ml	***	***	**	*
			1 µg/ml	*	*	ns	***
R1	ROS (30 minutes)		10 µg/ml	ns	ns	ns	*
			1 µg/ml	ns	ns	*	***
	ROS (24 hours)		10 µg/ml	*	**	ns	*
			1 µg/ml	*	***	ns	***

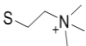
p-value is less than 0.05, marked with one star (*), p-value is less than 0.01, marked with two stars (**), p-value is less than 0.001, marked with three stars (***), ns for not significant.

Table 75 Significance of EH3-mediated PDT (at 624 nm with light fluence 2 joules/cm²), two-way ANOVA results.

EH3	Assay	Wavelength	Concentration	A253	FaDu	HT29	T47D
Center metal Zn	Cytotoxicity	624 nm	10 µg/ml	**	***	**	***
			1 µg/ml	**	***	**	*
R1	ROS (30 minutes)		10 µg/ml	**	*	ns	***
			1 µg/ml	*	ns	*	*
	ROS (24 hours)		10 µg/ml	ns	**	**	***
			1 µg/ml	ns	**	*	*

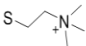
p-value is less than 0.05, marked with one star (*), p-value is less than 0.01, marked with two stars (**), p-value is less than 0.001, marked with three stars (***), ns for not significant.

Table 76 Significance of EH3-mediated PDT (at 650-670 nm with light fluence 2 joules/cm²), two-way ANOVA results.

EH3	Assay	Wavelength	Concentration	A253	FaDu	HT29	T47D
Center metal Zn	Cytotoxicity	650-670 nm	10 µg/ml	***	***	**	**
			1 µg/ml	***	***	*	**
R1	ROS (30 minutes)		10 µg/ml	**	*	**	**
			1 µg/ml	**	ns	*	**
S 	ROS (24 hours)		10 µg/ml	ns	***	***	**
			1 µg/ml	ns	**	ns	**

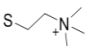
p-value is less than 0.05, marked with one star (*), p-value is less than 0.01, marked with two stars (**), p-value is less than 0.001, marked with three stars (***), ns for not significant.

Table 77 Significance of EH3-mediated PDT (at 690-710 nm with light fluence 2 joules/cm²), two-way ANOVA results.

EH3	Assay	Wavelength	Concentration	A253	FaDu	HT29	T47D
Center metal Zn	Cytotoxicity	690-710 nm	10 µg/ml	***	***	**	*
			1 µg/ml	**	***	*	***
R1	ROS (30 minutes)		10 µg/ml	*	**	**	*
			1 µg/ml	*	ns	**	***
S 	ROS (24 hours)		10 µg/ml	**	**	**	*
			1 µg/ml	**	ns	**	***

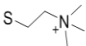
p-value is less than 0.05, marked with one star (*), p-value is less than 0.01, marked with two stars (**), p-value is less than 0.001, marked with three stars (***), ns for not significant.

Table 78 Significance of EH3-mediated PDT (at 720-740 nm with light fluence 2 joules/cm²), two-way ANOVA results.

EH3	Assay	Wavelength	Concentration	A253	FaDu	HT29	T47D
Center metal Zn	Cytotoxicity	740-740 nm	10 µg/ml	***	***	**	*
			1 µg/ml	***	***	**	*
R1	ROS (30 minutes)		10 µg/ml	**	**	**	*
			1 µg/ml	ns	ns	**	*
S 	ROS (24 hours)		10 µg/ml	*	ns	*	*
			1 µg/ml	ns	**	ns	*

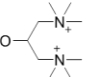
p-value is less than 0.05, marked with one star (*), p-value is less than 0.01, marked with two stars (**), p-value is less than 0.001, marked with three stars (***), ns for not significant.

Table 79 Significance of EH3-mediated PDT (at 725-755 nm with light fluence 2 joules/cm²), two-way ANOVA results.

EH3	Assay	Wavelength	Concentration	A253	FaDu	HT29	T47D
Center metal Zn	Cytotoxicity	725-755 nm	10 µg/ml	***	***	**	**
			1 µg/ml	**	***	**	*
R1	ROS (30 minutes)		10 µg/ml	**	ns	**	**
			1 µg/ml	*	**	*	*
S- 	ROS (24 hours)		10 µg/ml	***	*	***	**
			1 µg/ml	*	**	ns	*

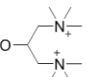
p-value is less than 0.05, marked with one star (*), p-value is less than 0.01, marked with two stars (**), p-value is less than 0.001, marked with three stars (***), ns for not significant.

Table 80 Significance of EH4-mediated PDT (at 624 nm with light fluence 2 joules/cm²), two-way ANOVA results.

EH4	Assay	Wavelength	Concentration	A253	FaDu	HT29	T47D
Center metal Zn	Cytotoxicity	624 nm	10 µg/ml	***	***	**	**
			1 µg/ml	***	***	ns	ns
R2	ROS (30 minutes)		10 µg/ml	**	*	*	**
			1 µg/ml	*	ns	*	ns
O- 	ROS (24 hours)		10 µg/ml	ns	***	***	**
			1 µg/ml	***	***	***	ns

p-value is less than 0.05, marked with one star (*), p-value is less than 0.01, marked with two stars (**), p-value is less than 0.001, marked with three stars (***), ns for not significant.

Table 81 Significance of EH4-mediated PDT (at 650-670 nm with light fluence 2 joules/cm²), two-way ANOVA results.

EH4	Assay	Wavelength	Concentration	A253	FaDu	HT29	T47D
Center metal Zn	Cytotoxicity	650-670 nm	10 µg/ml	***	***	**	***
			1 µg/ml	**	***	*	ns
R2	ROS (30 minutes)		10 µg/ml	**	*	**	***
			1 µg/ml	*	*	*	ns
O- 	ROS (24 hours)		10 µg/ml	*	***	**	***
			1 µg/ml	***	***	**	ns

p-value is less than 0.05, marked with one star (*), p-value is less than 0.01, marked with two stars (**), p-value is less than 0.001, marked with three stars (***), ns for not significant.

Table 82 Significance of EH4-mediated PDT (at 690-710 nm with light fluence 2 joules/cm²), two-way ANOVA results.

EH4	Assay	Wavelength	Concentration	A253	FaDu	HT29	T47D
Center metal Zn	Cytotoxicity	690-710 nm	10 µg/ml	***	***	**	**
			1 µg/ml	**	**	ns	**
R2	ROS (30 minutes)		10 µg/ml	**	*	***	**
			1 µg/ml	**	*	*	**
R2	ROS (24 hours)		10 µg/ml	ns	***	**	**
			1 µg/ml	***	**	*	**

p-value is less than 0.05, marked with one star (*), p-value is less than 0.01, marked with two stars (**), p-value is less than 0.001, marked with three stars (***), ns for not significant.

Table 83 Significance of EH4-mediated PDT (at 720-740 nm with light fluence 2 joules/cm²), two-way ANOVA results.

EH4	Assay	Wavelength	Concentration	A253	FaDu	HT29	T47D
Center metal Zn	Cytotoxicity	720-740 nm	10 µg/ml	***	***	**	**
			1 µg/ml	**	**	ns	*
R2	ROS (30 minutes)		10 µg/ml	***	*	***	**
			1 µg/ml	***	*	**	*
R2	ROS (24 hours)		10 µg/ml	*	***	ns	**
			1 µg/ml	ns	**	*	*

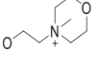
p-value is less than 0.05, marked with one star (*), p-value is less than 0.01, marked with two stars (**), p-value is less than 0.001, marked with three stars (***), ns for not significant.

Table 84 Significance of EH4-mediated PDT (at 725-755 nm with light fluence 2 joules/cm²), two-way ANOVA results.

EH4	Assay	Wavelength	Concentration	A253	FaDu	HT29	T47D
Center metal Zn	Cytotoxicity	725-755 nm	10 µg/ml	***	***	ns	***
			1 µg/ml	**	**	ns	**
R2	ROS (30 minutes)		10 µg/ml	**	*	**	***
			1 µg/ml	*	ns	*	**
R2	ROS (24 hours)		10 µg/ml	**	***	*	***
			1 µg/ml	ns	***	ns	**

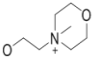
p-value is less than 0.05, marked with one star (*), p-value is less than 0.01, marked with two stars (**), p-value is less than 0.001, marked with three stars (***), ns for not significant.

Table 85 Significance of HQH₂Pc-mediated PDT (at 624 nm with light fluence 2 joules/cm²), two-way ANOVA results.

HQH2Pc	Assay	Wavelength	Concentration	A253	FaDu	HT29	T47D
Center metal 2H	Cytotoxicity	624 nm	10 µg/ml	ns	**	ns	**
			1 µg/ml	*	ns	ns	**
R2	ROS (30 minutes)		10 µg/ml	ns	ns	ns	**
			1 µg/ml	ns	ns	ns	**
	ROS (24 hours)		10 µg/ml	ns	**	ns	**
			1 µg/ml	***	***	**	**

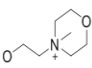
p-value is less than 0.05, marked with one star (*), p-value is less than 0.01, marked with two stars (**),
p-value is less than 0.001, marked with three stars (***), ns for not significant.

Table 86 Significance of HQH₂Pc-mediated PDT (at 650-670 nm with light fluence 2 joules/cm²), two-way ANOVA results.

HQH2Pc	Assay	Wavelength	Concentration	A253	FaDu	HT29	T47D
Center metal 2H	Cytotoxicity	650-670 nm	10 µg/ml	*	**	ns	**
			1 µg/ml	ns	ns	ns	**
R2	ROS (30 minutes)		10 µg/ml	*	ns	ns	**
			1 µg/ml	ns	ns	ns	**
	ROS (24 hours)		10 µg/ml	ns	**	ns	**
			1 µg/ml	ns	**	ns	**

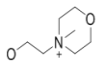
p-value is less than 0.05, marked with one star (*), p-value is less than 0.01, marked with two stars (**),
p-value is less than 0.001, marked with three stars (***), ns for not significant.

Table 87 Significance of HQH₂Pc-mediated PDT (at 690-710 nm with light fluence 2 joules/cm²), two-way ANOVA results.

HQH2Pc	Assay	Wavelength	Concentration	A253	FaDu	HT29	T47D
Center metal 2H	Cytotoxicity	690-710 nm	10 µg/ml	ns	*	ns	***
			1 µg/ml	*	ns	ns	**
R2	ROS (30 minutes)		10 µg/ml	*	ns	ns	***
			1 µg/ml	ns	ns	ns	**
	ROS (24 hours)		10 µg/ml	**	**	*	***
			1 µg/ml	ns	***	ns	**

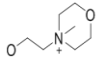
p-value is less than 0.05, marked with one star (*), p-value is less than 0.01, marked with two stars (**),
p-value is less than 0.001, marked with three stars (***), ns for not significant.

Table 88 Significance of HQH₂Pc-mediated PDT (at 720-740 nm with light fluence 2 joules/cm²), two-way ANOVA results.

HQH ₂ Pc	Assay	Wavelength	Concentration	A253	FaDu	HT29	T47D
Center metal 2H	Cytotoxicity	720-740 nm	10 µg/ml	ns	*	ns	**
			1 µg/ml	ns	ns	ns	***
R2	ROS (30 minutes)		10 µg/ml	**	ns	ns	**
			1 µg/ml	ns	ns	ns	***
	ROS (24 hours)		10 µg/ml	**	***	**	**
			1 µg/ml	**	***	***	***

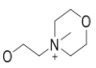
p-value is less than 0.05, marked with one star (*), p-value is less than 0.01, marked with two stars (**),
p-value is less than 0.001, marked with three stars (***), ns for not significant.

Table 89 Significance of HQH₂Pc-mediated PDT (at 725-755 nm with light fluence 2 joules/cm²), two-way ANOVA results.

HQH ₂ Pc	Assay	Wavelength	Concentration	A253	FaDu	HT29	T47D
Center metal 2H	Cytotoxicity	725-755 nm	10 µg/ml	ns	*	ns	*
			1 µg/ml	*	ns	ns	***
R2	ROS (30 minutes)		10 µg/ml	*	ns	*	*
			1 µg/ml	ns	ns	*	***
	ROS (24 hours)		10 µg/ml	***	**	***	*
			1 µg/ml	**	***	**	***

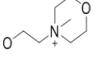
p-value is less than 0.05, marked with one star (*), p-value is less than 0.01, marked with two stars (**),
p-value is less than 0.001, marked with three stars (***), ns for not significant.

Table 90 Significance of HQZnPc-mediated PDT (at 624 nm with light fluence 2 joules/cm²), two-way ANOVA results.

HQZnPc	Assay	Wavelength	Concentration	A253	FaDu	HT29	T47D
Center metal Zn	Cytotoxicity	624 nm	10 µg/ml	***	***	*	ns
			1 µg/ml	**	ns	ns	*
R2	ROS (30 minutes)		10 µg/ml	*	ns	ns	ns
			1 µg/ml	*	*	**	*
	ROS (24 hours)		10 µg/ml	**	ns	***	ns
			1 µg/ml	***	**	**	*

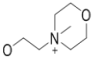
p-value is less than 0.05, marked with one star (*), p-value is less than 0.01, marked with two stars (**),
p-value is less than 0.001, marked with three stars (***), ns for not significant.

Table 91 Significance of HQZnPc-mediated PDT (at 650-670 nm with light fluence 2 joules/cm²), two-way ANOVA results.

HQZnPc	Assay	Wavelength	Concentration	A253	FaDu	HT29	T47D
Center metal Zn	Cytotoxicity	650-670 nm	10 µg/ml	***	***	**	*
			1 µg/ml	**	ns	ns	ns
R2	ROS (30 minutes)		10 µg/ml	*	*	ns	*
			1 µg/ml	ns	*	ns	ns
	ROS (24 hours)		10 µg/ml	**	ns	**	*
			1 µg/ml	ns	**	ns	ns

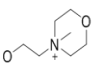
p-value is less than 0.05, marked with one star (*), p-value is less than 0.01, marked with two stars (**), p-value is less than 0.001, marked with three stars (***), ns for not significant.

Table 92 Significance of HQZnPc-mediated PDT (at 690-710 nm with light fluence 2 joules/cm²), two-way ANOVA results.

HQZnPc	Assay	Wavelength	Concentration	A253	FaDu	HT29	T47D
Center metal Zn	Cytotoxicity	690-710 nm	10 µg/ml	**	***	**	*
			1 µg/ml	***	ns	ns	ns
R2	ROS (30 minutes)		10 µg/ml	**	**	*	*
			1 µg/ml	***	ns	*	ns
	ROS (24 hours)		10 µg/ml	ns	*	ns	*
			1 µg/ml	***	**	**	ns

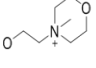
p-value is less than 0.05, marked with one star (*), p-value is less than 0.01, marked with two stars (**), p-value is less than 0.001, marked with three stars (***), ns for not significant.

Table 93 Significance of HQZnPc-mediated PDT (at 720-740 nm with light fluence 2 joules/cm²), two-way ANOVA results.

HQZnPc	Assay	Wavelength	Concentration	A253	FaDu	HT29	T47D
Center metal Zn	Cytotoxicity	720-740 nm	10 µg/ml	**	***	*	**
			1 µg/ml	*	ns	ns	ns
R2	ROS (30 minutes)		10 µg/ml	***	*	**	**
			1 µg/ml	ns	ns	ns	ns
	ROS (24 hours)		10 µg/ml	ns	*	ns	**
			1 µg/ml	*	***	*	ns

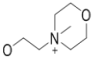
p-value is less than 0.05, marked with one star (*), p-value is less than 0.01, marked with two stars (**), p-value is less than 0.001, marked with three stars (***), ns for not significant.

Table 94 Significance of HQZnPc-mediated PDT (at 725-755 nm with light fluence 2 joules/cm²), two-way ANOVA results.

HQZnPc	Assay	Wavelength	Concentration	A253	FaDu	HT29	T47D
Center metal Zn	Cytotoxicity	725-755 nm	10 µg/ml	***	***	**	*
			1 µg/ml	*	ns	ns	ns
R2	ROS (30 minutes)		10 µg/ml	**	*	*	*
			1 µg/ml	**	ns	*	ns
	ROS (24 hours)		10 µg/ml	**	*	*	*
			1 µg/ml	***	**	***	ns

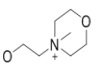
p-value is less than 0.05, marked with one star (*), p-value is less than 0.01, marked with two stars (**), p-value is less than 0.001, marked with three stars (***), ns for not significant.

Table 95 Significance of HQInPc-mediated PDT (at 624 nm with light fluence 2 joules/cm²), two-way ANOVA results.

HQInPc	Assay	Wavelength	Concentration	A253	FaDu	HT29	T47D
Center metal InCl	Cytotoxicity	624 nm	10 µg/ml	***	***	**	**
			1 µg/ml	***	***	*	***
R2	ROS (30 minutes)		10 µg/ml	***	ns	**	**
			1 µg/ml	*	ns	**	***
	ROS (24 hours)		10 µg/ml	ns	*	ns	**
			1 µg/ml	***	**	***	***

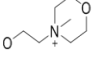
p-value is less than 0.05, marked with one star (*), p-value is less than 0.01, marked with two stars (**), p-value is less than 0.001, marked with three stars (***), ns for not significant.

Table 96 Significance of HQZnPc-mediated PDT (at 650-670 nm with light fluence 2 joules/cm²), two-way ANOVA results.

HQZnPc	Assay	Wavelength	Concentration	A253	FaDu	HT29	T47D
Center metal Zn	Cytotoxicity	650-670 nm	10 µg/ml	***	***	**	*
			1 µg/ml	**	ns	ns	ns
R2	ROS (30 minutes)		10 µg/ml	*	*	ns	*
			1 µg/ml	ns	*	ns	ns
	ROS (24 hours)		10 µg/ml	**	**	**	*
			1 µg/ml	ns	**	ns	ns

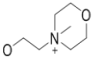
p-value is less than 0.05, marked with one star (*), p-value is less than 0.01, marked with two stars (**), p-value is less than 0.001, marked with three stars (***), ns for not significant.

Table 97 Significance of HQZnPc-mediated PDT (at 690-710 nm with light fluence 2 joules/cm²), two-way ANOVA results.

HQInPc	Assay	Wavelength	Concentration	A253	FaDu	HT29	T47D
Center metal InCl	Cytotoxicity	690-710 nm	10 µg/ml	***	***	**	***
			1 µg/ml	**	***	ns	**
R2	ROS (30 minutes)		10 µg/ml	**	ns	ns	***
			1 µg/ml	*	*	ns	**
	ROS (24 hours)		10 µg/ml	ns	***	*	***
			1 µg/ml	**	**	**	**

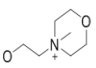
p-value is less than 0.05, marked with one star (*), p-value is less than 0.01, marked with two stars (**),
p-value is less than 0.001, marked with three stars (***), ns for not significant.

Table 98 Significance of HQZnPc-mediated PDT (at 720-740 nm with light fluence 2 joules/cm²), two-way ANOVA results.

HQInPc	Assay	Wavelength	Concentration	A253	FaDu	HT29	T47D
Center metal InCl	Cytotoxicity	720-740 nm	10 µg/ml	***	***	**	**
			1 µg/ml	*	***	ns	**
R2	ROS (30 minutes)		10 µg/ml	**	ns	ns	**
			1 µg/ml	*	ns	ns	**
	ROS (24 hours)		10 µg/ml	*	*	*	**
			1 µg/ml	*	**	**	**

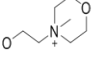
p-value is less than 0.05, marked with one star (*), p-value is less than 0.01, marked with two stars (**),
p-value is less than 0.001, marked with three stars (***), ns for not significant.

Table 99 Significance of HQZnPc-mediated PDT (at 725-755 nm with light fluence 2 joules/cm²), two-way ANOVA results.

HQInPc	Assay	Wavelength	Concentration	A253	FaDu	HT29	T47D
Center metal InCl	Cytotoxicity	725-755 nm	10 µg/ml	***	***	**	***
			1 µg/ml	***	***	ns	***
R2	ROS (30 minutes)		10 µg/ml	*	*	*	***
			1 µg/ml	ns	ns	ns	***
	ROS (24 hours)		10 µg/ml	**	**	**	***
			1 µg/ml	ns	**	*	***

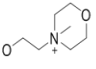
p-value is less than 0.05, marked with one star (*), p-value is less than 0.01, marked with two stars (**),
p-value is less than 0.001, marked with three stars (***), ns for not significant.

Table 100 Significance of SQH₂Pc-mediated PDT (at 624 nm with light fluence 2 joules/cm²), two-way ANOVA results.

SQH ₂ Pc	Assay	Wavelength	Concentration	A253	FaDu	HT29	T47D
Center metal 2H	Cytotoxicity	624 nm	10 µg/ml	**	**	***	**
			1 µg/ml	ns	ns	ns	*
R1	ROS (30 minutes)		10 µg/ml	*	*	**	**
			1 µg/ml	ns	**	*	*
	ROS (24 hours)		10 µg/ml	ns	*	ns	**
			1 µg/ml	***	**	**	*

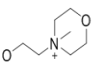
p-value is less than 0.05, marked with one star (*), p-value is less than 0.01, marked with two stars (**),
p-value is less than 0.001, marked with three stars (***), ns for not significant.

Table 101 Significance of SQH₂Pc-mediated PDT (at 650-670 nm with light fluence 2 joules/cm²), two-way ANOVA results.

SQH ₂ Pc	Assay	Wavelength	Concentration	A253	FaDu	HT29	T47D
Center metal 2H	Cytotoxicity	650-670 nm	10 µg/ml	***	***	**	**
			1 µg/ml	ns	ns	ns	ns
R1	ROS (30 minutes)		10 µg/ml	ns	ns	ns	**
			1 µg/ml	*	*	*	ns
	ROS (24 hours)		10 µg/ml	ns	**	ns	**
			1 µg/ml	**	**	***	ns

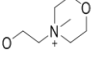
p-value is less than 0.05, marked with one star (*), p-value is less than 0.01, marked with two stars (**),
p-value is less than 0.001, marked with three stars (***), ns for not significant.

Table 102 Significance of SQH₂Pc-mediated PDT (at 670-710 nm with light fluence 2 joules/cm²), two-way ANOVA results.

SQH ₂ Pc	Assay	Wavelength	Concentration	A253	FaDu	HT29	T47D
Center metal 2H	Cytotoxicity	690-710 nm	10 µg/ml	**	**	**	**
			1 µg/ml	ns	*	ns	*
R1	ROS (30 minutes)		10 µg/ml	*	*	ns	**
			1 µg/ml	*	*	ns	*
	ROS (24 hours)		10 µg/ml	*	**	*	**
			1 µg/ml	**	**	*	*

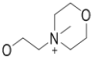
p-value is less than 0.05, marked with one star (*), p-value is less than 0.01, marked with two stars (**),
p-value is less than 0.001, marked with three stars (***), ns for not significant.

Table 103 Significance of SQH₂Pc-mediated PDT (at 720-740 nm with light fluence 2 joules/cm²), two-way ANOVA results.

SQH ₂ Pc	Assay	Wavelength	Concentration	A253	FaDu	HT29	T47D
Center metal 2H	Cytotoxicity	720-740 nm	10 µg/ml	***	**	**	**
			1 µg/ml	ns	*	ns	**
R1	ROS (30 minutes)		10 µg/ml	ns	ns	ns	**
			1 µg/ml	ns	ns	ns	**
	ROS (24 hours)		10 µg/ml	**	***	**	**
			1 µg/ml	ns	**	ns	**

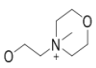
p-value is less than 0.05, marked with one star (*), p-value is less than 0.01, marked with two stars (**), p-value is less than 0.001, marked with three stars (***), ns for not significant.

Table 104 Significance of SQH₂Pc-mediated PDT (at 725-755 nm with light fluence 2 joules/cm²), two-way ANOVA results.

SQH ₂ Pc	Assay	Wavelength	Concentration	A253	FaDu	HT29	T47D
Center metal 2H	Cytotoxicity	725-755 nm	10 µg/ml	***	***	**	**
			1 µg/ml	*	ns	ns	***
R1	ROS (30 minutes)		10 µg/ml	**	ns	*	**
			1 µg/ml	**	*	ns	***
	ROS (24 hours)		10 µg/ml	***	**	**	**
			1 µg/ml	ns	ns	ns	***

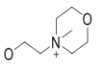
p-value is less than 0.05, marked with one star (*), p-value is less than 0.01, marked with two stars (**), p-value is less than 0.001, marked with three stars (***), ns for not significant.

Table 105 Significance of SQZnPc-mediated PDT (at 624 nm with light fluence 2 joules/cm²), two-way ANOVA results.

SQZnPc	Assay	Wavelength	Concentration	A253	FaDu	HT29	T47D
Center metal Zn	Cytotoxicity	624 nm	10 µg/ml	***	***	ns	*
			1 µg/ml	ns	*	ns	**
R1	ROS (30 minutes)		10 µg/ml	*	*	ns	*
			1 µg/ml	ns	ns	ns	**
	ROS (24 hours)		10 µg/ml	**	**	**	*
			1 µg/ml	ns	***	*	**

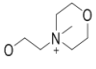
p-value is less than 0.05, marked with one star (*), p-value is less than 0.01, marked with two stars (**), p-value is less than 0.001, marked with three stars (***), ns for not significant.

Table 106 Significance of SQZnPc-mediated PDT (at 650-670 nm with light fluence 2 joules/cm²), two-way ANOVA results.

SQZnPc	Assay	Wavelength	Concentration	A253	FaDu	HT29	T47D
Center metal Zn	Cytotoxicity	650-670 nm	10 µg/ml	**	***	*	**
			1 µg/ml	ns	*	ns	*
R1	ROS (30 minutes)		10 µg/ml	**	**	*	**
			1 µg/ml	ns	ns	*	*
	ROS (24 hours)		10 µg/ml	***	**	**	**
			1 µg/ml	*	ns	ns	*

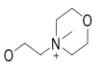
p-value is less than 0.05, marked with one star (*), p-value is less than 0.01, marked with two stars (**), p-value is less than 0.001, marked with three stars (***), ns for not significant.

Table 107 Significance of SQZnPc-mediated PDT (at 690-710 nm with light fluence 2 joules/cm²), two-way ANOVA results.

SQZnPc	Assay	Wavelength	Concentration	A253	FaDu	HT29	T47D
Center metal Zn	Cytotoxicity	690-710 nm	10 µg/ml	**	**	ns	**
			1 µg/ml	*	*	ns	**
R1	ROS (30 minutes)		10 µg/ml	*	**	***	**
			1 µg/ml	ns	ns	ns	**
	ROS (24 hours)		10 µg/ml	*	*	*	**
			1 µg/ml	ns	**	ns	**

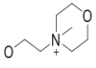
p-value is less than 0.05, marked with one star (*), p-value is less than 0.01, marked with two stars (**), p-value is less than 0.001, marked with three stars (***), ns for not significant.

Table 108 Significance of SQZnPc-mediated PDT (at 720-740 nm with light fluence 2 joules/cm²), two-way ANOVA results.

SQZnPc	Assay	Wavelength	Concentration	A253	FaDu	HT29	T47D
Center metal Zn	Cytotoxicity	720-740 nm	10 µg/ml	***	***	ns	*
			1 µg/ml	*	*	ns	**
R1	ROS (30 minutes)		10 µg/ml	**	**	***	*
			1 µg/ml	*	ns	*	**
	ROS (24 hours)		10 µg/ml	***	***	***	*
			1 µg/ml	**	**	**	**

p-value is less than 0.05, marked with one star (*), p-value is less than 0.01, marked with two stars (**), p-value is less than 0.001, marked with three stars (***), ns for not significant.

Table 109 Significance of SQZnPc-mediated PDT (at 725-755 nm with light fluence 2 joules/cm²), two-way ANOVA results.

SQZnPc	Assay	Wavelength	Concentration	A253	FaDu	HT29	T47D
Center metal Zn	Cytotoxicity	725-755 nm	10 µg/ml	***	**	ns	*
			1 µg/ml	*	*	*	**
R1	ROS (30 minutes)		10 µg/ml	*	**	**	*
			1 µg/ml	*	ns	**	**
	ROS (24 hours)		10 µg/ml	**	ns	*	*
			1 µg/ml	***	**	**	**

p-value is less than 0.05, marked with one star (*), p-value is less than 0.01, marked with two stars (**),
p-value is less than 0.001, marked with three stars (***), ns for not significant.



5. DISCUSSION

Photodynamic therapy is two-step cancer treatment alternatives to other treatments with its low side effects. Photosensitizer, light and molecular oxygen are the components of PDT which have an impact on the efficiency of the treatment. In this thesis study, in vitro characterization of nine specifically synthesized cationic phthalocyanine molecules has been studied.

In the light of the aim, several questions were studied in order to understand “in vitro PDT effects” of the molecules. Firstly, cellular uptake capacities of the molecules were studied. Furthermore, biocompatibility and appropriate concentrations were also calculated where the molecules did not have cytotoxic effects on the cell lines under dark conditions, and proper light fluence for PDT was determined.

After all these experiments, PDT-mediated cytotoxicity and ROS formation were evaluated at the determined concentration and light fluency.

To see the biocompatibility of the EH1, EH2, EH3, EH4, HQH₂Pc, HQZnPc, HQInPc, and SQH₂Pc, and SQZnPc Cationic Tetra Substituted Symmetrical Phthalocyanine molecules, cytotoxicity assay was performed on the L929 line as considering prescription of International Organization for Standardization. Effect of different doses of cytotoxicity in the dark environment (10 µg /mL and 1 µg /mL) were determined and then was used as working doses for the following studies. As a result of the light studies performed in the visible spectrum, the molecules were considered as biocompatible at the determined doses.

Cytotoxicity studies were performed by WST-1 assay in four different concentrations to determine the concentration range without toxic effects on A253,

FaDu, and HT29 and T47D cell lines in the dark environment. Phthalocyanines at a dose of 1 $\mu\text{g/mL}$ and 10 $\mu\text{g/mL}$ with a viability of 70% and above were determined as the non-toxic range.

Light-irradiated cytotoxicity studies were performed at two concentrations, 1 $\mu\text{g/mL}$ and 10 $\mu\text{g/mL}$ determined as non-toxic by dark cytotoxicity study. This study was carried out by WST-1 assay and verified by resazurin assay.

Although the molecules have absorbance spectrums at wavelengths with higher energies such as 300 nm, these wavelengths are not sufficient for depth penetration into the tissues. The other absorbance range (600-800 nm) of these molecules is suitable for PDT applications. For each molecule, their specific wavelengths in their absorbance spectrums which is higher than 600 nm were considered. However, at the other wavelengths (624-755 nm) that were studied, cellular response was obtained like their specific wavelengths. The reason for this situation could be that the wavelength intervals were close to the specific ones. Also, the absorbance spectrums could be affected from the ingredients of culture media since the molecules has different behavior in different substance such as DMSO and water.

Taking into account the absorption spectrum, at a wavelength of 650-670 nm with 2 joules/cm² of light fluence, EH1-mediated photodynamic therapy was the most effective on the FaDu cell line (with a p-value is smaller than 0.001 according to ANOVA analysis) where high and low doses of EH1 molecule lead to appx. 90 percent of cell death followed by HT29, A253, and T47D cell lines. EH1 induced immediate ROS production was seen the highest on FaDu cell line (with a p-value is smaller than 0.05 according to ANOVA analysis) caused by the high dose of the molecule with approx. 300% ROS production relative to non-treated control. It was followed by A253, T47D and HT29 cell lines, respectively. Further, EH1-induced PDT triggered late ROS production on FaDu cell line with approx. 10000% ROS production (with a p-value is smaller than 0.001 according to ANOVA analysis) relative to control,

followed by HT29, A253, and T47D cell lines, respectively. When gathering cytotoxicity and ROS results, it can be said that PDT-induced cytotoxicity of EH1 molecule was mostly dependent on ROS production.

Taking into account the absorption spectrum, at the wavelength of 650-670 nm with 2 joules/cm² light fluence, EH2-mediated photodynamic therapy was the most effective on FaDu cell line (with a p-value is smaller than 0.001 according to ANOVA analysis), followed by HT29, A253. EH2 induced immediate ROS production was seen only on A253 cell line (with a p-value is smaller than 0.05 according to ANOVA analysis) caused by the high dose of the molecule with approx. 150% ROS production relative to the non-treated control. Further, EH2-induced PDT triggered late ROS production on FaDu cell line (with a p-value is smaller than 0.01 according to ANOVA analysis) with approx. 750% ROS production relative to control, followed by HT29, and T47D cell lines, respectively. In contrast to the immediate ROS production of A253 cell line, there was no ROS measured lately. When gathering cytotoxicity and ROS results, it can be said that PDT-induced cytotoxicity of EH2 molecule was mostly dependent on ROS production, however, it can be triggered by immediate or late ROS production.

Taking into account the absorption spectrum, at the wavelength of 650-670 nm with 2 joules/cm² light fluence, EH3-mediated photodynamic therapy was the most effective on FaDu cell line (with a p-value is smaller than 0.001 according to ANOVA analysis) where both high and low doses of EH3 molecule lead to appx. 90% cell death relative to the non-treated control. It was followed by A253, HT29, and T47D cell lines. EH3 induced immediate ROS production was seen the highest on T47D cell line (with a p-value is smaller than 0.01 according to ANOVA analysis) caused by the high dose of the molecule with approx. 250% ROS production relative to the non-treated control. It was followed by FaDu, HT29, and A253 cell lines, respectively. Further, EH3-induced PDT triggered late ROS production on FaDu cell line (with a p-value is smaller than 0.001 according to ANOVA analysis) with approx. 10000% ROS production relative to control, followed by A253, HT29, and T47D cell lines,

respectively. When the cytotoxicity and ROS results were analyzed, it can be said that PDT-induced cytotoxicity of EH3 molecule was mostly dependent on ROS production.

Taking into account the absorption spectrum, at the wavelength of 650-670 nm with 2 joules/cm² light fluence, EH4-mediated photodynamic therapy was the most effective on FaDu cell line (with a p-value is smaller than 0.001 according to ANOVA analysis), followed by HT29, A253, and T47D cell lines. EH4 induced immediate ROS production was seen the highest on T47D cell line (with a p-value is smaller than 0.001 according to ANOVA analysis) caused by high dose of the molecule with approx. 350% ROS production relative to the non-treated control. It was followed by FaDu, A253, and HT29 cell lines, respectively. Further, EH4-induced PDT triggered late ROS production on FaDu cell line (with a p-value is smaller than 0.001 according to ANOVA analysis) with approx. 7500% ROS production relative to control, followed by A253, HT29, and T47D cell lines, respectively. When gathering cytotoxicity and ROS results, it can be said that PDT-induced cytotoxicity of EH4 molecule was mostly dependent on ROS production.

Taking into account the absorption spectrum, at the wavelength of 650-670 nm with 2 joules/cm² light fluence, HQH₂Pc-mediated photodynamic therapy did not trigger cellular damage on any cell lines. Further, neither immediate nor late PDT-induced ROS was not formed. HQH₂Pc molecule is not suitable for PDT.

Taking into account the absorption spectrum, at the wavelength of 650-670 nm with 2 joules/cm² light fluence, HQZnPc-mediated photodynamic therapy was the most effective on FaDu cell line (with a p-value is smaller than 0.001 according to ANOVA analysis) where both high and low doses of HQZnPc molecule lead to appx. 90% cell death relative to the non-treated control. It was followed by A253, HT29, and T47D cell lines, respectively. HQZnPc induced immediate ROS production was seen the highest on T47D cell line (with a p-value is smaller than 0.05 according to ANOVA

analysis) caused by the high dose of the molecule with approx. 350% ROS production relative to the non-treated control. It was followed by FaDu, A253, and HT29 cell lines, respectively. Further, HQZnPc-induced PDT triggered late ROS production on FaDu cell line (with a p-value is smaller than 0.01 according to ANOVA analysis) with approx. 7500% ROS production relative to control, followed by HT29, T47D, and A253 cell lines, respectively. When gathering cytotoxicity and ROS results, it can be said that PDT-induced cytotoxicity of HQZnPc molecule was mostly dependent on ROS production.

Taking into account the absorption spectrum, at the wavelength of 650-670 nm with 2 joules/cm² light fluence, HQInPc-mediated photodynamic therapy was the most effective on FaDu cell line (with a p-value is smaller than 0.001 according to ANOVA analysis), followed by T47D, HT29, and A253 cell lines, respectively. HQInPc induced immediate ROS production was seen the highest on A253 cell line (with a p-value is smaller than 0.01 according to ANOVA analysis) caused by the high dose of the molecule with approx. 250% ROS production relative to the non-treated control. It was followed by T47D, FaDu, and HT29 cell lines, respectively. Further, HQInPc-induced PDT triggered late ROS production on T47D cell line (with a p-value is smaller than 0.01 according to ANOVA analysis) with approx. 400% ROS production relative to control, followed by FaDu, and HT29 cell lines, respectively. When gathering cytotoxicity and ROS results, it can be said that PDT-induced cytotoxicity of HQInPc molecule was mostly dependent on ROS production, however, it can be triggered by immediate or late ROS production.

Taking into account the absorption spectrum, at the wavelength of 690-710 nm with 2 joules/cm² light fluence, SQH₂Pc-mediated photodynamic therapy was the moderately effective only on FaDu and HT29 cell lines (with a p-value is smaller than 0.01 according to ANOVA analysis) when were applied with the high dose of the molecule. SQH₂Pc induced immediate ROS production was seen the highest on A253 cell line (with a p-value is smaller than 0.05 according to ANOVA analysis) caused by the high dose of the molecule with approx. 150% ROS production relative to the non-

treated control. It was followed by FaDu cell line. Further, SQH₂Pc-induced PDT triggered late ROS production on HT29 cell line (with a p-value is smaller than 0.05 according to ANOVA analysis) with approx. 150% ROS production relative to control, followed by T47D cell line. When gathering cytotoxicity and ROS results, it can be said that PDT-induced cytotoxicity of SQH₂Pc molecule was mostly dependent on ROS production, however, it can be triggered by immediate or late ROS production.

Taking into account the absorption spectrum, at the wavelength of 690-710 nm with 2 joules/cm² light fluence, SQZnPc-mediated photodynamic therapy was the moderately effective only on A253 and FaDu cell lines (with a p-value is smaller than 0.01 according to ANOVA analysis). SQZnPc induced immediate ROS production was seen the highest on FaDu cell line (with a p-value is smaller than 0.01 according to ANOVA analysis) caused by the high dose of the molecule with approx. 350% ROS production relative to the non-treated control. It was followed by T47D, A253, and HT29 cell lines, respectively. Further, SQZnPc-induced PDT triggered late ROS production on HT29 cell line (with a p-value is smaller than 0.05 according to ANOVA analysis) with approx. 150% ROS production relative to control, followed by T47D cell line. When gathering cytotoxicity and ROS results, it can be said that PDT-induced cytotoxicity of SQZnPc molecule was mostly dependent on ROS production, however, it can be triggered by immediate or late ROS production.

When all the data that were presented among the phthalocyanine molecules were collected, the most cytotoxic response was obtained from EH1-induced PDT, followed by EH3, HQZnPc, EH4, SQZnPc, EH2, HQInPc, and SQH₂Pc.

Two different methods (WST-1 and Resazurin methods) were used in cell viability studies and the results were compared. In most of the cases in the study, although the resazurin assay results were similar to the WST-1 assay, in some cases, there were some differences. Even though the experiments were repeated to eliminate the differences, the same differences were experienced. The results obtained by WST-

1 experiments have been considered more reliable and reproducible than those obtained by resazurin experiments. Since, for resazurin assay, the evaluation is based on fluorescence intensity whereas for WST-1 assay, it is based on absorbance, and each experiment was carried out using clear surface plates that are not suitable for fluorescence readings and can scatter taken fluoresces. For this reason, the results of WST-1 experiments were taken as a basis in cell viability / proliferation assays in this thesis study.

When the relationship between cytotoxicity and ROS production after Pc-mediated PDT was considered, it can be said that for each cancer cell line, the cytotoxic response was mostly depending on ROS formation following PDT.

It is known that the molecules can generate enough energy to form singlet oxygen. However, the PDT-mediated singlet oxygen formation on cells could not be studied because of its very short half-life. Therefore, in this study, we could only show PDT mediated responses of type-1 reaction (electron/photon is transferred from Pc to O₂) that triggers cellular damage through ROS. Further, at different times, PDT-mediated ROS amounts were measured. We may say that given the findings, PDT begins to trigger ROS formation right after the treatment. However, the most significant ROS formation was obtained later on the treatment. It could be better to take kinetic models of ROS formation to make more precious comments on when the highest amount of ROS produced after treatment.

In some cases, ROS production did not lead to cell death. This situation could be due to that each cell line requires a different amount of ROS to trigger cell death, and although there was ROS production, the requirement of the cell to trigger death could not be meet.

Further, the cytotoxic response against Pc-based PDT and cellular uptake capacities of Pc molecules was evaluated together. Flow cytometry assay at Fluorochrome (Ex-Max 650 nm/Em-Max 785 nm) to see cellular uptake of these nine phthalocyanine molecules on the A253, FaDu, HT29, and T47D cell lines due to their fluorescence was performed. Consequently, a higher capacity of binding is found at SQ group phthalocyanines, SQH₂Pc and SQZnPc, further EH4 and EH2 showed relatively agreeable binding capacities on each cell lines relative to control. In contradiction to cellular uptake results, EH1, EH3, and HQZnPc molecules have higher light-dependent toxicity compared to the molecules that have higher binding capacities. This contradiction could be explained by the higher energy transfer capacities of these molecules.

In conclusion, at wavelength range between 624-755 nm with 2 joules/cm² light fluence, each cell line used in this thesis responded to Pc-based PDT, even to varying degrees. The highest cytotoxicity was mostly measured in the FaDu cell line. Between the phthalocyanine molecules, the most cytotoxic response was obtained from EH1-induced PDT, followed by EH3, HQZnPc, EH4, SQZnPc, EH2, HQInPc, and SQH₂Pc. PDT-induced cytotoxicity of the molecules was mostly ROS-dependent. Each molecule also had cellular uptake capacities. Since their high binding capacities, fluorescence features, and non-cytotoxic effect at low dose of the EH2, SQH₂Pc, and SQZnPc molecules, they can be used as a diagnostic reagent for solid tumors of cancer. According to the in vitro experimental results, Pc derivatives used in this thesis can be considered as strong candidates that can be used as photosensitizing agents for further studies due to their binding capacities, biocompatibility and high level of cancer cytotoxicity.

6. BIBLIOGRAPHY

1. Dummin H, Cernay T, Zimmermann HW. Selective photosensitization of mitochondria in HeLa cells by cationic Zn (II)phthalocyanines with lipophilic sidechains. *J Photochem Photobiol B Biol.* 1997; 37(3):219–29.
2. van Straten D, Mashayekhi V, de Bruijn HS, Oliveira S, Robinson DJ. Oncologic photodynamic therapy: Basic principles, current clinical status and future directions. 2017; 9(2).
3. Dougherty TJ, Gomer CJ, Henderson BW, Jori G, Kessel D, Korbek M, et al. Photodynamic therapy. *Journal of the National Cancer Institute.* 1998; 90(12): 889–905.
4. Castano AP, Demidova TN, Hamblin MR. Mechanisms in photodynamic therapy: Part One- Photosensitizers, photochemistry and cellular localization. *Photodiagnosis and Photodynamic Therapy.* 2004; 1(4): 279–93.
5. Abrahamse H, Hamblin MR. New photosensitizers for photodynamic therapy. *Biochemical Journal.* 2016; 473(4): 347–64.
6. Moor ACE. Signaling pathways in cell death and survival after photodynamic therapy. *Journal of Photochemistry and Photobiology B: Biology.* 2000; 57(1): 1–13.
7. Li B, Lin L, Lin H, Wilson BC. Photosensitized singlet oxygen generation and detection: Recent advances and future perspectives in cancer photodynamic therapy. *J Biophotonics.* 2016; 9(11–12): 1314–1325.
8. DeRosa MC, Crutchley RJ. Photosensitized singlet oxygen and its applications. *Coordination Chemistry Reviews.* 2002; 233-234: 351–371.
9. Henderson BW, Dougherty TJ. How does photodynamic therapy work? *Photochemistry and Photobiology.* 1992; 55(1): 145–57.
10. Plaetzer K, Kiesslich T, Verwanger T, Krammer B. The modes of cell death induced by PDT: An overview. *Medical Laser Application.* 2003; 18(1): 7–19.
11. Dlugaszewska J, Szczolko W, Koczorowski T, Skupin-Mrugalska P, Teubert A, Konopka K, et al. Antimicrobial and anticancer photodynamic activity of a phthalocyanine photosensitizer with N-methyl morpholiniumethoxy substituents in non-peripheral positions. *J Inorg Biochem.* 2017; 172: 67–79.
12. Zheng BY, Ke MR, Lan WL, Hou L, Guo J, Wan DH, et al. Mono- and tetra-substituted zinc (II) phthalocyanines containing morpholinyl moieties: Synthesis, antifungal photodynamic activities, and structure-activity relationships. *Eur J Med Chem.* 2016; 114: 380–389.
13. Skupin-Mrugalska P, Szczolko W, Gierlich P, Konopka K, Goslinski T, Mielcarek J, et al. Physicochemical properties of liposome-incorporated 2-(morpholin-4-yl) ethoxy phthalocyanines and their photodynamic activity against oral cancer cells. *J Photochem Photobiol A Chem.* 2018; 353: 445–457.

14. Marino J, García Vior MC, Dixelio LE, Roguin LP, Awruch J. Photodynamic effects of isosteric water-soluble phthalocyanines on human nasopharynx KB carcinoma cells. *Eur J Med Chem.* 2010; 45(9): 4129–4139.
15. Wöhrle D, Iskander N, Grashew G, Sinn H, Friedrich EA, Maier-Borst W, et al. Synthesis of positively charged phthalocyanines and their activity in the photodynamic therapy of cancer cells. *Photochem Photobiol.* 1990; 51(3): 351–356.
16. De Filippis MP, Dei D, Fantetti L, Roncucci G. Synthesis of a new water-soluble octa-cationic phthalocyanine derivative for PDT. *Tetrahedron Lett.* 2000; 41(47): 9143–9147.
17. Tuncer S, Ozcesmeci I, Sesalan BS. Spectroscopic and thermodynamic approach to the interaction of nonperipherally substituted cationic phthalocyanines with calf thymus (CT)-DNA. *Turkish Journal of Chemistry.* 2018; 42: 274 – 290.
18. Koçan H, Kaya K, Ozcesmeci I, Sesalan BS, Goksel M, Durmus M, Burat AK. Photophysicochemical, calf thymus DNA binding and in vitro photocytotoxicity properties of tetramorpholinoethoxy-substituted phthalocyanines and their water-soluble quaternized derivatives. *J Biol Inorg Chem.* 2017; 22(8): 1251-1266.
19. Moses C, Garcia-Bloj B, Harvey AR, Blancafort P. Hallmarks of cancer: The CRISPR generation. *European Journal of Cancer.* 2018; 93: 10–8.
20. Hanahan D, Weinberg RA. The hallmarks of cancer. *Cell.* 2000; 100(1): 57–70.
21. Hanahan D, Weinberg RA. Hallmarks of cancer: The next generation. *Cell.* 2011; 144(5): 646–674.
22. Anioogo EC, Plackal Adimuriyil George B, Abrahamse H. The role of photodynamic therapy on multidrug resistant breast cancer. *Cancer Cell International.* 2019; 19(1).
23. Ackroyd R, Kelty C, Brown N, Reed M. The History of Photodetection and Photodynamic Therapy. *Photochem Photobiol.* 2001; 74(5): 656.
24. Celli JP, Spring BQ, Rizvi I, Evans CL, Samkoe KS, Verma S, et al. Imaging and photodynamic therapy: Mechanisms, monitoring, and optimization. *Chem Rev.* 2010; 110(5): 2795–2838.
25. Spikes JD. The origin and meaning of the term “photodynamic” (as used in “photodynamic therapy”, for example). *Journal of Photochemistry and Photobiology, B: Biology.* 1991; 9(3-4): 369–371.
26. Berg K, Selbo PK, Weyergang A, Dietze A, Prasmickaite L, Bonsted A, et al. Porphyrin-related photosensitizers for cancer imaging and therapeutic applications. *Journal of Microscopy.* 2005; 218(2): 133–47.
27. Lipson RL, Baldes EJ, Olsen AM. The use of a derivative of hematoporphyrin in tumor detection. *J Natl Cancer Inst.* 1961; 26(1): 1–11.
28. Agostinis P, Berg K, Cengel KA, Foster TH, Girotti AW, Gollnick SO, et al. Photodynamic therapy of cancer: An update. *CA Cancer J Clin.* 2011; 61(4): 250–281.
29. Hamblin MR, Newman EL. Photosensitizer targeting in photodynamic therapy I. conjugates of haematoporphyrin with albumin and transferrin. *J Photochem Photobiol B Biol.* 1994; 26(1): 45–56.
30. Korbelik M, Kroszl G, Chaplin DJ, Chaplin DJ, Korbelik M. photofrin uptake by murine macrophages. *Cancer Res.* 1991; 51(9): 2251–2255.

31. Vaupel P. Tumor microenvironmental physiology and its implications for radiation oncology. *Semin Radiat Oncol.* 2004; 14(3): 198–206.
32. Tan X, Luo S, Wang D, Su Y, Cheng T, Shi C. A NIR heptamethine dye with intrinsic cancer targeting, imaging and photosensitizing properties. *Biomaterials.* 2012; 33(7): 2230–2239.
33. Kwiatkowski S, Knap B, Przystupski D, Saczko J, Kędzierska E, Knap-Czop K, et al. Photodynamic therapy – mechanisms, photosensitizers and combinations. *Biomedicine and Pharmacotherapy.* 2018; 106: 1098–1107.
34. Ariffin AB, Forde PF, Jahangeer S, Soden DM, Hinchion J. Releasing pressure in tumors: What do we know so far and where do we go from here a review. *Cancer Research.* 2014; 74(10): 2655–2662.
35. Jori G. Tumour photosensitizers: Approaches to enhance the selectivity and efficiency of photodynamic therapy. *Journal of Photochemistry and Photobiology B: Biology.* 1996; 36(2): 87–93.
36. Castano AP, Demidova TN, Hamblin MR. Mechanisms in photodynamic therapy: Part three - Photosensitizer pharmacokinetics, biodistribution, tumor localization and modes of tumor destruction. *Photodiagnosis and Photodynamic Therapy.* 2005; 2(2): 91–106.
37. Kessel D. Correlation between subcellular localization and photodynamic efficacy. *Journal of Porphyrins and Phthalocyanines.* 2004; 8(8): 1009–1014.
38. Bonnett R. Photosensitizers of the porphyrin and phthalocyanine series for photodynamic therapy. *Chemical Society Reviews.* 1995; 24(1): 19–33.
39. Kucinska M, Skupin-Mrugalska P, Szczolko W, Sobotta L, Sciepura M, Tykarska E, et al. Phthalocyanine derivatives possessing 2-(morpholin-4-yl)ethoxy groups as potential agents for photodynamic therapy. *J Med Chem.* 2015; 58(5): 2240–2255.
40. Rosenthal I. Phthalocyanines as photodynamic sensitizers. *Photochemistry and Photobiology.* 1991; 53(6): 859–870.
41. Lukyanets EA. Phthalocyanines as photosensitizers in the photodynamic therapy of cancer. *J Porphyr Phthalocyanines.* 1999; 3(6–7): 424–32.
42. Jamali Z, Hejazi SM, Ebrahimi SM, Moradi-Sardareh H, Paknejad M. Effects of LED-Based photodynamic therapy using red and blue lights, with natural hydrophobic photosensitizers on human glioma cell line. *Photodiagnosis Photodyn Ther.* 2018; 21: 50–54.
43. Plaetzer K, Krammer B, Berlanda J, Berr F, Kiesslich T. Photophysics and photochemistry of photodynamic therapy: Fundamental aspects. *Lasers in Medical Science.* 2009; 24(2): 259–268.
44. Weston MA, Patterson MS. Validation and application of a model of oxygen consumption and diffusion during photodynamic therapy in vitro. *Photochem Photobiol.* 2014; 90(6): 1359–1367.
45. Sharman WM, Allen CM, Van Lier JE. Role of activated oxygen species in photodynamic therapy. *Methods Enzymol.* 2000; 319: 376–400.
46. Hou H, Huang X, Wei G, Xu F, Wang Y, Zhou S. Fenton Reaction-Assisted Photodynamic Therapy for Cancer with Multifunctional Magnetic Nanoparticles. *ACS Appl Mater Interfaces.* 2019; 11(33): 29579–29592.

47. Baptista MS, Cadet J, Di Mascio P, Ghogare AA, Greer A, Hamblin MR, et al. Type I and Type II Photosensitized Oxidation Reactions: Guidelines and Mechanistic Pathways. *Photochemistry and Photobiology*. 2017; 93(4): 912–919.
48. Castano AP, Demidova TN, Hamblin MR. Mechanisms in photodynamic therapy: Part two - Cellular signaling, cell metabolism and modes of cell death. *Photodiagnosis and Photodynamic Therapy*. 2005; 2(1): 1–23.
49. Morris RL, Azizuddin K, Lam M, Berlin J, Nieminen AL, Kenney ME, et al. Fluorescence resonance energy transfer reveals a binding site of a photosensitizer for photodynamic therapy. *Cancer Res*. 2003; 63(17): 5194–5197.
50. Plaetzer K, Kiesslich T, Krammer B, Hammerl P. Characterization of the cell death modes and the associated changes in cellular energy supply in response to AIPcS4-PDT. *Photochem Photobiol Sci*. 2002; 1(3): 172–177.
51. Nagata S, Obana A, Gohto Y, Nakajima S. Necrotic and apoptotic cell death of human malignant melanoma cells following photodynamic therapy using an amphiphilic photosensitizer, ATX-S10 (Na). *Lasers Surg Med*. 2003; 33(1): 64–70.
52. Castano AP, Mroz P, Hamblin MR. Photodynamic therapy and anti-tumour immunity. *Nature Reviews Cancer*. 2006; 6(7): 535–545.
53. Garg AD, Nowis D, Golab J, Agostinis P. Photodynamic therapy: Illuminating the road from cell death towards anti-tumour immunity. *Apoptosis*. 2010; 15(9): 1050–1071.
54. Rashid F, Horobin RW. Interaction of molecular probes with living cells and tissues. Part 2. *Histochemistry*. 1990; 94(3).
55. Lam M, Oleinick NL, Nieminen A-L. Photodynamic Therapy-induced Apoptosis in Epidermoid Carcinoma Cells. *J Biol Chem*. 2001; 276(50): 47379–47386.
56. Granville DJ, Carthy CM, Jiang H, Shore GC, McManus BM, Hunt DWC. Rapid cytochrome c release, activation of caspases 3, 6, 7 and 8 followed by Bap31 cleavage in HeLa cells treated with photodynamic therapy. *FEBS Lett*. 1998; 437(1–2): 5–10.
57. Zhuang S, Lynch MC, Kochevar IE. Caspase-8 mediates caspase-3 activation and cytochrome c release during singlet oxygen-induced apoptosis of HL-60 cells. *Exp Cell Res*. 1999; 250(1): 203–212.
58. Mroz P, Yaroslavsky A, Kharkwal GB, Hamblin MR. Cell death pathways in photodynamic therapy of cancer. *Cancers*. 2011; 3(2): 2516–2539.

7. RESUME

Personal Information

Name	Şeyma	Surname	Işık
Birthplace	Bahçelievler/İstanbul	Birthday	16.02.1992
Nationality	T.C.	Phone Number	
E-mail	seymaxisik@gmail.com		

Education

	Institution	Graduation Year
Master of Science	Acıbadem Mehmet Ali Aydınlar University	2020
Bachelor of Science	Yeditepe University	2016
High School	Pertevniyal Lisesi	2010

Experience

	Position	Organization	Duration (Year – Year)
	Scholar	TÜBİTAK	2018-

Language	Reading	Speaking	Writing
English	Advanced	Advanced	Advanced

Foreign Language Examination Grade									
KPDS	ÜDS	IELTS	TOEFL IBT	TOEFL PBT	TOEFL CBT	FCE	CAE	CPE	YÖK DİL

KPDS: Kamu Personeli Yabancı Dil Sınavı; ÜDS: ÜniversitelereRası Kurul Yabancı Dil Sınavı; IELTS: International English Language Testing System; TOEFL IBT: Test of English as a Foreign Language-Internet-Based Test TOEFL PBT: Test of English as a Foreign Language-Paper-Based Test; TOEFL CBT: Test of English as a Foreign Language-Computer-Based Test; FCE: First Certificate in English;
CAE: Certificate in Advanced English; CPE: Certificate of Proficiency in English

	Quantitative	Equally Weighted	Verbal
ALES Note			

Computer Skills

Program	
Gen5	Image J
VMD	Office Package
NAMD	Novo Express

